

Cite this: *Chem. Soc. Rev.*, 2012, **41**, 480–520

www.rsc.org/csr

CRITICAL REVIEW**Anion receptor chemistry: highlights from 2010****Marco Wenzel, Jennifer R. Hiscock and Philip A. Gale****Received 20th September 2011*

DOI: 10.1039/c1cs15257b

This *critical review* covers advances in anion complexation in the year 2010. The review covers both organic and inorganic systems and also highlights the applications to which anion receptors can be applied such as sensing, anion transport, control of molecular motion and gelation (179 references).

Introduction

This review is the latest in a series covering recent advances in anion complexation.^{1–6} It highlights developments in 2010 in the fields of new receptors, modes of binding, transport and extraction of anions, and sensing mechanisms. It is not intended to be a comprehensive overview of the area. The structure of the review is primarily according to the dominant functional group used to complex the anion and by the potential application of these systems. Many receptors use more than one functional group to bind anions or have various applications and the organisation of this review should be regarded as a flexible guide to the classification of these systems.

Amide/carbamate containing receptors

Secondary amides have been widely employed in synthetic anion receptor systems. Yatsimirsky and co-workers have

investigated a series of known isomeric *N,N'*-bis(pyridyl)-2,6-pyridine-dicarboxamides^{7,8} **4–6** and their dicationic pyridinium analogues **1–3** in solution and the solid state.⁹ The stability constants of the neutral receptors with chloride and acetate were determined by ¹H NMR titrations in CD₃CN. The NMR titration curve of the *m*-isomer **4** illustrates the formation of 1:1 and 1:2 (L:A) complexes with both anions (chloride: log *K* = 1.8, log β_{21} = 4.23; acetate: log *K* = 2.6, log β_{21} = 4.7). For the *p*-isomer **5** the formation of 1:1 complexes was observed for chloride (log *K* = 2.85) whereas 1:1 and 1:2 complexes are formed with acetate (log *K* = 3.48, log β_{21} = 6.5). No interaction and weak binding were observed during the titration of the *o*-isomer **6** with chloride and acetate (log *K* = 0.7) respectively. The binding affinities of the related pyridinium receptors **1–3** towards halides and nitrate are higher. Spectrophotometric titrations for the *m*- and *p*-isomers **1** and **2**, and competition experiments by deprotonation with pyridine for *o*-isomer **3** were carried out in CH₃CN in order to calculate the stability constant of the 1:1 complexes. A summary of the obtained stability constants is shown in Table 1. The highest affinities were observed with the *o*-isomer **3** over the *m*- and *p*-isomers **1**

*Chemistry, University of Southampton, Southampton, SO17 1BJ, UK.
E-mail: philip.gale@soton.ac.uk; Fax: +44 (0)23 8059 6805;
Tel: +44 (0)23 8059 3332*

**Marco Wenzel**

Marco Wenzel studied Chemical Engineering at the HTW Dresden, Germany. He completed his PhD at the University of Dresden in 2008 under the supervision of Prof Karsten Gloe with research stays at the University of Nottingham, UK (Marie Curie Fellowship), University of Saga, Japan (DAAD) and University of Sydney, Australia (DFG). Before he joined the group of Prof Philip Gale in 2010 he carried out 2 years of Post-Doctoral research with Dr Paul

Plieger at Massey University, New Zealand. His main research interests in supramolecular chemistry are membrane transport and liquid–liquid extraction of anionic species and metal salts.

**Jennifer R. Hiscock**

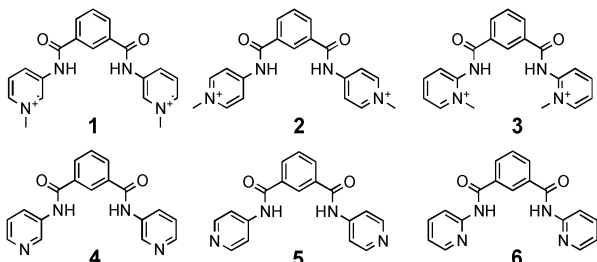
Jennifer Hiscock graduated in biomedicinal chemistry at the University of Exeter 2007. In 2010 she received her PhD from the University of Southampton where she has continued as a Post Doctoral researcher under the supervision of Prof Philip Gale. Her research interests include the supramolecular chemistry of anionic species and the utilisation of organic molecules in catalysis.

Table 1 Stability constants ($\log K_a$) for receptors **1–3** in CH_3CN .^{a,b}
Anions added as their tetrabutylammonium salts

Anion	1	2	3
F^-	5.28(8)	4.36(7)	
Cl^-	5.27(9)	5.65(6)	5.85(9)
Br^-	5.24(7)	4.29(7)	5.40(8)
I^-	3.80(7)	3.57(9)	3.80(8)
H_2PO_4^-	4.20(6)	5.18(9)	
AcO^-	4.40(7)	5.38(8)	
NO_3^-	4.11(9)	4.34(5)	4.40(6)

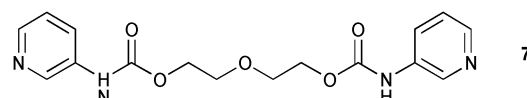
^a Stability constants for **1** and **2** were obtained by spectrophotometric titrations, for **3** by competition experiments by deprotonation with pyridine. ^b Values in parentheses are standard deviation in the last significant digit.

and **2**, respectively. Four crystal structures of chloride and triflate complexes of the three isomers illustrate the binding of the anion in the ligand cleft *via* multiple hydrogen bonds with the amide groups and *via* CH-interactions with adjacent methyl-pyridinium rings. The observed $\text{NH}\cdots\text{Cl}$ distances are between 3.194 and 3.307 Å and the $\text{CH}\cdots\text{Cl}$ distances range from 3.342 to 3.614 Å. The triflate anions in **2** and **3** are bound by $\text{NH}\cdots\text{O}$ interactions with distances between 2.878 and 3.127 Å and by $\text{CH}\cdots\text{O}$ interactions between 3.089 to 3.371 Å. The orientation of the methyl substituents towards the centre of the ligand cleft prevents the formation of inclusion complexes with *o*-isomer **3** for both chloride and triflate in the solid state. The proximity of the positive charge of the pyridinium function and the ligand NH binding side may result in the observed order of stability in solution.



Solid phase investigation of the sulfate, perchlorate and chloride complexes of the protonated aliphatic bis-3-pyridinium carbamate receptor **7** show different modes of interaction with

different anionic guests.¹⁰ Perchlorate was found to bind *via* pyridinium NH \cdots O interactions between 2.801 and 2.961 Å. Interactions with the carbamate NH hydrogen bond donor occur *via* a co-crystallised water molecule, but no direct hydrogen bonds were observed between the anion and these groups. The NH \cdots O_{water} distances are between 3.012 and 3.039 Å and the OH_{water} \cdots O ClO_4^- distance is 2.858 Å. Direct hydrogen bonds between the carbamate NH and the anion are observed in the sulfate and chloride complexes. The NH \cdots Cl distances are between 3.192 and 3.267 Å whereas the pyridinium NH \cdots Cl distances are significantly shorter (3.021 to 3.039 Å) presumably due to electrostatic attraction. A similar differentiation was observed for the NH \cdots O SO_4^{2-} interactions: the pyridinium NH \cdots O distances are 2.614 and 2.659 Å whereas the carbamate NH \cdots O distance is 2.789 Å.



Simple diamide receptors **8–11** based on anthracene or carbazole linked *via* amide bonds to pendant pyrrole or phenyl substituents were synthesised and investigated by Sessler and co-workers.¹¹ Proton NMR titrations in $\text{DMSO}-d_6$ with chloride, benzoate and dihydrogen phosphate, added as their tetrabutylammonium ($n\text{-Bu}_4\text{N}^+$) salts, show selective complexation of H_2PO_4^- over PhCOO^- and Cl^- for all receptors. Furthermore, the stability constants show an increase in the anion binding affinity in agreement with the number of N-donor atoms present in the receptor. For example K_a [M^{-1}] for H_2PO_4^- for **8**: 2000, for **9**: 1400 for **10**: 2600 and for **11**: 160 (see Table 2). Interestingly, the pyrrolic NH protons do not participate in the coordination of the Cl^- ion in the crystal structure of the complex $[\text{Cl} \subset \mathbf{8}] (n\text{-Bu}_4\text{N})$ (Fig. 1), and the anion is bound by only three of the possible five NH-groups. Instead, the pyrrole protons are involved in the formation of a hydrogen-bonded network with the amide oxygen of another molecule of **8** to form a 1-D hydrogen bonded polymer.

A series of amide hosts based on a benzene^{12,13} and tris(2-aminoethyl)amine^{14,15} (tren) platform have been investigated by Ghosh and co-workers. The bistripodand ligand **12** coordinates multiple anions by dividing the six pendant arms into two compartments with an ababab arrangement or unfavourable aaabbb fashion in the solid state (Fig. 2).¹² The latter was found in the 1:2 (L:A) acetate complex with the anion bound by three amide NH \cdots O hydrogen bonds (NH \cdots O distances in the range 2.677 to 2.792 Å). In the crystal two receptors form a pseudo-cage, composed of six arms that hold two anions separated by 6.101 Å. The authors quote four intermolecular C–F \cdots F–C interactions with a F \cdots F distance of 2.938 Å as the driving force

Table 2 Stability constants (K_a [M^{-1}]) for receptors **8–11** in $\text{DMSO}-d_6$ at 298 K. Anions added as their tetrabutylammonium salts

Anion	Receptor			
	8	9	10	11
Cl^-	<50	<50	80	83
PhCOO^-	1600	790	310	65
H_2PO_4^-	2000	1400	2600	165



Philip A. Gale is Professor of Supramolecular Chemistry at the University of Southampton. A major focus of his research concerns the molecular recognition, sensing and lipid bilayer transport of anionic species.

Philip A. Gale

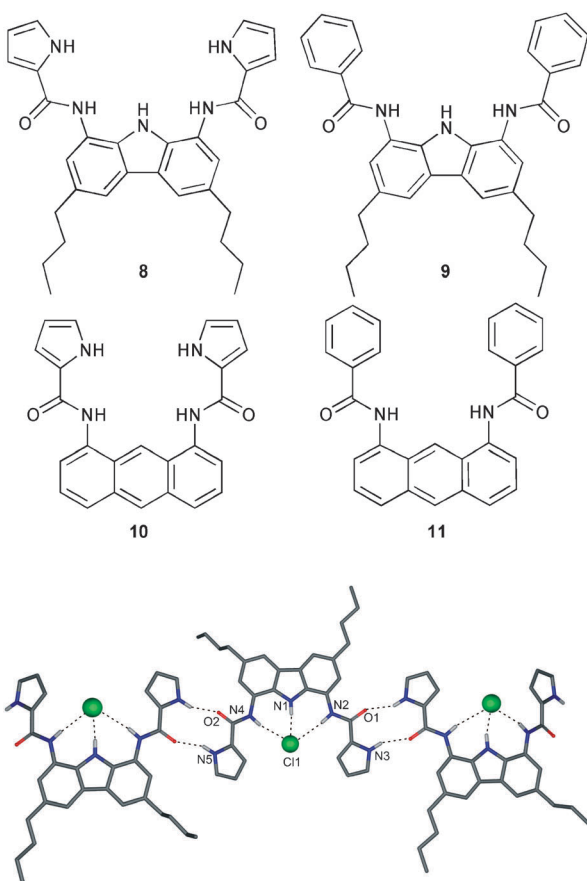


Fig. 1 Schematic representation of the crystal structure of $[\text{Cl} \subset 8]$ - $(n\text{-Bu}_4\text{N})$, non-acidic hydrogen atoms and tetrabutylammonium counter cations are omitted for clarity, hydrogen bonds are represented as dotted lines.

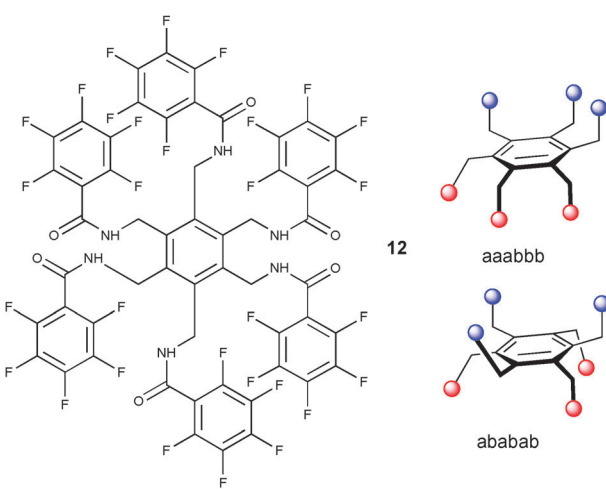


Fig. 2 Schematic draw of **12** (left) and aaabbb and ababab orientation of pendant arms in solid phase (right).

for pseudo-cage formation. In the nitrate complex of **12** the pendant arms are orientated in an ababab alternate arrangement. A total of four nitrate anions are coordinated by one ligand. Two anions are bound as pair, bridged with one water molecule on either side of the benzene platform ($\text{OH}_{\text{water}} \cdots \text{O}-\text{NO}_2^-$ distance between 2.795 and 3.035 Å). Each of the nitrate anions is

coordinated by the ligand *via* one amide $\text{NH} \cdots \text{O}$ hydrogen bond ($\text{NH} \cdots \text{O}$ distances are 2.893 and 3.135 Å) and an anion- π interaction towards the pentafluoro-phenyl substituent. The anion-centroid distances are 3.201 and 3.511 Å. The anion binding ability of **12** towards the tetrabutylammonium salts of H_2PO_4^- , OAc^- and NO_3^- was studied in acetone- d_6 using ^1H NMR titrations. Job plot experiments, monitoring the shift of the amide-NH for NO_3^- and the CH_2 resonance for OAc^- and H_2PO_4^- show a stoichiometry of 1:4 (L:A) for acetate and dihydrogen phosphate, and a 1:2 host-guest binding for NO_3^- . The calculated binding constants $\log K_n$ for NO_3^- are 2.83 and 4.91, respectively.

The influence of *p*- and *o*-nitrophenyl substituents on anion encapsulation in tripodal amide receptors, based on 1,3,5-trimethylbenzene has been reported by the same research group.¹³ Comparison of the crystal structures of the nitrate, acetate, fluoride and chloride complexes of *p*-isomer **13** with known complexes of *o*-isomer **14**¹⁶ shows the formation of 2:2 host-guest capsules of **13** with all studied anions. A similar assembly of *o*-isomer **14** was only observed upon the complexation of $[\text{F}_2(\text{H}_2\text{O})_6]^{2-}$. The mutual interdigitation of the six pendant arms of two molecules of **13** in a sandwiched arrangement hosts two NO_3^- (Fig. 3), $[(\text{AcO})_2(\text{H}_2\text{O})_4]^{2-}$, $[\text{F}_2(\text{H}_2\text{O})_6]^{2-}$ and $[\text{Cl}_2(\text{H}_2\text{O})_4]^{2-}$ inside the capsule. The incorporated water molecules in the latter three complexes act as bridges to overcome anion-anion repulsion and are involved in numerous hydrogen bonds with the ligand and the anionic guests. However no water was found in the nitrate structure of **13** ($[\text{NO}_3 \subset 13_2]^{2-}$). In this case the two anions are arranged in a staggered planar orientation relative to one another with a central $\text{N} \cdots \text{N}$ distance of 3.562 Å. Further, both nitrate anions are in short contact to the respective π -cloud of the aryl platform with N -centroid distances of 3.225 and 3.229 Å. Numerous $\text{NH} \cdots \text{O}$ and $\text{CH} \cdots \text{O}$ hydrogen bonds are formed from the amide groups and the *p*-nitrophenyl substituents towards the anions. The distances of the observed $\text{NH} \cdots \text{O}-\text{NO}_2^-$ interactions range from 2.984 to 3.297 Å, where the $\text{CH} \cdots \text{O}$ distances are between 3.279 and 3.451 Å. The distance of the $\text{NH} \cdots \text{anion}$ interaction in the

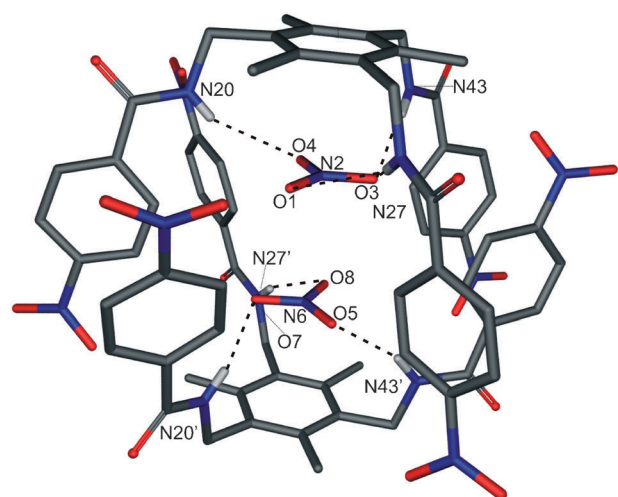
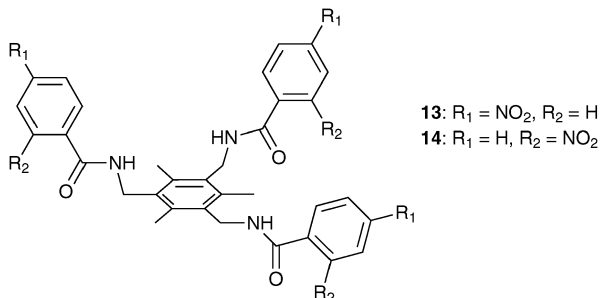
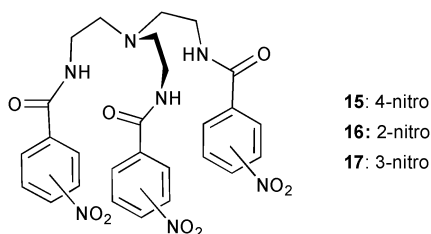


Fig. 3 X-Ray structure of $[(\text{NO}_3)_2 \subset 13_2]^{2-}$ with selected atom labels and $\text{N}-\text{H} \cdots \text{O}$ hydrogen bonds as dotted lines, tetrabutylammonium cations and non-acidic hydrogen atoms are omitted for clarity.

acetate complex is 2.893 Å, where a NH···F distance of 2.805 Å was obtained in $[(\text{F}_2(\text{H}_2\text{O})_6 \subset \mathbf{13}_2)^{2-}]$. The chloride ions in $[(\text{Cl}_2(\text{H}_2\text{O})_4 \subset \mathbf{13}_2)^{2-}]$ are bound by an NH···Cl interaction of 3.290 Å and CH···Cl contacts of 3.466 and 3.636 Å. The subsequent X-ray analysis of the reaction of **13** with 3 equivalents of the tetrabutylammonium salts of nitrate, acetate, fluoride and chloride from dioxane yields the previously observed complex $[(\text{F}_2(\text{H}_2\text{O})_6 \subset \mathbf{13}_2)(n\text{-Bu}_4\text{N})_2]_2$ dioxane. Qualitative ¹H NMR studies in DMSO-*d*₆ underline the preferred uptake of fluoride over chloride, nitrate and acetate.



More detailed studies on the influence of positional isomers in solution on anion affinity were performed with the series of tren-based nitrophenyl-amide receptors **15–17**.¹⁴ Proton NMR titration experiments in DMSO-*d*₆ of the known *m*-isomer¹⁷ **17** and the two new receptors **15** and **16** with chloride and fluoride show selective binding of fluoride over chloride for the latter two isomers. The calculated stability constants log K_a for a 1:1 binding mode are 4.06 and 2.29 for fluoride and chloride, respectively, with *p*-isomer **15**. A binding constant log K_a of 5.63 was obtained for fluoride with *o*-isomer **16**, whilst no shift in the NH was observed upon addition of tetrabutylammonium chloride. The binding constants are the same order of magnitude for both anions with *m*-isomer **17** (log K_a = 3.76 and 3.32 for fluoride and chloride, respectively). No uptake of the anion into the pseudo-cage was observed in the solid state. Crystal structures of the iodide, perchlorate and hexafluorosilicate complex of the *p*-isomer **15** show anion coordination on the ligand periphery only. Presumably strong intermolecular N–H···O hydrogen bonds between the amide groups of at least two pendant arms (N···O distances between 2.792 and 3.057 Å) prevent the uptake of the anion into the pseudo-cage.



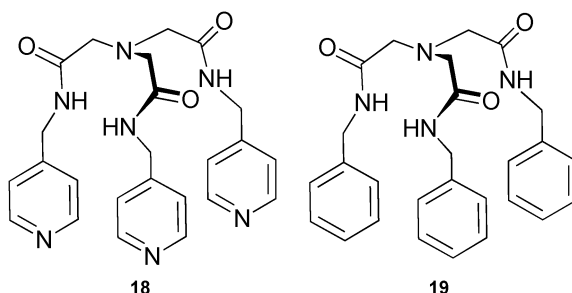
Öztürk and co-workers conducted the solvent free synthesis of two amide-based tripodal receptors.¹⁵ The direct treatment of nitrilotriacetic acid with benzylamine and picolyamine under microwave conditions gives receptor **18** and previously reported ligand **19**¹⁸ in high yield (>80%) and in very short reaction times (<45 min). Binding studies in DMSO-*d*₆ show a pronounced selectivity of both receptors for H₂PO₄[−] and PhCOO[−] over HSO₄[−], ClO₄[−], PF₆[−] and Br[−] (Table 3).

Table 3 Binding constants K_a [M^{−1}] for the 1:1 complexes of **18** and **19** in DMSO-*d*₆ at 298 K.^a Anions added as their tetrabutylammonium salts

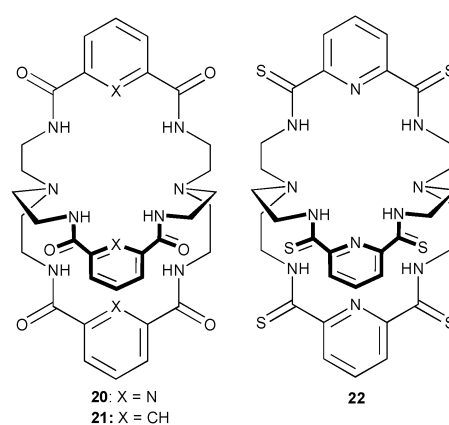
Anion	18	19
H ₂ PO ₄ [−]	810	241
PhCOO [−]	286	110
HSO ₄ [−]	39	43
ClO ₄ [−]	59	—
PF ₆ [−]	73	—
Br [−]	—	—

^a Errors estimated to be not more than ±10%.

Overall higher binding constants were observed for the 4-pyridyl-methyl substituted receptor **18** (K_a (M^{−1}) = 810 for H₂PO₄[−] and 286 for PhCOO[−]) than for the benzyl substituted receptor **19** (K_a (M^{−1}) = 241 and 110 for H₂PO₄[−] and PhCOO[−], respectively).



Two known amido-cryptands (**20** and **21**) and a new thioamido-cryptand **22** have been studied for their fluoride binding ability in solution and the solid state by Bowman-James and co-workers.¹⁹ Proton NMR studies in DMSO-*d*₆ reveal binding constants K_a (M^{−1}) of 8.1×10^5 , 3.3×10^4 and 3.2×10^4 for **20**, **21** and **22**, respectively. The significantly lower anion affinity of the thioamide receptor **22** as compared to compound **20** was explained by the authors as being due to the presence of a negative charge on the partly deprotonated thioamide group during ongoing hydrogen/deuterium exchange repelling the incoming fluoride anion. Extensive ¹⁹F NMR studies demonstrated the presence of enhanced deuterium-exchange reactions in DMSO for this receptor. The enhanced hydrogen bonding capability of the thioamide group has resulted in higher binding affinities for anions in previous studies of monocyclic thioamides from the same group.²⁰ Two crystal structures of the



F^- complexes of **20** and **21** show the 1:1 encapsulation of the anion within the pseudo C_3 -symmetric host. The F^- anions are coordinated by $\text{N}-\text{H}\cdots\text{F}$ hydrogen bonds with all amide groups in both examples. The observed $\text{N}\cdots\text{F}$ distances range from 2.822 to 2.889 Å in $[\text{F} \subset \textbf{20}]^-$ and between 2.948 and 3.111 Å in $[\text{F} \subset \textbf{21}]^-$, which is longer than most amide $\text{N}-\text{H}\cdots\text{F}$ interactions. In the F^- complex of **21** additional $\text{C}-\text{H}\cdots\text{F}$ interactions are formed between the three isophthaloyl hydrogen atoms and the central anion. The $\text{C}\cdots\text{F}$ distances range from 3.032 to 3.077 Å.

The same group has also reported tricyclic 2,6-pyridinedicarboxamide host **23**.²¹ This larger receptor forms more stable complexes with linear anions, such as FHF^- and N_3^- over anions such as Cl^- , Br^- and I^- . Crystal structures of both bifluoride and azide complexes show encapsulation of the guest inside the receptor cavity. Internal multi-atom hydrogen bonding networks involving the pyridine nitrogen, amido hydrogen and amine nitrogen atom ($\text{N}_{\text{py}} \cdots \text{H}_{\text{amide}} \cdots \text{N}_{\text{amine}}$) provide a preorganised hydrogen bonding pocket for the coordination of the guest anions (Fig. 4). The observed $\text{N}_{\text{amide}} \cdots \text{N}_{\text{amine}}$ distances range from 2.839 to 2.944 Å where $\text{N}_{\text{amide}} \cdots \text{N}_{\text{py}}$ interactions between 2.734 and 2.772 Å have been observed. In both complexes the anions are coordinated by multiple hydrogen bonds from the remaining amide groups. The $\text{N} \cdots \text{F}$ interactions range from 2.724 to 2.754 Å where the fluorine atoms are separated by 2.475 Å with a FHF^- angle of 168°. The azide ion is bound via $\text{N}_{\text{amide}} \cdots \text{N}_{\text{azide}}$ interactions between 2.854 and 2.906 Å. The $\text{N}=\text{N}=\text{N}$ separation is 2.355 Å with nearly equal N–N distances of 1.162 and 1.193 Å in the linear ion (N_3^- angle 179.3°). In contrast, the receptor in the sulfate complex is protonated with the two sulfate anions coordinated by **23** neutralised by the charge on the four protonated bridgehead amine groups. The anions are located outside the receptor cavity and are bound by multiple hydrogen bonds to the amide and ammonium groups. The $\text{N}_{\text{amine}} \cdots \text{O}$ interactions range from 2.638 to 2.704 Å with

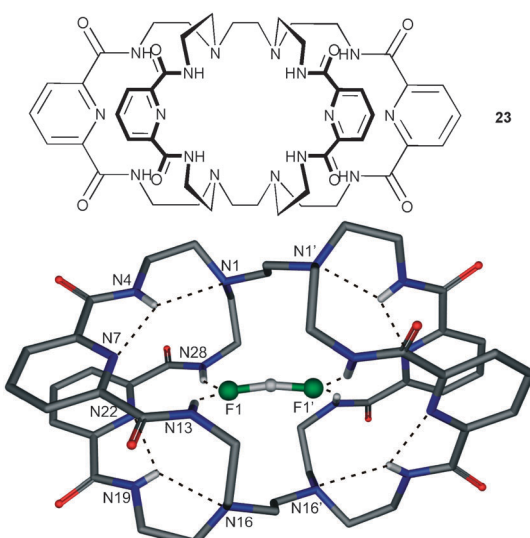
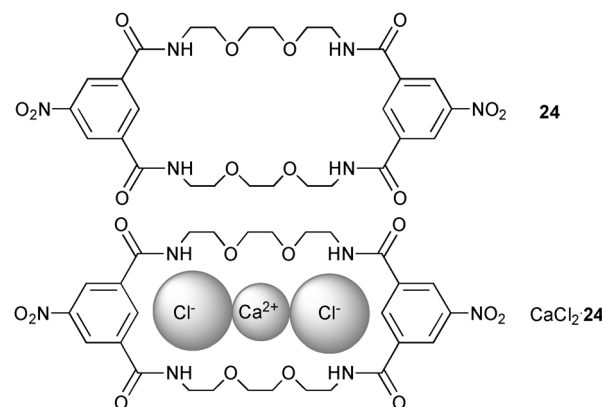


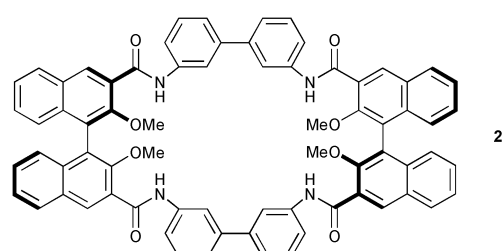
Fig. 4 X-Ray structure of $[(\text{FHF})_2\text{C}_2\text{H}_5](n\text{-Bu}_4\text{N})\cdot 3\text{H}_2\text{O}$ with selected atom labels and hydrogen bonds as dotted lines, tetrabutylammonium counter cations, co-crystallised H_2O molecules and non-acidic hydrogen atoms are omitted for clarity.

$\text{N}_{\text{amide}} \cdots \text{O}$ distances between 2.874 and 2.891 Å. In addition two co-crystallised water molecules are present, which act as hydrogen bonding bridges between the sulfate ions and the ligand ($\text{S}-\text{O} \cdots \text{O}_{\text{water}}$ interaction of 2.672 and 2.836 Å, $\text{NH} \cdots \text{O}_{\text{water}}$ distances 2.854 and 2.937 Å). Proton NMR titration experiments in $\text{DMSO}-d_6$ show preferential binding of FHF^- over N_3^- , H_2PO_4^- and CH_3COO^- by 23. A shift of the HF_2^- proton resonance from 15.4 to 17.5 ppm was observed upon complexation. The calculated stability constants employing a 1:1 binding mode results in a $\log K_a$ of 3.74 for FHF^- , 2.87 for H_2PO_4^- , 2.53 for N_3^- and 2.00 for AcO^- , and negligible binding for HSO_4^- , Cl^- , Br^- , I^- , NO_3^- , SCN^- and ClO_4^- .

Another extended amide based macrocycle has been employed by Lünig and co-workers to bind chloride as its calcium salt in a cascade-like complex.²² The 2 + 2 condensation of 5-nitroisophthaloyl dichloride and 1,8-diamino-3,6-dioxa-octane in THF results in macrocycle **24**. Both isophthalamide residues provide the binding pocket for anions where the four oxygen atoms of the diethylene glycol linker act as donor atoms for the coordination of the metal centre. Electrospray ionisation mass spec (ESI-MS) investigations give evidence for the coordination of chloride (molecular weight ($\text{Cl}\cdot\text{24}$)⁻ = 681.2, m/z observed = 681.2 (negative mode)) and the calcium salt ($\text{CaCl}\cdot\text{24}$)⁺ (m/z = 721.14, calc mass: 721.2). Quantitative ¹H NMR experiments of **24** in CDCl_3 with 5% $\text{DMSO}-d_6$ over an excess of $n\text{-Bu}_4\text{NCl}$, CaCl_2 , MgCl_2 and BaCl_2 , present as solids, show a pronounced shift of the amide protons in the case of $n\text{-Bu}_4\text{NCl}$ or CaCl_2 , only, illustrating the extraction and uptake of CaCl_2 over MgCl_2 and BaCl_2 into **24**.

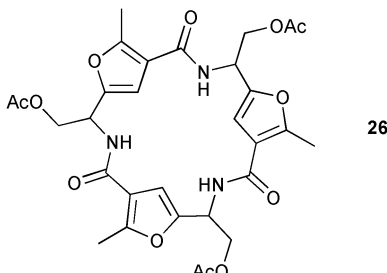


The chiral amide based macrocycle **25** has been synthesised and studied by the group of Pasini.²³ The receptor shows no particular interaction towards halide ions (Cl^- and Br^-) or towards numerous mono- and di-carboxylates, with exception of glutarate ($K_a = 30 \text{ M}^{-1}$, ^1H NMR titration in CDCl_3).

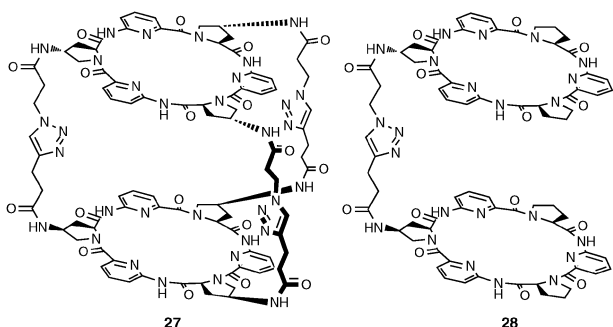


The authors explain this modest anion affinity with the rigid receptor structure and strong intermolecular $\text{NH}\cdots\text{O}$ hydrogen bonds.

Robina and co-workers have reported the synthesis and anion binding ability of furyl-cyclopeptide receptor **26**.²⁴ ESI-MS and ^1H NMR in CD_3CN studies demonstrate the formation of 1:1 complexes with chloride, acetate and cyanide. The calculated stability constants $K_a (\text{M}^{-1})$ show selectivity for chloride ($K_a = 16\,000$) over cyanide ($K_a = 1600$) and acetate ($K_a = 1000$) by the receptor.

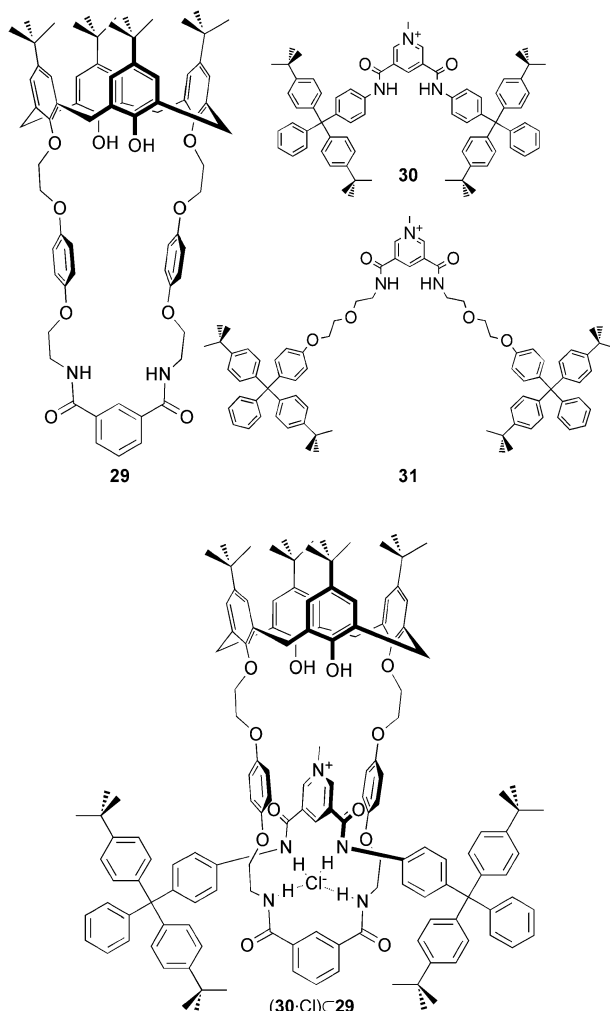


Kubik and co-workers conducted binding studies with sulfate for cyclopeptide based cages **27** and **28** in highly competitive solvents, such as $\text{H}_2\text{O}/\text{CH}_3\text{OH}$.²⁵ The results of isothermal titration calorimetry (ITC) experiments in $\text{H}_2\text{O}/\text{CH}_3\text{OH}$ mixture with water content between 35 and 65% are summarized in Table 4. A stability constant ($\log K_a$) of 5.70 for **27** and 4.96 for **28** in $\text{H}_2\text{O}/\text{CH}_3\text{OH}$ (1:1 v/v) reveals slightly enhanced binding upon increasing the number of linkers and subsequent higher preorganisation of **27**. After detailed analysis of the thermodynamic data (Table 4) the authors conclude that the additional linker stabilises a favourable arrangement of the two cyclopeptide rings. The results show that coordination of sulfate is entropically favourable but enthalpically disfavoured.



Amides have also been employed in the formation of anion templated interlocked molecular assembles. Beer and co-workers reported the first example of the calix[4]arene based rotaxane host for anion recognition.²⁶ The Cl^- -templated ring closure reaction of macrocycle **29** with isophthaloyl chloride in the presence of threads **30** and **31** results in rotaxanes $(\mathbf{30}\cdot\text{Cl})\subset\mathbf{29}$ and $(\mathbf{31}\cdot\text{Cl})\subset\mathbf{29}$. The structure of the interlocked assembly is confirmed by the X-ray crystal structure of the calix[4]arene based rotaxane anion host. The Cl^- ion is bound by $\text{NH}\cdots\text{Cl}$ interactions between 3.222 and 3.544 Å, with the amide groups of the macrocycle and the thread. In addition close aryl $\text{CH}\cdots\text{Cl}$ contacts between 3.276 and 3.366 Å are observed. Following the removal of the chloride anion template, the anion binding properties of the resulting rotaxanes $(\mathbf{30}\cdot\text{PF}_6)\subset\mathbf{29}$ and

$(\mathbf{31}\cdot\text{PF}_6)\subset\mathbf{29}$ have been studied by ^1H NMR titration experiments in $\text{CDCl}_3/\text{CD}_3\text{OD}$ (1:1). The calculated binding constants $K_a [\text{M}^{-1}]$ show preferred uptake of Cl^- ($K_a = 3820$) over Br^- ($K_a = 1560$), H_2PO_4^- ($K_a = 1140$) and AcO^- ($K_a = 530$) by rotaxane $(\mathbf{30}\cdot\text{PF}_6)\subset\mathbf{29}$. Significantly reduced binding constants were found for rotaxane $(\mathbf{31}\cdot\text{PF}_6)\subset\mathbf{29}$ ($K_a [\text{M}^{-1}] = 650$ for Cl^- , 630 for Br^- , 420 for H_2PO_4^- and 140 for AcO^-), which incorporates a conformationally flexible thread **31**. Comparable binding experiments of the thread **31** only show preferred binding of H_2PO_4^- ($K_a = 710$) over Br^- ($K_a = 440$), Cl^- ($K_a = 300$) and AcO^- ($K_a = 160$).



The novel thiazine-1,1-dioxide based receptors **32** and **33**²⁷ were employed by Wisner and co-workers as hosts for anions.²⁷ Proton NMR titrations in acetone- d_6 show 1:1 (L:A) stoichiometry in solution and higher stability constants for anion complexes with **32** than for receptor **33**, presumably due to

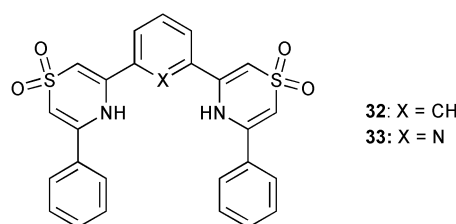


Table 4 Stability constants $\log K_a$, Gibbs free energies ΔG , enthalpies ΔH and entropies $T\Delta S$ of binding Na_2SO_4 to **27** and **28** in $\text{H}_2\text{O}/\text{CH}_3\text{OH}$ of varying ratios at 298 K

H ₂ O : CH ₃ OH	27			28		
	35 : 65	50 : 50	65 : 35	35 : 65	50 : 50	65 : 35
$\log K_a^a$	6.34 (± 0.02)	5.70 (± 0.03)	5.19 (± 0.05)	5.67 (± 0.02)	4.96 (± 0.05)	4.26 (± 0.02)
$\Delta G [\text{kJ mol}^{-1}]^a$	-36.2 (± 0.1)	-32.6 (± 0.2)	-29.6 (± 0.3)	-32.3 (± 0.1)	-28.4 (± 0.3)	-24.3 (± 0.1)
$\Delta H [\text{kJ mol}^{-1}]^a$	13.3 (± 0.1)	10.1 (± 0.1)	6.9 (± 0.3)	-12.4 (± 0.1)	-13.5 (± 0.3)	-11.8 (± 0.2)
$T\Delta S [\text{kJ mol}^{-1}]^a$	49.5 (± 0.1)	42.7 (± 0.2)	36.5 (± 0.1)	19.9 (± 0.2)	14.9 (± 0.5)	12.5 (± 0.3)

^a Standard deviations of at least three independent measurements are specified in brackets.

the repulsion of the anionic guest by the lone pair of the pyridine nitrogen. The binding of tetrabutylammonium chloride by **32** includes a much weaker 2:1 (L:A) component. The order of anion affinity for **32** is $\text{Cl}^- (K_{21} = 300 \text{ M}^{-1}, K_{11} = 59\,000 \text{ M}^{-1})$ over $\text{AcO}^- (K_a = 12\,500 \text{ M}^{-1})$, $\text{H}_2\text{PO}_4^- (K_a = 540 \text{ M}^{-1})$, $\text{Br}^- (K_a = 380 \text{ M}^{-1})$, $\text{HSO}_4^- (K_a = 220 \text{ M}^{-1})$ and $\text{I}^- (K_a = 53 \text{ M}^{-1})$. Whereas **33** shows a preferred binding of $\text{AcO}^- (K_a = 480 \text{ M}^{-1})$ over $\text{H}_2\text{PO}_4^- (K_a = 360 \text{ M}^{-1})$, $\text{Cl}^- (K_a = 300 \text{ M}^{-1})$, $\text{HSO}_4^- (K_a = 130 \text{ M}^{-1})$ and $\text{Br}^- (K_a = 83 \text{ M}^{-1})$.

Urea containing receptors

Urea based receptors have proven very effective anion hosts, particularly in the recognition of oxo-anions. Tris-urea receptor **34** has recently been reported by Wu and co-workers for the complexation of tetrahedral oxo-anions such as phosphate and sulfate.²⁸ Single crystals, obtained from a DMSO/25% water solution of *n*-Bu₄NH₂PO₄ and **34**, revealed deprotonation of the anion upon coordination by two ligand molecules. The urea groups chelate the anion on the edge of the tetrahedron and form twelve N-H···O hydrogen bonds with N···O distances between 2.752 and 2.901 Å. Proton NMR studies in DMSO-*d*₆/25% water in the presence of PO_4^{3-} (as Na⁺ salt) and Et₃N show the same 2:1 (L:A) stoichiometry in solution. The addition of H_3PO_4 or HClO_4 results in proton transfer to the coordinated anion and subsequently complex dissociation. Extended NMR studies show that this process is reversible upon addition of Et₃N (Fig. 5). The same reversible binding of the deprotonated anion was observed for SO_4^{2-} , whilst HSO_4^- was not coordinated. UV-Vis titration experiments in DMSO/25% water were used to assess stability constants of the formed complexes. Fitting of the titration curve to a 2:1 (L:A) model results in $\log K_{11} = 5.0$ and $\log K_{21} = 12.0$ for PO_4^{3-} (as Na⁺ salt). Job plot experiments reveal a 1:1 binding mode of SO_4^{2-} (as the tetrabutylammonium salt) under comparable experimental conditions. The calculated binding constant in this case was $\log K_a = 4.72$.

The strong affinity for carbonate ions of the known pentafluorophenyl-tren-based receptor **35**²⁹ has been demonstrated by Ghosh and co-workers.³⁰ Aerial CO₂ is fixed in basic DMSO solutions and the resulting carbonate complex of **35** crystallised as 2:1 (L:A) complex. The anion is coordinated via sixteen N-H···O bonds from the urea groups with N···O distances between 2.705 and 3.346 Å. A closer examination reveals that thirteen out of the sixteen hydrogen bonds are in the strong hydrogen bonding interaction region with N···O distances <3.2 Å and N-H···O angles >140°. Proton NMR titration experiments of **35** with tetrethylammonium bicarbonate

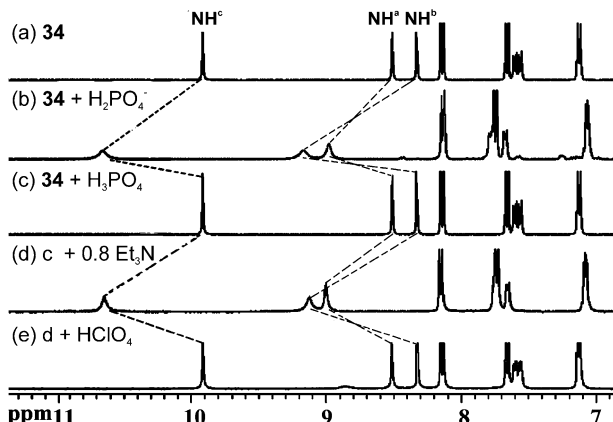
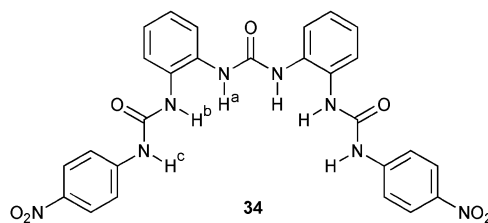
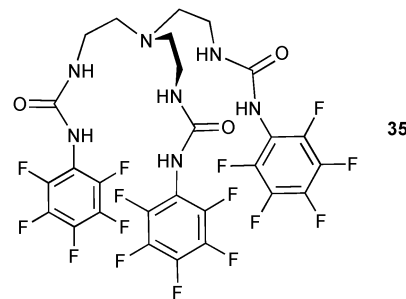


Fig. 5 $\text{HClO}_4/\text{Et}_3\text{N}$ modulated reversible binding of phosphate by **34** in DMSO-*d*₆/25% water (H_2PO_4^- added as tetrabutylammonium salt, H_3PO_4 as DMSO-*d*₆ solution diluted from 85% H_3PO_4). *Chem. Commun.* 2010, **46**, 5376–5378. Reproduced with permission of The Royal Society of Chemistry.

show the formation of the 2:1 (L:A) complex in solution with a stability constant $\log \beta_{21}$ of 4.04. The authors demonstrate further that the free receptor **35** can be regenerated and collected by filtration upon addition of CH₃OH/water (1:4) to the complex $[\text{CO}_3^{2-}\text{---}35]^{2-}$.



The same group has reported the first example of $(n\text{-Bu}_4\text{N}^+)_2\text{SO}_4$ bound as an ion pair by the pentafluorophenyl tripodal host **36** in polar solvents and in the solid state (Fig. 6).³¹

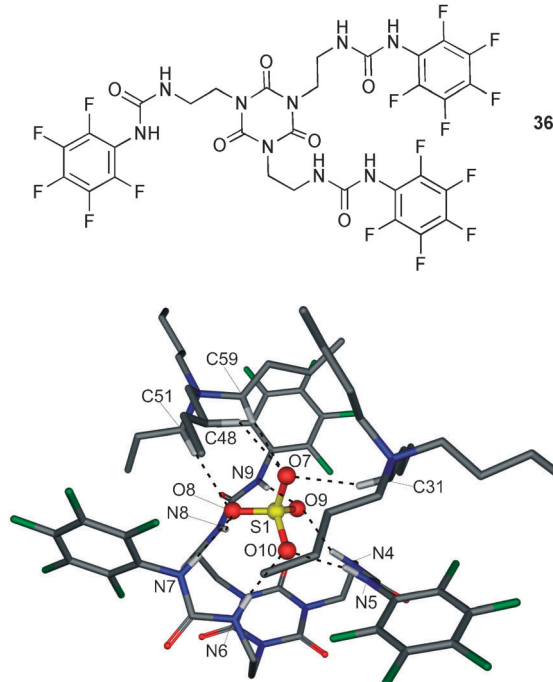


Fig. 6 The X-ray structure of $((n\text{-Bu}_4\text{N})_2\text{SO}_4)\cdot\text{36}$ with selected atom labels and hydrogen bonds as dotted lines, co-crystallised solvent molecules and non-acidic hydrogen atoms omitted for clarity.

The cyanuric acid based receptor coordinates the sulfate ion *via* six N–H···O hydrogen bonds with N···O distances between 2.733 and 2.994 Å. On the exposed side the anion is bound by C–H···O interaction towards the tetrabutylammonium counterion. The C···O distances range from 3.304 to 3.523 Å. Extensive 2-dimensional diffusion ordered spectroscopy (2D-DOSY) and proton NMR studies show the presence of the ion pair complex in DMSO-*d*₆ at 298 K. Where comparable experiments at 333 K point to a separation of $[\text{SO}_4\cdot\text{36}]^{2-}$ and the $n\text{-Bu}_4\text{N}^+$ cation, which reassemble after the solution is cooled down to 298 K. However no evidence for the coordination of an ion pair was observed with the tetrabutylammonium salts of dihydrogen phosphate, acetate or chloride at 298 K. Proton NMR titrations in DMSO-*d*₆ show the strong binding of sulfate ($\log K_a = 5.74$) over dihydrogen phosphate ($\log K_a = 4.39$), acetate ($\log K_a = 3.41$) and chloride ($\log K_a = 3.38$) in 1:1 binding stoichiometry.

Moyer and co-workers³² have carried out extensive solution studies with receptor **37** which binds sulfate, selenate, sulfite and carbonate strongly forming a 2:1 (L:A) capsule upon the coordination of $\text{Mg}(\text{H}_2\text{O})_6^{2+}$.³³ These types of capsule often do not persist in aqueous solution. The determination of the solubility product K_{sp} in borax buffered aqueous solution by inductively coupled plasma (ICP) determinations of the magnesium concentration give a value K_{sp} of 2.0×10^{-17} at 25 °C. Comparable experiments at 35, 45 and 52 °C result in $\Delta H^\circ = -99.1 \text{ kJ mol}^{-1}$ and $T\Delta S^\circ = -3.8 \text{ kJ mol}^{-1}$ for the sulfate complex $[\text{SO}_4\cdot\text{37}]_2\text{Mg}(\text{H}_2\text{O})_6$, K_{sp} of 5.5×10^{-16} with $\Delta H^\circ = -108.5 \text{ kJ mol}^{-1}$ and $T\Delta S^\circ = -21.4 \text{ kJ mol}^{-1}$ for the selenite complex $[\text{SeO}_4\cdot\text{37}]_2\text{Mg}(\text{H}_2\text{O})_6$ and for the sulfite complex $[\text{SO}_3\cdot\text{37}]_2\text{Mg}(\text{H}_2\text{O})_6$ $K_{sp} = 6.6 \times 10^{-16}$, $\Delta H^\circ = -64.6 \text{ kJ mol}^{-1}$ and $T\Delta S^\circ = 22.0 \text{ kJ mol}^{-1}$ were obtained. Further, the group carried out potentiometric titrations to

obtain the protonation constants of **37** and stability constants of the SO_4^{2-} binding. The four observed protonation steps of **37** (in 75 mM KNO_3) correspond to the three pyridine groups and the tertiary amine group with pK_a values of 3.58, 4.37, 5.23 and 7.11. The stability constants for a 1:1 binding mode of the protonated species $\text{H}_n\text{37}^{(n+)}$ ($n = 2-4$) for sulfate are $\log K_a = 1.8$ for $\text{SO}_4\subset\text{H}_2\text{37}$, $\log K_a = 2.45$ for $\text{SO}_4\subset\text{H}_3\text{37}^+$ and $\log K_a = 2.62$ for $\text{SO}_4\subset\text{H}_4\text{37}^{2+}$. These values are comparable to the stability constants of the SO_4^{2-} complexes observed for the mono-, di-, and triprotonated parental tren ligand ($\log K_a$ for $\text{SO}_4^{2-} = 1.66$ (mono-), 1.72 (di-), and 2.22 (triprotonated), respectively),³⁴ and give evidence for the dominance of the electrostatic effect in anion recognition in aqueous media, as observed in crystal structure of $([\text{SO}_4\subset\text{H}_4\text{37}] \text{SO}_4)_2$ (Fig. 7).

Yatsimirsky and co-workers have compared the anion binding abilities of thiocalix[4]arenes functionalised with thiourea **38** and urea **39** moieties and with model compounds **40** and **41**.³⁵ The crystal structures of all receptors reveal the *cis*-orientation of the urea N–H groups in both ligands where the N–H groups in the thiourea derivatives are present in the *trans*-orientation in the solid state. Nevertheless, spectrophotometric titrations in CHCl_3 show a stronger binding of the anion by thiourea derivatives **38** and **40** over the urea receptors **39** and **41**. Further, the thiocalix[4]arene receptors give higher stability constants than model compounds **40** and **41** due to the greater number of urea/thiourea groups. Overall a preferred binding of acetate over fluoride, dihydrogen phosphate and chloride was observed as shown in Table 5.

A series of urea functionalised cyclophanes (**42–45**) was prepared by Rissanen and co-workers.³⁶ Crystal structures of the tetramethylphosphonium chloride and phosphoric acid complexes of ligand **44** illustrate the anion binding ability of these compounds. The chloride ion is bound by one urea

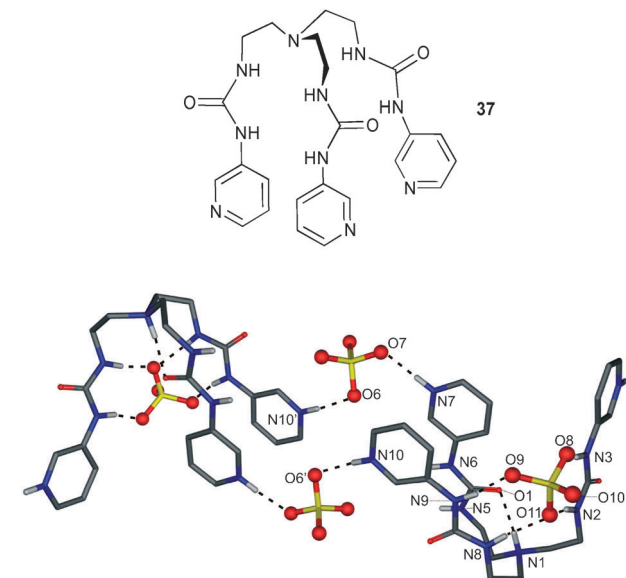
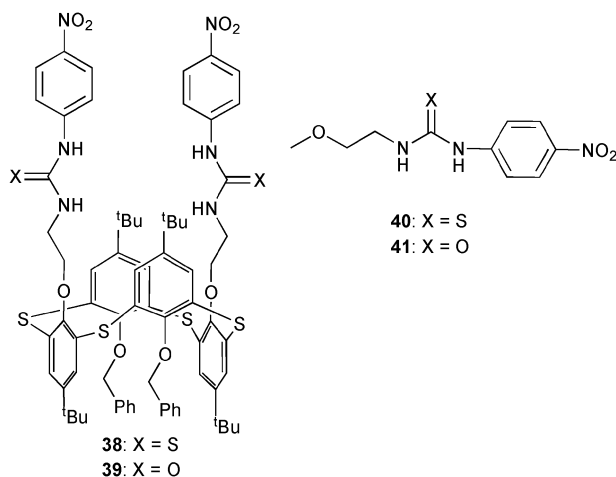


Fig. 7 Schematic draw of X-ray structure of $([\text{SO}_4\subset\text{H}_4\text{37}] \text{SO}_4)_2$ with selected atom labels and hydrogen bonds as dotted lines, co-crystallised solvent molecules and non-acidic hydrogen atoms omitted for clarity.

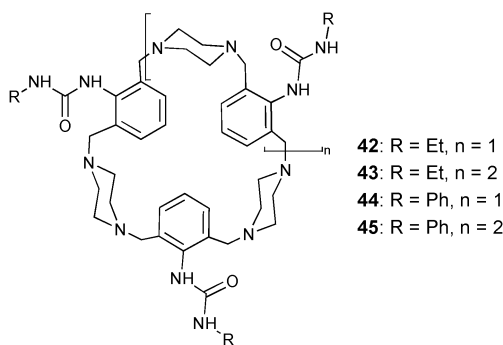
Table 5 Stability constants ($\log K_a$) in CHCl_3 of receptors **38–41** at 298 K.^a Anions added as their tetrabutylammonium salts

Anion	38		39 $\log K_{11}$	40 $\log K_{11}$	41 $\log K_{11}$
	$\log K_{11}$	$\log K_{12}$			
Cl^-	3.87	<1.7	3.17	4.26	3.52
F^-	4.57	2.00	3.86	4.42	3.90
AcO^-	5.30	3.32	4.46	4.65	4.01
H_2PO_4^-	4.00		4.58	4.30	3.88

^a Errors of the K_a values are not more than $\pm 10\%$ (± 0.04 in $\log K_a$).

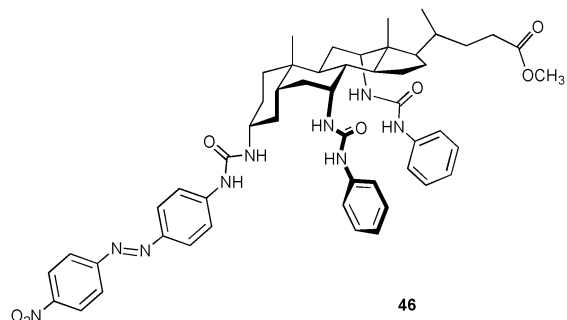


N–H···Cl interaction (N···Cl distance of 3.307 Å) from the ligand and two O–H···Cl interactions from co-crystallised CH_3OH (O···Cl distances of 3.026 and 3.200 Å). The treatment of **44** with phosphoric acid and subsequent crystallisation results in the triprotonated ligand, with one ammonium group present in each of the three piperazine linkers, coordinated to a hydrogen bonded H_2PO_4^- – HPO_4^{2-} anion pair. Two P–O–H···O=P hydrogen bonds (O···O distances of 2.583 and 2.679 Å) link the anion pair. The H_2PO_4^- anion is bound by one urea N–H···O interaction (N···O distance of 2.881 Å) to the ligand, whereas the HPO_4^{2-} anion is coordinated by the ammonium groups of three different ligands with N···O distances between 2.590 and 2.668 Å.

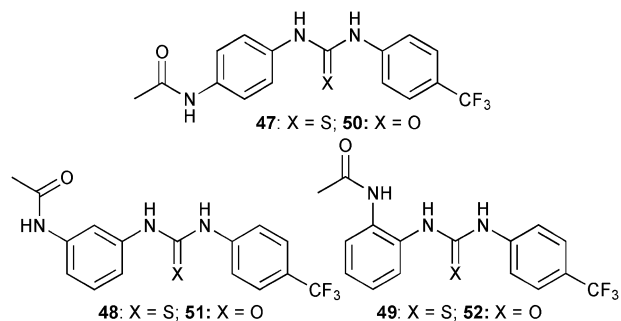


Davis and co-workers employed steroid-based receptor **46** for the recognition of unprotected amino acids.³⁷ Proton NMR titration experiments in $\text{DMSO}-d_6$ reveal a preferred binding of L-tryptophan (Trp) over D-Trp in a 1:1 binding mode.

The calculated stability constants K_a are 480 M^{-1} for L-Trp and 260 M^{-1} for D-Trp, whereas the interactions towards D/L-Phe (phenylalanine), D/L-Leu (leucine) and D/L-Ala (alanine) are too weak to determine stability constants using this method. NOESY and computer simulation (Density functional theory (DFT) (B3LYP/6-31G(d)) studies of the complexes [L-Trp]–**46**] and [D-Trp]–**46**] suggest the presence of CH–π interactions between both the L- and D-Trp guest and the receptor. Thus, differences in the hydrogen bond pattern between the carboxylate group of the two enantiomers and the host presumably results in the observed enhanced binding of the L-enantiomer.



Gunnlaugsson and co-workers³⁸ have synthesised a series of diaryl thiourea receptors **47–49** with acetamide moieties in the *para*-, *meta*- and *ortho*-positions and compared their anion binding properties to the known urea counterparts **50–52**.³⁹ UV-Vis titration experiments in CH_3CN showed a shift in the absorption band upon addition of the tetrabutylammonium salts of H_2PO_4^- , AcO^- , $\text{HP}_2\text{O}_7^{3-}$, F^- and Cl^- . The dominant species for all receptors is a 1:2 (L:A) complex. The expected 1:1 complex due to cooperative binding of the amide and thiourea group in **49** (*ortho*) was not obtained. However 1:1 complexes were formed by the urea counterpart **52**.³⁹ In general the ligands bind acetate more strongly than hydrogen pyrophosphate, fluoride, dihydrogen phosphate and chloride. A summary of the stability constants is listed in Table 6. Compared to their urea counterparts, the thioureas **47** and **48** show a higher anion affinity than **50** and **51**.



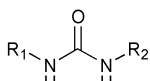
The remote electronic effect on the binding of F^- and AcO^- by the urea group was studied by Ghosh and co-workers.⁴⁰ Density functional theory (B3LYP/6-311+G**) studies of $\text{NH}\cdots\text{F}$ and $\text{NH}\cdots\text{O-COCH}_3$ hydrogen bond lengths in the 1:1 complex of **53–61** reveal shorter distances for the NH binding side adjacent the substituent containing the electron withdrawing nitro or trifluoromethane groups. Closer examination of the positional isomers **58–60** show binding in the

Table 6 Stability constants of **47–49** for 1:1 and 1:2 (L:A) binding mode in CH₃CN at room temperature.^a Anions added as their tetrabutylammonium salts

Anion	47		48		49	
	log K_{11}	log K_{12}	log K_{11}	log K_{12}	log K_{11}	log K_{12}
AcO ⁻	6.31 (± 0.17)	5.12 (± 0.37)	5.61 (± 0.11)	2.93 (± 0.23)	5.46 (± 0.05)	3.44 (± 0.28)
F ⁻	4.84 (± 0.1)	4.3 (± 0.28)	5.39 (± 0.07)	3.71 (± 0.25)	5.30 (± 0.05)	3.47 (± 0.21)
H ₂ PO ₄ ⁻	5.34 (± 0.24)	4.66 (± 0.46)	4.42 (± 0.19)	4.945 (± 0.39)	4.81 (± 0.01)	4.60 (± 0.14)
HP ₂ O ₇ ³⁻	5.76 (± 0.007)	1.52 (± 0.13)	5.46 (± 0.15)	2.77 (± 0.30)	6.33 (± 0.06)	2.13 (± 0.19)
Cl ⁻	4.1 (± 0.13)	3.26 (± 0.31)	3.69 (± 0.05)	—	3.20 (± 0.07)	2.0 (± 0.01)

^a Standard deviations are specified in brackets.

order **60** > **59** > **58** for both anions highlighting the important role of the relative positions of the substituents.



53: R₁ = H, R₂ = H

58: R₁ = o-NO₂-C₆H₄, R₂ = Ph

54: R₁ = Ph, R₂ = H

59: R₁ = m-NO₂-C₆H₄, R₂ = Ph

55: R₁ = Ph, R₂ = Ph

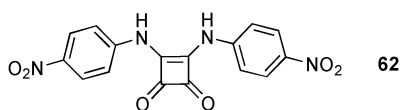
60: R₁ = p-NO₂-C₆H₄, R₂ = Ph

56: R₁ = p-CH₃-C₆H₄, R₂ = Ph

61: R₁ = p-NO₂-C₆H₄, R₂ = p-NO₂-C₆H₄

57: R₁ = p-CF₃-C₆H₄, R₂ = Ph

Fabbrizzi and co-workers have synthesised simple squaramide receptor **62**⁴¹ and compared its anion binding properties to those of known urea receptor **61**.⁴² Spectrophotometric titrations with tetraalkylammonium salts were performed in CH₃CN to assess the stability constants. A 1:1 binding mode was found for the studied anions, except for F⁻ and CH₃COO⁻. These anions showed more complex behaviour and the authors suggest deprotonation of the receptor and subsequent formation of hydrogen bonded anion pairs ([F-H···F]⁻ and [CH₃COO-H···OOCCH₃]⁻, respectively) in the presence of excess of these anions, as observed previously.^{42,43} Overall, both receptors show decreasing complex stability along the series F⁻ > Cl⁻ > Br⁻ > I⁻ and CH₃COO⁻ > H₂PO₄⁻ > NO₂⁻ > HSO₄⁻ > NO₃⁻. The observed stability constants are higher for the squaramide receptor **62** than the urea analogue **61** (Table 7), except for HSO₄⁻ and AcO⁻. Interestingly, the

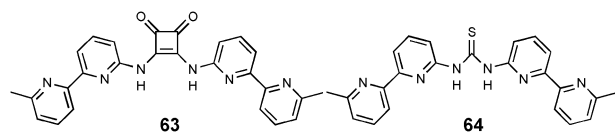
**Table 7** Stability constants log K_a of **61** and **62** for 1:1 binding mode in MeCN at 298 K.^a Anions added as their tetraalkylammonium salts

Anion	61	62
F ⁻	7.4(1)	8.0(2)
Cl ⁻	4.55(1)	6.05(2)
Br ⁻	3.22(3)	4.70(1)
I ⁻	<2	3.51(2)
NO ₃ ⁻	3.65(5)	3.68(1)
NO ₂ ⁻	4.33(1)	4.75(2)
HSO ₄ ⁻	4.26(1)	4.02(3)
H ₂ PO ₄ ⁻	5.37(1)	5.42(7)
AcO ⁻	6.61(1)	6.5(2)

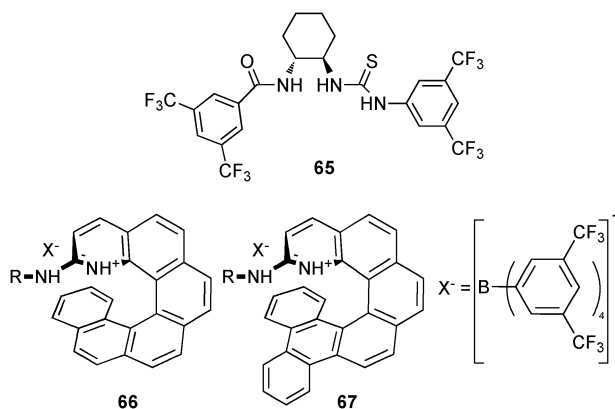
^a The standard deviations are given parentheses.

enhanced affinity of **62** towards the halide ions is more pronounced than for the oxo-anions. The authors point out the presence of additional C-H···anion interactions from the C_α aryl group in the crystal structure of the Cl⁻ and Br⁻ complexes of **62** to explain this behaviour. The observed C···Cl distances are 3.784 and 3.862 Å, whereas the C···Br distances are 3.868 and 3.930 Å.

In a similar fashion Al-Sayah and Branda have compared the anion binding ability of thiourea and squaramide groups.⁴⁴ Proton NMR titration studies with tetrabutylammonium acetate in CD₃CN/CDCl₃, fitted to a 1:1 binding mode, reveal a higher stability constant for the squaramide receptor **63** ($K_a = 7390 \text{ M}^{-1}$) than for the thiourea **64** ($K_a = 5790 \text{ M}^{-1}$). Calorimetric titration studies show that the binding is both enthalpically and entropically driven. An enthalpy change ΔH of $-505 \text{ cal mol}^{-1}$ and entropy change ΔS of $8.7 \text{ cal mol}^{-1} \text{ K}^{-1}$ were calculated for **64** in DMSO, whereas a ΔH of $-2209 \text{ cal mol}^{-1}$ and a ΔS of $10.3 \text{ cal mol}^{-1} \text{ K}^{-1}$ were obtained for **63** in CH₃CN/CHCl₃.



The application of a series of chiral thiourea-amide ligands such as compound **65** as co-catalyst in combination with 4-(dimethylamino)-pyridine was investigated by Seidel and co-workers.⁴⁵ The authors observed significantly improved discrimination rates between the reaction rate of faster and slower reacting enantiomers (s-factor) of up to 56 times for the conversion of various propargylic amines with benzoic anhydride.



Another series of catalysts for asymmetric introduction based on the formation of hydrogen bonds have been reported by Takenaka and co-workers.⁴⁶ The 2-aminopyridinium ion based catalysts of the general type **66** and **67** were tested against the addition of 4,7-dihydroindole to nitroalkenes.

Amine, ammonium and pyridinium based receptors

Anion binding by amine based receptors requires protonation of the host. Thus, the receptor's binding ability is pH dependent and can be tuned by the substituents close to the ammonium groups and the type of amine present in the molecule (*e.g.* primary, secondary, tertiary). The determination of the protonation and stability constants of triphosphate with a series of tripodal tris(tetraamine) ligands described by Tripier and co-workers illustrates this strikingly.⁴⁷ The protonation constants were investigated by potentiometric titrations in aqueous solution at 25 °C and summarised in Table 8. The calculated species distribution diagrams (Fig. 8) illustrate the presence of the higher protonated species for **68**, which contains primary, secondary and tertiary ammonium groups, over **69** and **70**. The last (**70**) contains tertiary ammonium groups only and is present as $\text{H}_3\text{70}^{3+}$, $\text{H}_4\text{70}^{4+}$ and $\text{H}_5\text{70}^{5+}$ at significant lower pH only. For example at pH 6 the major species for **70** is $\text{H}_3\text{70}^{3+}$, for **69** $\text{H}_6\text{69}^{6+}$ and for **68** $\text{H}_6\text{68}^{6+}$ and $\text{H}_7\text{68}^{7+}$ are present at approximately 50% each. At pH 3 the major species of **70** is $\text{H}_5\text{70}^{5+}$, where **69** is

Table 8 Logarithmic protonation constants of **68–70** (H_2O , $I = 0.1 \text{ M}$ (NaCl), $T = 25^\circ\text{C}$)

Equilibrium ^a	68 ^b	69 ^b	70 ^b
$\text{L} + \text{H}=\text{LH}$	10.55(3)	11.00(1)	—
$\text{LH} + \text{H}=\text{LH}_2$	9.85(2)	9.80(1)	—
$\text{LH}_2 + \text{H}=\text{LH}_3$	9.38(2)	9.21(1)	—
$\text{LH}_3 + \text{H}=\text{LH}_4$	8.71(3)	8.30(1)	4.60(1)
$\text{LH}_4 + \text{H}=\text{LH}_5$	8.26(1)	8.20(1)	4.26(1)
$\text{LH}_5 + \text{H}=\text{LH}_6$	6.63(2)	6.92(2)	3.23(2)
$\text{LH}_6 + \text{H}=\text{LH}_7$	5.93(2)	3.00(2)	
$\text{LH}_7 + \text{H}=\text{LH}_8$	4.30(2)		
$\text{LH}_8 + \text{H}=\text{LH}_9$	4.25(2)		

^a Charges omitted for clarity. ^b Values in parentheses are standard deviation in the last significant digit.

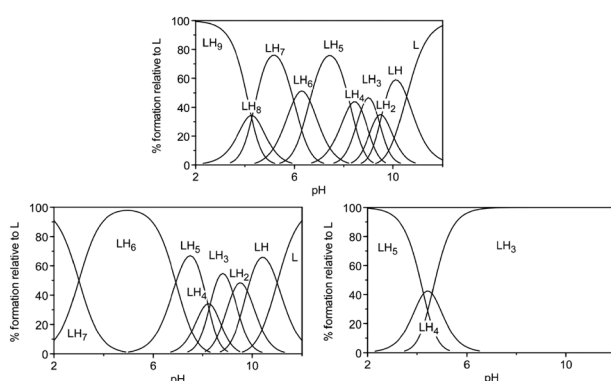


Fig. 8 Species distribution diagrams for **68** (top), **69** (bottom left) and **70** (bottom right) as a function of pH. Tripier *et al.*, *J. Org. Chem.* 2010, 5380–5390. Reproduced with permission of Wiley-VCH Verlag GmbH & Co. KGaA, Weinheim.

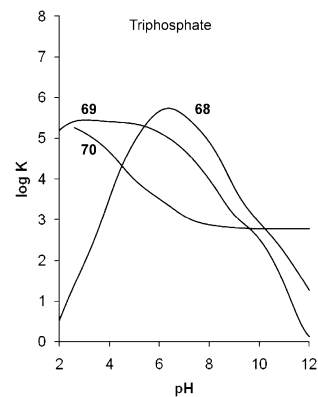
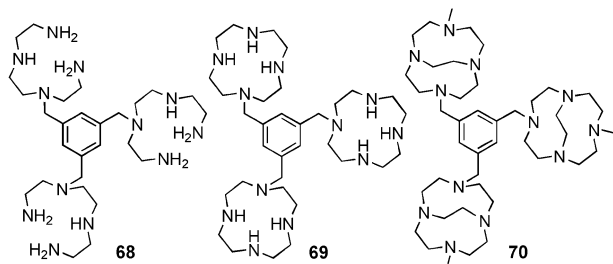
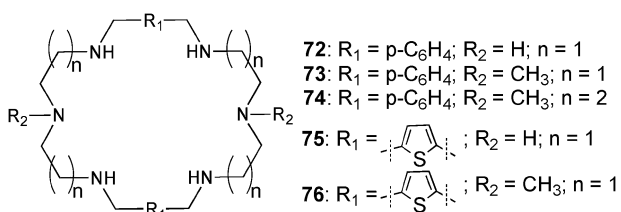


Fig. 9 Logarithms of the conditional constant for triphosphate versus pH for **68**, **69** and **70**. Tripier *et al.*, *Eur. J. Org. Chem.*, 2010, 5380–5390. Reproduced with permission of Wiley-VCH Verlag GmbH & Co. KGaA, Weinheim.

present as $\text{H}_7\text{69}^{7+}$ and $\text{H}_6\text{69}^{6+}$ (approximately 50% each) and **68** as $\text{H}_9\text{69}^{9+}$. Due to this different level of protonation a comparison of the triphosphate complex stability $\log K_{\text{dh}}$ is not practical and the authors utilise a plot of the logarithmic conditional constants $\log K$ over pH to illustrate the order of anion binding at a given pH (Fig. 9).⁴⁷ For example, the affinity towards triphosphate at pH 6 was found to decrease from **68** > **69** > **70** whereas at pH 3 the stability constants increase in the order is **70** < **68** < **69**.



Numerous hexa-aza-macrocycles (**72–76**) containing secondary and tertiary ammonium groups for binding halides and oxo-anions, have been described by Hossain and co-workers.^{48–52} Proton NMR titrations carried out in D_2O with the hexatosylated salt of **73** at pH 2.1⁴⁹ and the tetratosylated salt of **74** at pH 1.7⁴⁸ show a selectivity for sulfate over perchlorate, nitrate and halides. The binding studies fitted to a 1 : 1 binding mode result in stability constants $K_a [\text{M}^{-1}]$ with **73** and **74** of 3600 and 580 for sulfate, >20 and 120 for perchlorate, 120 and 40 for nitrate, 15 each for chloride, 90 and 20 for bromide and 25 and 30 for iodide, respectively. Crystal structures of the sulfate complexes of *p*-xylyl⁴⁹ (**72**) and 1,5-thiophene⁵⁰ (**76**) linked macrocycles agree with the 1 : 1 binding stoichiometry. The anion is bound by N–H···O and C–H···O interactions of the ammonium groups and the ligand backbone with N···O



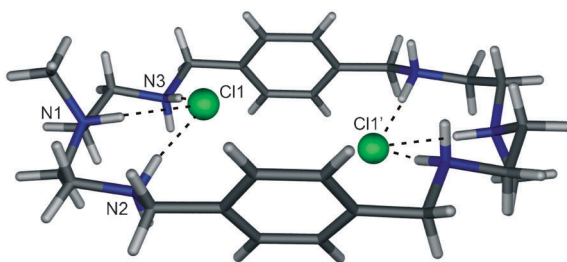


Fig. 10 Crystal structure of $\text{Cl}_6\subset\text{H}_6\text{73}$ with selected atom labels and hydrogen bonds as dotted lines, Cl^- atoms located in ligand periphery, co-crystallised solvent molecules and non-interacting hydrogen atoms omitted for clarity.

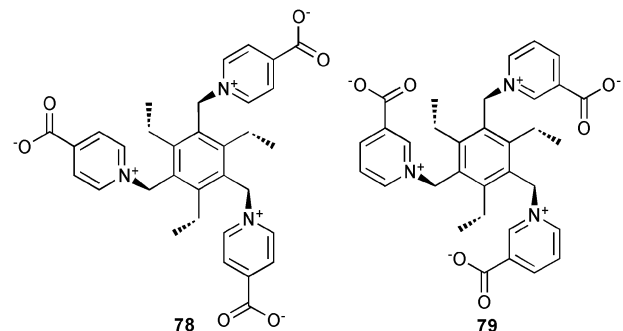
distance between 2.688 and 3.366 Å and $\text{C}\cdots\text{O}$ distance between 3.100 and 3.207 Å.

In contradistinction to these results, the perchlorate^{48,52} complex of **72**, **74** and **75** as well as the chloride⁵¹ complexes of **73** were isolated with a 1:2 ligand to anion ratio with the anion bound inside the macrocycle. The latter example is a complex with complete encapsulation of two chloride anions within the protonated aza-macrocyclic **73** (Fig. 10).⁵¹ The intramolecular chloride-chloride distance is 4.433 Å and each of the chloride atoms is bound by three hydrogen bonds with $\text{NH}\cdots\text{Cl}$ distances between 3.067 and 3.146 Å.

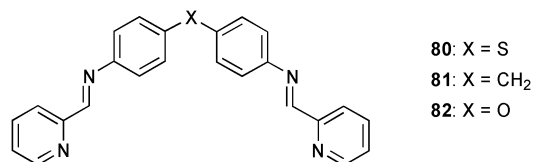
In a related octa-protonated aza-cryptand, compound **77**, an unusual bridged binding mode of three nitrate anions was observed in the complex in the solid state (Fig. 11).⁵³ The three anions are located in close proximity in a triangular arrangement between the two tertiary bridgehead N–H groups and each nitrate anion is coordinated *via* one oxygen atom. The intermolecular $\text{NH}\cdots\text{O}$ distances are between 3.099 and 3.370 Å and show no particular order. The bound O atoms of the three nitrate anions are separated by 2.494, 2.602 and 3.000 Å. Proton NMR titrations in D_2O at pH 3.3 revealed a 1:1 binding mode in solution.⁵⁴ The calculated stability constant are $\log K_a = 4.23$ for NO_3^- and $\log K_a = 3.75$ for NO_2^- .

To avoid the formation of a highly charged hosts for the binding of anions in water Steed and co-workers⁵⁵ have reported the synthesis of two tripodal zwitterionic receptors **78** and **79** based on the combination of pyridinium and carboxylate subunits on a 2,4,6-triethylbenzene platform. Both receptors show no affinity towards NaCl , NaI , NaAcO , MgATP and $\text{K}[\text{Al}(\text{oxalate})]$ in NMR titration experiments in

high competitive solvents such as D_2O and CD_3OD . However, the PF_6^- complex ($\text{HPF}_6\subset\text{79}$) shows moderate binding of chloride ($\log K_{11} = 2.17$) and bromide ($\log K_{11} = 1.98$) in $\text{DMSO}-d_6$. In contrast, the *para* isomer **78** was not isolated as a halide-free receptor, due to the strong coordination of bromide in the self-assembled capsule. The mutual interdigitation of the six pendant arms of two ligand molecules in a sandwiched arrangement of the carboxylate functions of one ligand between the pyridinium groups of the other results in the formation of a stable capsule such that even the addition of AgPF_6 was not sufficient to remove bromide completely.



An example of anion controlled self-assembly of Cu(II) complexes of the simple bis-pyridylimine ligands **80**–**82** has been reported by Gloe and co-workers.⁵⁶ Crystallisation in the presence of SO_4^{2-} results in the formation of hexanuclear circular *meso*-helicates with all three ligands, wherein the coordination sphere of the metal centres are saturated by a chelating interaction to the anion. The observed $\text{Cu}–\text{O}_{\text{ sulfate}}$ distances range from 1.959 to 2.792 Å. The authors observed the formation of non-cyclic triple helicate complexes when SO_4^{2-} was replaced with ClO_4^- or NO_3^- and used the different coordination mode of the metal centre as strong evidence for influence of the nature of the anion on the topology of the formed assembly.



Pyrrole based anion receptors

Pyrrole based anion receptors have been shown to be effective and selective receptors for a variety of anionic species.^{57–59} The anion binding ability of macrocyclic **83** and open chain dipyrrolylmethane receptor **84** were investigated by Mani and co-workers.⁶⁰ Proton NMR titration experiments in acetone- d_6 reveal a strong binding for F^- ($K_a > 10^4 \text{ M}^{-1}$) over Cl^- ($K_a = 4763 \text{ M}^{-1}$) and Br^- ($K_a = 317 \text{ M}^{-1}$) by **83** in a 1:1 binding mode. Slow exchange processes in acetone- d_6 and CDCl_3 were observed upon the titration of **83** with $n\text{-Bu}_4\text{NHSO}_4$. Comparable experiments with open chain receptor **84** in CDCl_3 result in stability constants $\log K_a > 4$ in a 1:2 (host to guest) binding mode. However, crystallisation of both receptors with two equivalents of $n\text{-Bu}_4\text{NHSO}_4$ results in the formation of the 1:1 complexes $[\text{SO}_4\subset\text{H}_2\text{83}]$ and $[\text{SO}_4\subset\text{H}_2\text{84}]$.

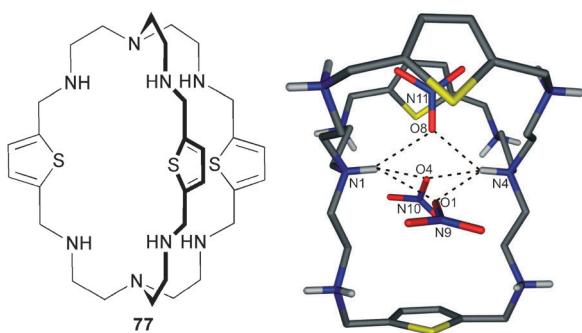


Fig. 11 Schematic draw of **77** (left) and crystal structure of $[\text{NO}_3\subset\text{H}_8\text{77}]^{5+}$ (right), hydrogen bonds as dotted line, external NO_3^- , H_2O and selected hydrogen atoms omitted for clarity.

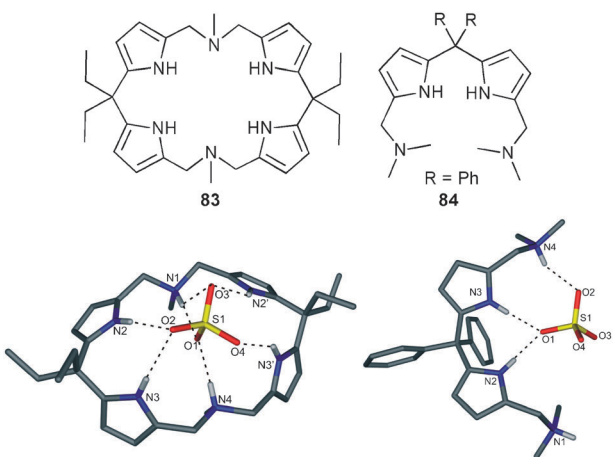
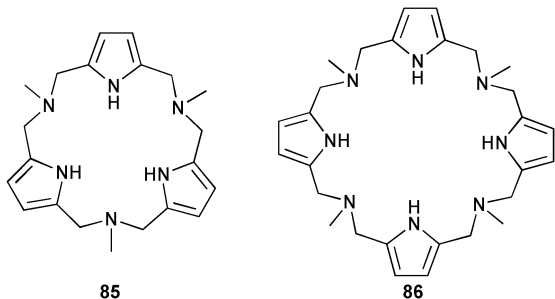


Fig. 12 Crystal structure of $[\text{SO}_4 \subset \text{H}_2]83$ (left) and $[\text{SO}_4 \subset \text{H}_2]84$ (right), hydrogen bonds as dotted line, co-crystallised solvent molecules and non-acidic hydrogen atoms are omitted for clarity.

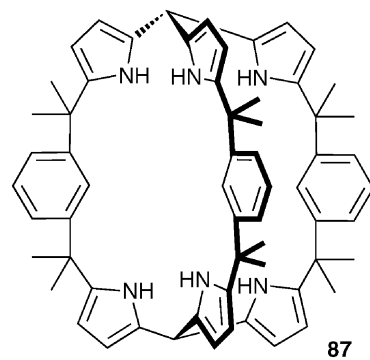
respectively (Fig. 12). The crystal structures reveal that both receptors are doubly protonated. The sulfate ion in $[\text{SO}_4 \subset \text{H}_2]83$ is coordinated by $\text{N}-\text{H} \cdots \text{O}$ hydrogen bonds to the pyrrole groups ($\text{N} \cdots \text{O}$ distances of 2.992 and 3.076 Å) and the formed ammonium group ($\text{N} \cdots \text{O}$ distances of 2.740 and 2.833 Å). In $[\text{SO}_4 \subset \text{H}_2]84$ the anion is bound by two $\text{N}-\text{H} \cdots \text{O}$ hydrogen bonds from the pyrrole groups ($\text{N} \cdots \text{O}$ distances of 2.800 and 2.821 Å) and by only one of the two ammonium groups with an $\text{N} \cdots \text{O}$ distance of 2.773 Å.

The same group have studied the anion binding of amine linked pyrrole based macrocycles **85** and **86** by proton NMR titration in acetone- d_6 .⁶¹ The smaller macrocycle **85** binds F^- in a 1:1 binding mode with a stability constant $K_a [\text{M}^{-1}]$ of 1138. A 2:1 ($\text{L} : \text{A}$) stoichiometry was obtained for the binding of Cl^- and Br^- with stability constants $K_{21} [\text{M}^{-1}]$ of 3182 and 243, respectively. The larger macrocycle **86** forms 1:1 complexes with Cl^- and Br^- and shows enhanced binding of halide anions ($K_a [\text{M}^{-1}] = 13586$ for Cl^- and 1181 for Br^-).



Proton NMR titrations of a new tripyrrole-methane based cryptand **87** reveal a preferred binding of F^- over Cl^- , NO_3^- , HSO_4^- , CH_3COO^- and H_2PO_4^- , added as their tetrabutylammonium salts.⁶² Complex formation is kinetically slow in CD_2Cl_2 . However, the integration of the resonances of free and complexed cryptand results in a calculated stability constant of 1562 M^{-1} in a 1:1 binding mode.⁶³

The ability to assemble anion complexes of the known *meso*-octamethylcalix[4]pyrrole **88** by bis-cations in the solid phase and in solution was reported by Gale, Sessler and co-workers.⁶⁴ Crystallisation experiments of **88** in the presence of dibromide



salt **89** and **90** results in assemblies where the bromide ions are coordinated by four $\text{N}-\text{H} \cdots \text{Br}$ hydrogen bonds ($\text{N} \cdots \text{Br}$ distances between 3.410 and 3.503 Å) of the calixpyrrole. The pyridinium or imidazolium rings of the bis-cation reside in the bowl shaped calixpyrrole-anion complex cavity with C-centroid distances of 3.640 and 3.679 Å for $(\text{Br} \subset 88)_2 89$ and 3.537 Å for $(\text{Br} \subset 88)_2 90$ (Fig. 13). Isothermal titration calorimetry experiments in acetonitrile point at the formation of similar 1:2 (bis-cationic salt to calixpyrrole) complexes in solution. The stability constant for the association of bis-bromide salt **90** and **88** was calculated to 2220 M^{-1} .

Sessler and co-workers have reported additional binding studies with bromide and benzoate of a series of known strapped calix[4]pyrroles⁶⁵ **91**–**93** and have demonstrated the pronounced anion selectivity of these compounds.⁶⁶ Proton NMR titrations of **93** and isothermal titration calorimetry studies of **91** and **92** and the parent calix[4]pyrrole **88** were performed in acetonitrile solutions. The calculated stability constants, employing a 1:1 binding mode, are summarized in Table 9 and reveal selective binding of Cl^- over Br^- and PhCOO^-

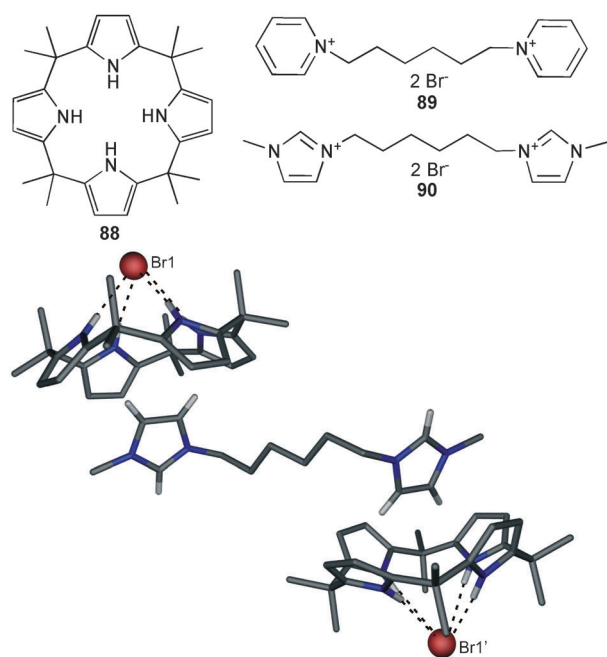
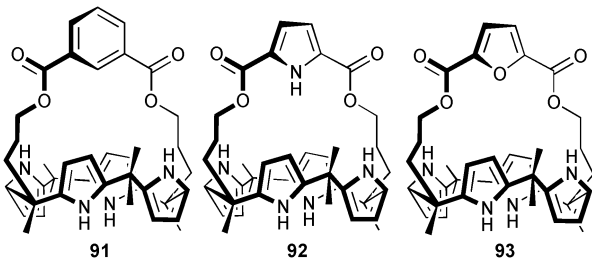


Fig. 13 Crystal structure of the ion pair assembly of $(\text{Br} \subset 88)_2 90$, hydrogen bonds as dotted line, selected hydrogen atoms omitted for clarity.

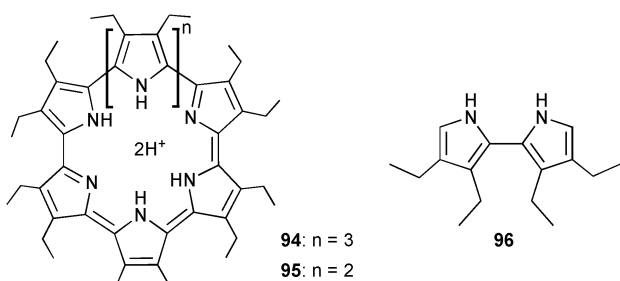
Table 9 Stability constants K_a [M^{-1}] of **88** and **91–93** in CH_3CN determined by ITC or^a NMR titration at 298 K^b at 303 K. Anions added as their tetrabutylammonium salts

Anion	88	91	92	93
Cl^-	2.2×10^5	2.2×10^6	1.8×10^7	1.9×10^5
Br^-	3.4×10^{3b}	2.1×10^3	4.5×10^5	5.4×10^{1a}
PhCOO^-	1.4×10^5	1.1×10^3	7.9×10^5	4.6×10^{1a}

for all receptors, with a pronounced Cl^- selectivity for the strapped system **91–93**. The highest binding for all anions was obtained with the pyrrole-strapped system **92**.



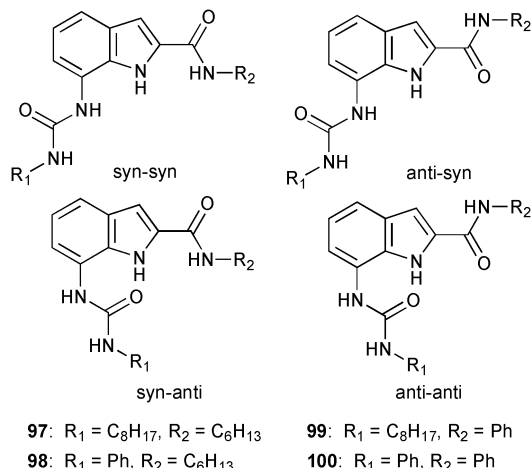
Sessler and co-workers also reported the use of anion templates to synthesise the large macrocycle cyclo[8]pyrrole (**94**) by electrochemical oxidation of bipyrrole **96**.⁶⁷ The electrolyses were carried out in dichloromethane in the presence of F^- , Cl^- , Br^- , NO_3^- , BF_4^- , HSO_4^- and ClO_4^- . The highest reaction yield of 68% was achieved in the presence of HSO_4^- . Further, the authors successfully synthesised cyclo[7]pyrrole **95** and cyclo[8]pyrrole **94** from the simple 3,4-diethylpyrrole by the same method, which was not achieved before by chemical oxidation.



The same group have also continued their work to apply various calix[4]pyrroles as liquid–liquid extractants to aid sulfate/nitrate exchange selectivity.⁶⁸

Indole based receptors

The relatively new area of indole based anion receptor systems^{69,70} continued to grow in 2010. Anion receptors containing a 7-indoleureido moiety may be used to provide additional hydrogen bond donors in a favourable position for the multidentate coordination of anions. Detailed proton NMR studies of the C2 and C7 substituted receptors **97–100** by Plavec and co-workers illustrate the conformational change of the ligand upon the addition of spherical halides and oxo-anions.⁷¹ NOE studies reveal the dominance of the *anti-anti* conformation of the free receptor in acetone, whereas the addition of chloride, bromide and acetate results in the *syn-syn* conformation of **97–100**. No conformational changes were observed upon the



addition of nitrate to all receptors, which also exhibits very weak binding.

Diindolyurea based receptors **101** and **102** were employed by Gale and co-workers to bind various oxo-anions in the flexible ligand cleft.⁷² Crystal structures reveal the coordination of SO_4^{2-} and HPO_4^{2-} via 8 and 9 N–H···O hydrogen bonds from all the N–H groups in **101**, respectively (Fig. 14).

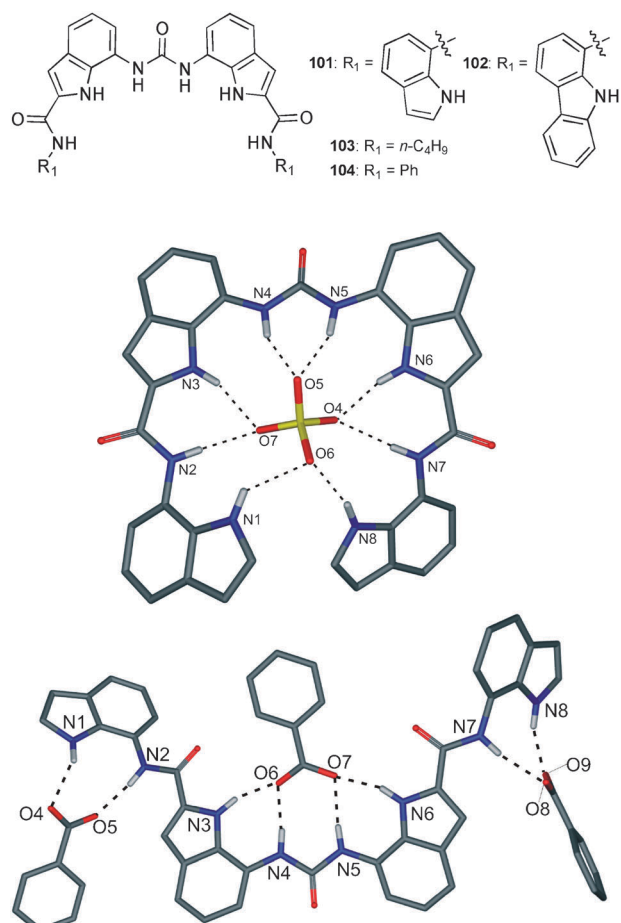


Fig. 14 Crystal structure of $[\text{SO}_4^{2-}] \subset \mathbf{101}^{2-}$ (top) and $[(\text{PhCOO})_3] \subset \mathbf{101}^{3-}$ (bottom) with selected atom labels, hydrogen bonds as dotted line, tetrabutylammonium cation, co-crystallised solvent molecules and non-interacting hydrogen atoms omitted for clarity.

The observed N···O distances in the SO_4^{2-} complex range from 2.788 to 2.953 Å, whilst the N···O distances are between 2.736 and 3.109 Å in $[\text{HPO}_4 \subset \mathbf{101}]^{2-}$. However the structure of the benzoate complex reveals a 1:3 (L:A) stoichiometry (Fig. 14). One anion is bound by four hydrogen bonds of the urea and the two adjacent indole groups in the central ligand cleft (N···O distances range from 2.717 to 2.820 Å) where the two amidoindole moieties coordinate to remaining anions by N–H···O interactions with N···O distances between 2.766 and 3.144 Å. Solution studies with carboxylates show that the first equivalent of anion binds to the central diindolylurea group, whilst the second and third equivalents bind to the terminal amidoindole groups. However, upon addition of one equivalent of tetrabutylammonium sulfate to the receptor all the NH groups bind the anion in a 1:1 stoichiometry. Addition of further equivalents of sulfate results in the formation of higher order complexes. Proton NMR studies in $\text{DMSO}-d_6/0.5\%$ water reveal deprotonation of H_2PO_4^- and HCO_3^- by free anions in solution when complexed by the receptors.

More detailed studies of anion–anion proton transfer of coordinated H_2PO_4^- were performed by the same group.⁷³ Proton NMR titration experiments of **103** in $\text{DMSO}-d_6/0.5\%$ water and $\text{DMSO}-d_6/10\%$ water show a new set of signals after the addition of more than one equivalent of $n\text{-Bu}_4\text{NH}_2\text{PO}_4$ with a considerable downfield shift. Comparable experiments where $n\text{-Bu}_4\text{NH}_2\text{PO}_4$ was added up to 1.4 equivalent followed by the addition of $n\text{-Bu}_4\text{NOH}$ yield the same set of signals in the proton NMR spectra (Fig. 15). The authors explain their observation with a reduced pK_a of the bound oxo-anion and subsequent proton transfer to the unbound anion. The solid-state structure of $[\text{HPO}_4 \subset \mathbf{104}]^{2-}$ supports the observed proton transfer (Fig. 16). Single crystals were isolated by slow evaporation of a DMSO solution of **104** in the presence of excess $n\text{-Bu}_4\text{NH}_2\text{PO}_4$. The coordinated anion is HPO_4^{2-} , which is bound by six N–H···O hydrogen bonds with N···O distances between 2.660 and 2.842 Å.

The same receptor **103** amongst others of the same type was also employed to recognise alkylcarbamate anions in solution

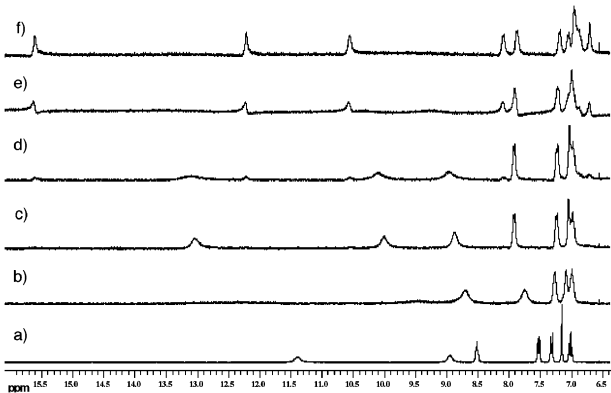


Fig. 15 Proton NMR titration of **104** in $\text{DMSO}-d_6/0.5\%$ water. (a) Free receptor; (b) 0.6 equivalents $n\text{-Bu}_4\text{NH}_2\text{PO}_4$; (c) 1.0 equivalents $n\text{-Bu}_4\text{NH}_2\text{PO}_4$; (d) 1.4 equivalents $n\text{-Bu}_4\text{NH}_2\text{PO}_4$; (e) 1.4 equivalents $n\text{-Bu}_4\text{NH}_2\text{PO}_4 + 0.7$ equivalents $n\text{-Bu}_4\text{NH}_2\text{PO}_4$; (f) 1.4 equivalents $n\text{-Bu}_4\text{NH}_2\text{PO}_4 + 1.4$ equivalents $n\text{-Bu}_4\text{NH}_2\text{PO}_4$. Gale *et al.*, *Chem. Asian J.* 2010, **5**, 555–561. Reproduced with permission of Wiley-VCH Verlag GmbH & Co. KGaA, Weinheim.

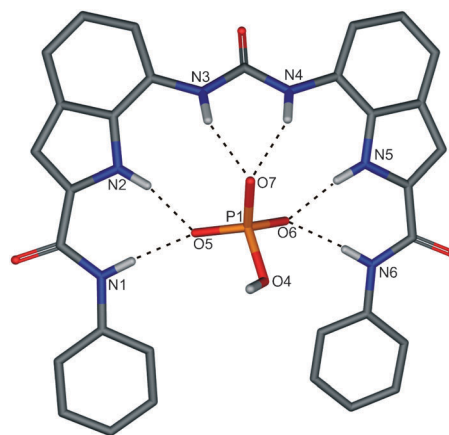


Fig. 16 Crystal structure of $[\text{HPO}_4 \subset \mathbf{104}]^{2-}$ with selected atom labels, hydrogen bonds as dotted line, tetrabutylammonium cation, co-crystallised water molecules and non-interacting hydrogen atoms omitted for clarity.

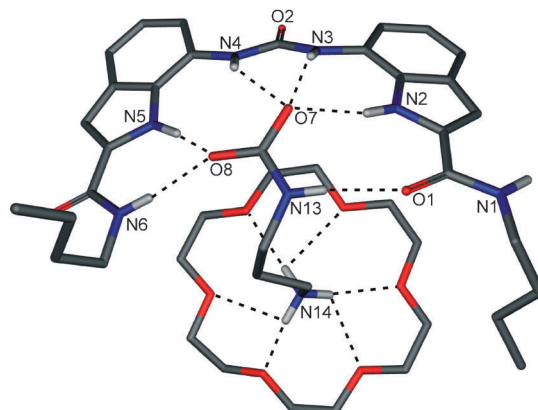


Fig. 17 Crystal structure of $[\text{AAAC} \subset \mathbf{103}]\text{-18-crown-6}$ with selected atom labels, hydrogen bonds as dotted line, co-crystallised solvent molecules and non-interacting hydrogen atoms omitted for clarity.

and the solid state.⁷⁴ A crystal structure reveals that the alkylammonium-alkylcarbamate (AAAC) salt, the reaction product of 1,3-diaminopropane and carbon dioxide, is coordinated by **103** (binding the carbamate group) and 18-crown-6 (binding the ammonium group) (Fig. 17). Both functional groups are bound by multiple hydrogen bonds with N···O distances ranging from 2.677 to 3.163 Å between the receptor and carbamate and N···O distances between 2.738 and 3.073 Å for the ammonium···18-crown-6 interactions. Significant proton NMR shifts indicate the interaction of the receptors and the carbamate substrates in $\text{DMSO}-d_6$ solutions.

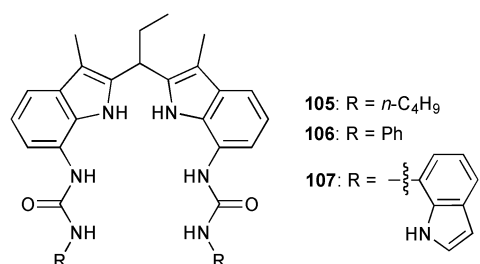
Jurczak and co-workers have reported the anion binding ability of a series of 7,7'-diureido-2,2'-diindolymethane based receptors **105**–**107**.⁷⁵ Proton NMR titrations in CD_3OD were employed to calculate the stability constants of the 1:1 anion complexes. The three receptors show selective binding of H_2PO_4^- over HSO_4^- , PhCOO^- , Cl^- and Br^- (Table 10). Interestingly, the additional 7-indole NH donor functions in **107** do not result in an enhanced binding of the anion. The obtained stability constants are evidence of a pronounced influence of n-butyl and phenol substituent in **105** and **106**, respectively. The crystal structure of the phosphate complex of

Table 10 Stability constants K_a [M^{-1}] of **105–107** in CD_3OD at 298 K.^a Anions added as their tetrabutylammonium salts

Anion	105	106	107
$H_2PO_4^-$	135	535	256
HSO_4^-	99 ^b	280	90
$PhCOO^-$	15	28	39 ^c
Cl^-	14	31	21
Br^-	13	23	15

^a Determined from the observed shift of the urea NH shift, errors estimated to be not more than $\pm 10\%$. ^b Errors $> 10\%$. ^c Shift of the indole NH employed.

106 shows a deprotonation of the anion upon crystallisation. The anion is bound *via* five N–H···O hydrogen bonds with N···O distances between 2.818 and 2.942 Å. Closer examination reveals the formation of a $[H_3PO_4 \cdot PO_4]^{3-}$ dimer, that is coordinated by two ligands **106**. The phosphate anions are bridged by three protons with O···O distances between 2.496 and 2.676 Å and a P–P distance of 3.677 Å.



The indolocarbazole oligomer **108** was employed by Jeong and co-workers for the recognition of sulfate in solution and the solid state.⁷⁶ Quantitative NMR analysis of **108** in the presence of one equivalent tetrabutylammonium sulfate shows significant shifts of the NH and OH signals, resulting from hydrogen bonding between the anion and the six N–H and two O–H donor groups. NOE cross-peaks of non-adjacent protons indicate folding of **108** upon the coordination of the anion in solution. This is in agreement to the observed arrangement in the solid state. The crystal structure of $[SO_4^2- \subset 108]^{2-}$ shows a folded structure of **108** and the coordination of the SO_4^{2-} anion by eight hydrogen bonds in the helical cavity. The six N–H···O hydrogen bonds range from 2.780 to 2.844 Å where the distances of the two O–H···O hydrogen bonds are 2.810 and 2.883 Å. Nonlinear fitting analyses were performed on the fluorescence emission change of **108** (excited at 320 nm) upon the addition of tetrabutylammonium salts in 10% CH_3OH – CH_3CN to determine the stability constants. The calculated constants (K_a [M^{-1}]) show preferential binding of SO_4^{2-} (640 000) over Cl^- (8800), AcO^- (5700), $H_2PO_4^-$ (3600), Br^- (2800), CN^- (1600), N_3^- (790) and I^- (< 100).

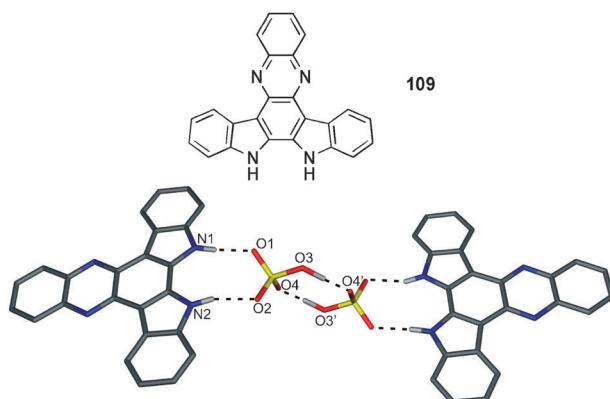
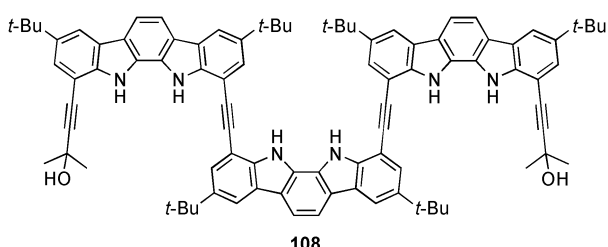


Fig. 18 Crystal structure of $[HSO_4^- \subset 109_2]^{2-}$ with selected atom labels, hydrogen bonds as dotted line, tetrabutylammonium cation and non-interacting hydrogen atoms omitted for clarity.

Yan and co-workers have reported a series of crystal structures illustrating the binding modes of known indolocarbazole-quinoxaline receptor **109**⁷⁷ with various anions such as F^- , Br^- , AcO^- , $PhCOO^-$, NO_3^- , HSO_4^- , $H_2PO_4^-$ and SiF_6^{2-} in the solid state.⁷⁸ The crystal structures reveal a 1:1 stoichiometry for F^- , Br^- , AcO^- and $PhCOO^-$ complex, whilst a 2:1 (L:A) complex is observed with SiF_6^{2-} and a 2:2 dimer with HSO_4^- . In the latter structure, two anions are bridged by two protons with an O···O distance of 2.527 Å to form the dimer (Fig. 18). The two indolocarbazole NH donor atoms are involved in two hydrogen bonds to the HSO_4^- anion with N···O distances of 2.748 and 2.821 Å. The NH···F interactions in $[SiF_6^- \subset 109_2]^{2-}$ range from 2.770 to 3.120 Å. The F^- ion in $[F^- \subset 109]^-$ is bound by N···F distances of 2.611 and 2.633 Å where N···Br distances of 3.281 and 3.383 Å were observed for $[Br^- \subset 109]^-$. The N···O distances of 2.676 and 2.676 Å in $[AcO^- \subset 109]^-$ are comparable to the observed N···O distances of 2.643 and 2.701 Å in $[PhCOO^- \subset 109]^-$.

The same group reported the anion binding properties of the pyrazino[2,3-*g*]quinoxaline linked indole based receptors **110–112**.⁷⁹ Significant absorption spectral changes upon addition of AcO^- and $H_2PO_4^-$ as their tetrabutylammonium salts were employed to determine the stability constants for the 1:2 (L:A) complexes in DMSO. The stability constants reveal enhanced binding by the biindolocarbazole receptor **112** (for AcO^- : $\log \beta_{11} = 5.0$, $\log \beta_{12} = 9.2$; for $H_2PO_4^-$: $\log \beta_{11} = 4.9$, $\log \beta_{12} = 9.1$) over the indole-indolocarbazole receptor **111** (for AcO^- : $\log \beta_{11} = 4.7$, $\log \beta_{12} = 8.3$; for $H_2PO_4^-$: $\log \beta_{11} = 4.5$, $\log \beta_{12} = 8.2$) and the biindole receptor **110** (for AcO^- : $\log \beta_{11} = 3.7$, $\log \beta_{12} = 7.5$; for $H_2PO_4^-$: $\log \beta_{11} = 3.3$, $\log \beta_{12} = 7.2$). The stronger binding may be due to the rigid indolocarbazole group possessing a higher degree of preorganisation than the flexible biindole receptor. The crystal structures of the $H_2PO_4^-$ complexes of the three receptors **110–112** result in distinct multi-dimensional networks as a result of the different binding modes of the indolocarbazole and biindole moieties towards the anion in the solid state. The biindole side tends to bind two respective $H_2PO_4^-$ ions, whereas the indolocarbazole moiety prefers only one (Fig. 19). Thus, in $[(H_2PO_4)_2 \subset 110_2]^{2-}$ each anion is bound by one N–H···O hydrogen bond from two ligands and two alternating O–H···O hydrogen bonds

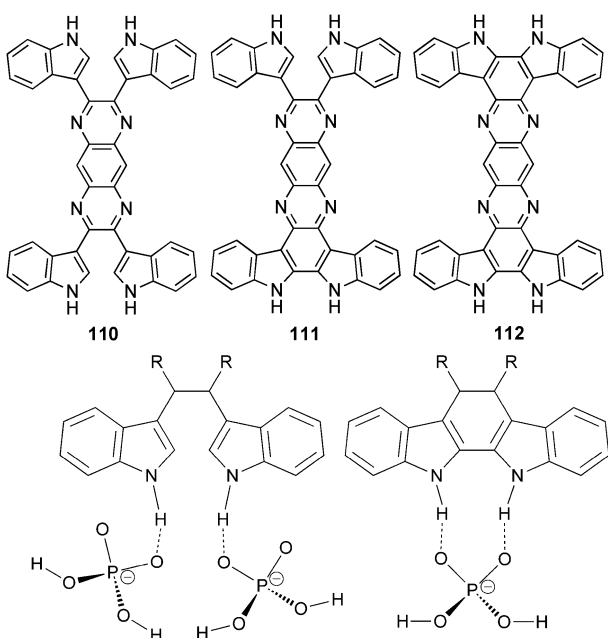
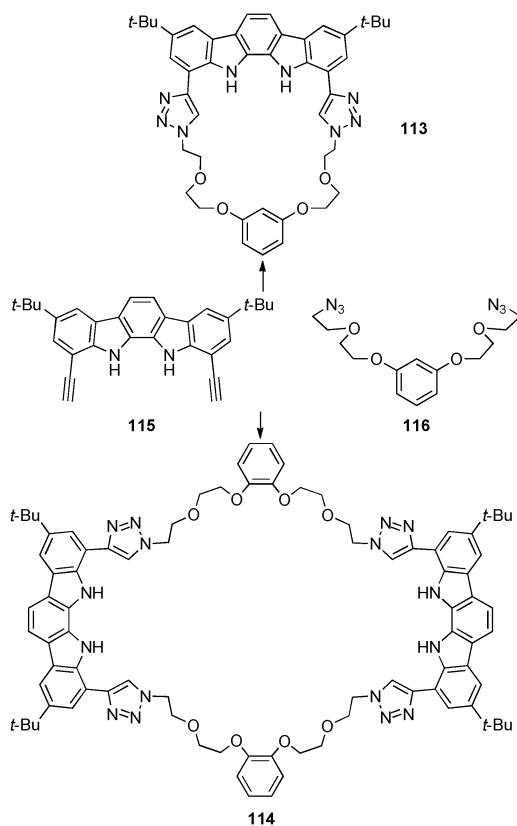


Fig. 19 Schematic representation of the preferred binding mode towards H_2PO_4^- by the biindole and the indolocarbazole moiety.

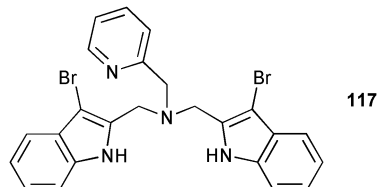
toward another H_2PO_4^- ion to form an anion dimer. This results in a two-dimensional network in the crystal packing. In $[(\text{H}_2\text{PO}_4)_2 \subset 111_2]^{2-}$ the anion dimer is bound by two indole N–H···O and four indolocarbazole N–H···O hydrogen bond of four ligands to form a one-dimensional 2+2 dimeric ribbon. In $[(\text{H}_2\text{PO}_4)_2 \subset 112]^{2-}$ the anion forms an infinite chain, which is alternate coordinated by the double N–H···O hydrogen bonds



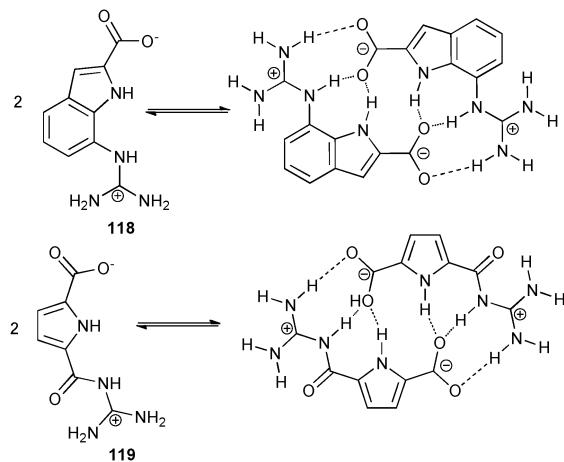
of the indolocarbazole moiety of 112 to form a two-dimensional coordination polymer.

Li and co-workers have reported the anion binding ability of macrocyclic indolocarbazole based receptors 113 and 114 in solution.⁸⁰ The ring closure of the macrocycles was achieved by ‘click chemistry’ on the 1:1 and 2:2 assemblies of the precursors 115 and 116, tuned by the reaction conditions. Proton NMR titration experiments fitted to a 1:1 binding model in CDCl_3 reveal a preferred binding of the spherical halide ions by the smaller macrocycle 113, even though only one indolocarbazole moiety is present in this system. Further, the stability constants show preferred binding of F^- ($K_a [\text{M}^{-1}] 11600$ for 113, 3010 for 114) over Cl^- ($K_a [\text{M}^{-1}] 1500$ for 113, 120 for 114), Br^- ($K_a [\text{M}^{-1}] 325$ for 113, 16 for 114) and I^- ($K_a [\text{M}^{-1}] 106$ for 113, 4 for 114) for both macrocyclic receptors.

The asymmetric tripodal amine bridged indole receptor 117 was employed by Fujita and co-workers for the binding of halide ions or alkali metal ions in solution.⁸¹ Proton NMR titration experiments in CD_3CN fitted to a 1:1 binding mode reveal a preferred binding of Cl^- ($K_a [\text{M}^{-1}] = 1042$) over Br^- ($K_a [\text{M}^{-1}] = 157$) and I^- ($K_a [\text{M}^{-1}] = 12$). No shift of the protons was observed if $n\text{-Bu}_4\text{NF}$ was added.



Schmuck and co-workers have continued their work on the dimerisation of zwitterionic guanidinium–carboxylates.⁸² This group have recently reported the synthesis of an indole-containing analogue 118 of their self-assembling guanidinio-carbonylpyrrole systems (e.g. 119). Proton NMR studies reveal a stability constant $K_{\text{ass}} > 10^5 \text{ M}^{-1}$ in $\text{DMSO}-d_6$ for the indole based ligand 118, which is significantly smaller than the estimated value $K_{\text{ass}} > 10^{10} \text{ M}^{-1}$ for the pyrrole based analogue 119.⁸³ The crystal structure of the dimer of 118 reveals a steric hindrance between the guanidinium group and the proton in the 6-position of the indole group. Consequently the guanidinium group is twisted out of the plane and the attractive nature of the additional hydrogen bonds is reduced.



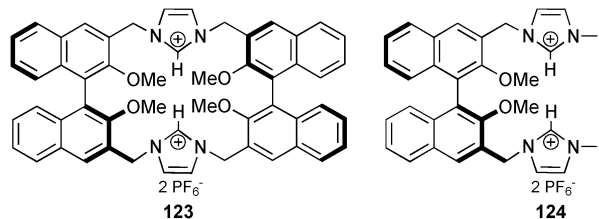
Imidazole and triazole base receptors

Imidazole and triazole based receptors provide different binding modes for the recognition of anions. Where imidazole derivatives require protonation and subsequently anion binding is accomplished by charged N⁺–H···X⁻-type hydrogen bonds, triazole based receptors form C–H···X⁻-type hydrogen bonds. Substitution of both functional groups results in imidazolium and triazolium based receptors, which form (C–H)⁺···X⁻ type hydrogen bonds with dominant electrostatic interactions.

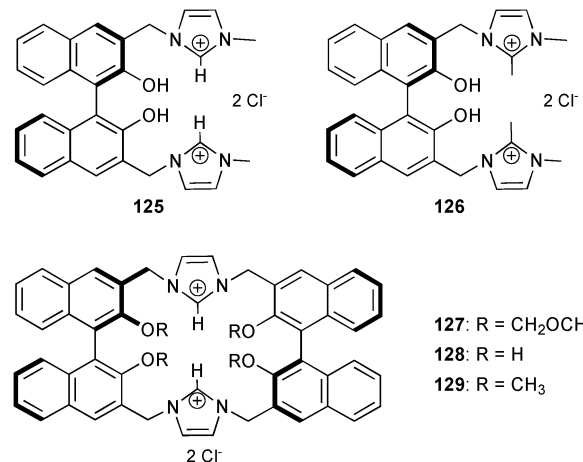
The nitrate complexes of a series of imidazole and pyrazole arene capped tripodal receptors **120**–**122** were investigated by Arunachalam and Ghosh.⁸⁴ Previous reports show that the solid state complex of protonated benzimidazole substituted receptor **120** forms a discrete dimeric capsule including all six NO₃⁻.⁸⁵ In contradistinction, the reaction product of the imidazole substituted receptor **121** and nitric acid crystallised in an infinite disordered capsular structure. Each nitrate anion is bound by one N–H···O hydrogen bond with N···O distances between 2.750 and 2.806 Å. The anions are linked by hydrogen bonds towards a co-crystallised water molecule. The replacement of imidazole with dimethyl pyrazole in **122** and subsequent crystallisation with nitric acid results in the formation of an anion bridged macrocycle (Fig. 20). The anion bridge is formed by two NO₃⁻ ions coordinated by the arms of two different ligand molecules with N···O distances between 2.730 and 2.803 Å. The three pyrazolium groups of the ligand are approximately planar and occupy the corners of the triangle. This results in a 1-D sheet like assembly of anion bridged macrocycles.

The anion binding ability of imidazolium receptors **123** and **124**, based on the 1,1'-bi-2-naphthol (BINOL) scaffold, were investigated by Yu and co-workers.⁸⁶ The treatment of the ligands with various anions as their tetrabutylammonium salts in CH₃CN–DMSO (9 : 1 v/v) results in a significant change in

the emission spectra upon excitation at 290 nm. The calculated stability constants show an enhanced anion binding in a 1 : 1 binding mode by the macrocyclic receptor **123** ($K_a [M^{-1}] \sim 2.6 \times 10^6$ for F⁻) over the monomer **124** ($K_a [M^{-1}] = 2.6 \times 10^5$ for F⁻). Furthermore, the titration experiments reveal a selectivity of **123** for F⁻ ($K_a [M^{-1}] \sim 2.6 \times 10^6$) over AcO⁻ ($K_a [M^{-1}] = 2.8 \times 10^5$), H₂PO₄⁻ ($K_a [M^{-1}] = 1.4 \times 10^4$), HSO₄⁻ ($K_a [M^{-1}] = 1.1 \times 10^3$), Cl⁻ ($K_a [M^{-1}] = 341$), Br⁻ ($K_a [M^{-1}] = 180$) and I⁻ ($K_a [M^{-1}] = 75$). The obtained stability constants of **124** point at a reduced selectivity of the more flexible receptor: $K_a [M^{-1}] = 1.4 \times 10^5$ for AcO⁻, 8.7×10^3 for H₂PO₄⁻, 1.4×10^3 for HSO₄⁻, 6.2×10^3 for Cl⁻, 933 for Br⁻ and 154 for I⁻. Preliminary titration experiments towards the chiral recognition of amino acids were carried out for **123** with the tetrabutylammonium salts of t-Boc-L-phenylalanine and t-Boc-D-phenylalanine. The calculated stability constants of 64 200 and 43 000 M⁻¹ respectively, point at a moderate selectivity of 1.5.



More detailed studies towards the binding of α -amino acids by 1,1-binaphthyl based imidazolium receptors **125**–**129** were reported by You and co-workers.⁸⁷ Fluorescence titration experiments in aqueous solution (HEPES buffer, pH 7.4) of **125** reveal a pronounced binding of L-Trp ($K_a [M^{-1}] = 1.73 \times 10^4$) over L-Phe ($K_a [M^{-1}] = 7.28 \times 10^3$), L-His ($K_a [M^{-1}] = 3.79 \times 10^3$), L-Tyr ($K_a [M^{-1}] = 2.96 \times 10^3$), L-Val ($K_a [M^{-1}] = 6.06 \times 10^3$), Gly ($K_a [M^{-1}] = 2.17 \times 10^3$) and L-Cys ($K_a [M^{-1}] = 1.45 \times 10^3$). No spectral changes were observed upon the addition of L-Pro, L-Glu, L-Ala and L-Ser. The chiral recognition of the two enantiomers of tryptophan (L-Trp and D-Trp) was investigated for **125**–**129**. The results are summarized in Table 11 and reveal a remarkable chiral recognition capability K_D/K_L of 6.2 by macrocyclic receptor **127**.



Sessler and co-workers have employed the tetracationic macrocycle **130**⁴⁺, containing four imidazolium moieties, for the formation of oligo-pseudorotaxanes with a mono-terephthalate anion.⁸⁸ The crystal structure shows a chair-like

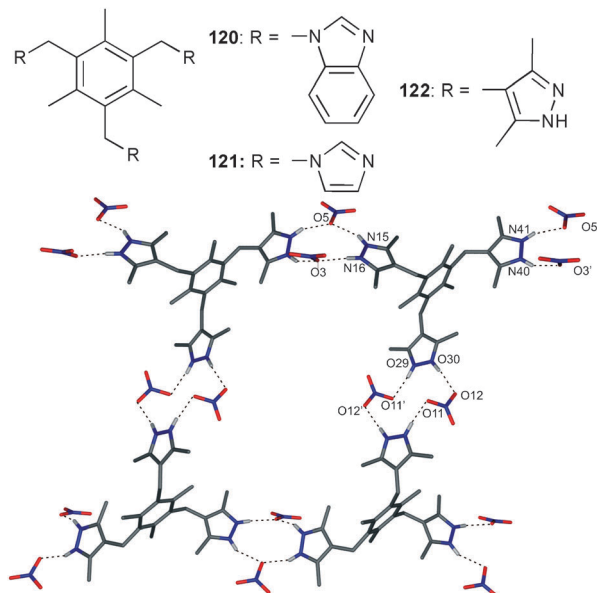


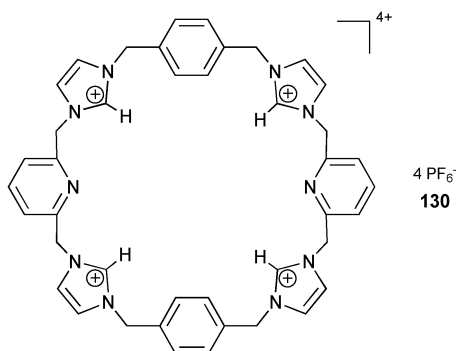
Fig. 20 Single macrocyclic unit formed in the crystal structure of (NO₃)₃ · H₃ **122** with selected atom labels, hydrogen bonds as dotted line, non-interacting hydrogen atoms omitted for clarity.

Table 11 Stability constants [M^{-1}] for the complexes of tryptophan (Trp) with **125–129** in water (10 mM HEPES buffer, pH = 7.4) at 25 °C^a

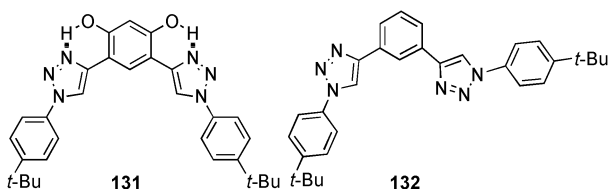
Receptor	$K_{L\text{-Trp}}/M^{-1}$	$K_{D\text{-Trp}}/M^{-1}$	$K_{D\text{-Trp}}/K_{L\text{-Trp}}$
125	$(1.73 \pm 0.01) \times 10^4$	$(1.09 \pm 0.03) \times 10^4$	0.6
126	$(8.04 \pm 1.62) \times 10$	$(8.34 \pm 2.20) \times 10$	1.0
127	$(2.89 \pm 0.12) \times 10^3$	$(1.79 \pm 0.03) \times 10^4$	6.2
128	$(4.78 \pm 0.07) \times 10^3$	$(3.38 \pm 0.13) \times 10^3$	0.7
129	$(2.59 \pm 0.12) \times 10^3$	$(5.42 \pm 0.02) \times 10^3$	2.1

^a Error values were obtained by the result of Benesi–Hildebrand plots and the correlation coefficient of linear fitting is over 0.99.

conformation for the macrocycle, with the mono-terephthalate anion bound within the central cavity. Hydrogen bonds between the head-to-head stacked mono-terephthalate anion result in a 1-D arrangement in the solid state, where electrostatic and C–H···π interactions stabilize the pseudorotaxane arrangement. Detailed NOESY NMR experiments in DMSO-*d*₆ reveal the presence of various aggregates of the pseudorotaxane in solution. Stability constants of $1.3 \times 10^2 M^{-1}$ (K_{a1}) and $8.8 \times 10^1 M^{-1}$ (K_{a2}) were calculated for the formation of the dimeric and trimeric oligomers $[(\mathbf{130}^{4+})\text{-}(\text{mono-terephthalate anion})_2]$ and $[(\mathbf{130}^{4+})\text{-}(\text{mono-terephthalate anion})_3]$, respectively. The 1:1 complex formation of the free host $\mathbf{130}^{4+}$ and mono-terephthalate anion gives a stability constant K_a of $2.1 \times 10^3 M^{-1}$.



The influence of preorganisation, due to intramolecular hydrogen bonding in the receptor backbone, on the chloride binding ability of aryl-triazole based receptors was investigated by Flood and co-workers.⁸⁹ Proton NMR titration experiments in CD₂Cl₂ reveal the expected significant enhanced affinity of the chloride anion for **131** ($K_a [M^{-1}] = 46\,800$) compared to **132** ($K_a [M^{-1}] = 1000$). The coordination of anions in both receptors is based on multiple C–H···Cl interactions only.



The same group reported the chloride binding of a photo-switchable triazole foldamer **133**.⁹⁰ The *cis*–*trans* photoisomerisation of azobenzene end groups was used to enable the wavelength dependent uptake and release of the anion. Electronic absorption spectra titration experiments with *n*-Bu₄NCl in CH₃CN

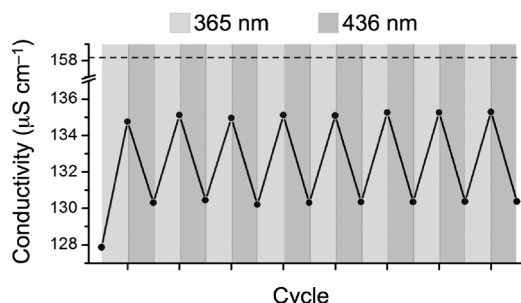
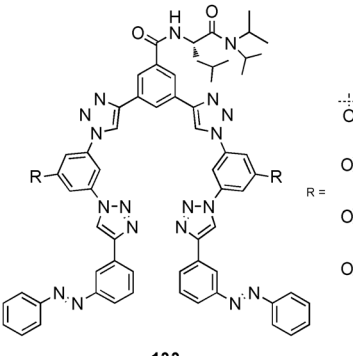
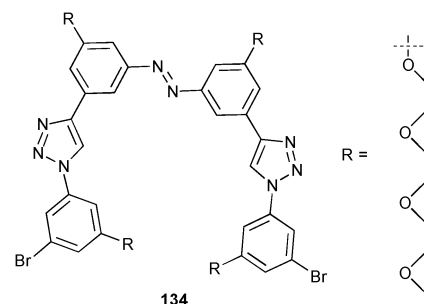


Fig. 21 Solution conductivity of *n*-Bu₄NCl in the presence of **133** (1 equivalent, 1mM, CH₃CN, 298 K) obtained upon exposure to UV (365 nm) and visible (436 nm) light. Dashed line corresponds to the conductivity in the absence of **133**. Reprinted with permission from *J. Am. Chem. Soc.* 2010, **132**, 12838–12840. Copyright 2011 American Chemical Society.

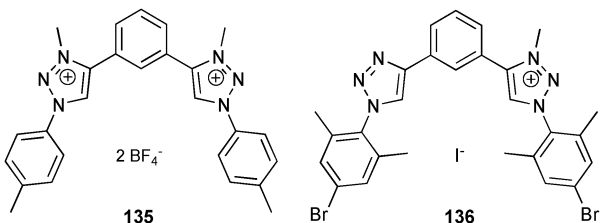
reveal stability constants of $K_a = 3000 M^{-1}$ for the *trans* and $K_a = 380 M^{-1}$ for the *cis* isomer. The authors demonstrate the reversible photo-switchable conformation of the receptor and the subsequent influence on the anion binding in conductivity experiments. Alternate radiation of the receptor in the presence of *n*-Bu₄NCl in CH₃CN with light at 365 and 436 nm results in significant changes in the observed conductivity (Fig. 21).

The anion binding ability of a similar photo-switchable triazole based receptor **134** was investigated by Jiang and co-workers.⁹¹ Proton NMR titration experiments in acetone-*d*₆ fitted to a 1:1 binding mode show the enhanced binding of the *cis* isomer ($K_a [M^{-1}] = 290$ for Cl[−]) compared to the *trans* isomer ($K_a [M^{-1}] = 70$). All other anions result in reduced stability constants of 66 M⁻¹ for HSO₄[−], 87 M⁻¹ for Br[−], 31 M⁻¹ for I[−] and 21 M⁻¹ for NO₃[−] with the *cis* isomer and $K_a = 38 M^{-1}$ for HSO₄[−], 22 M⁻¹ for Br[−], 11 M⁻¹ for I[−] and 10 M⁻¹ for NO₃[−] with the *trans* isomer.



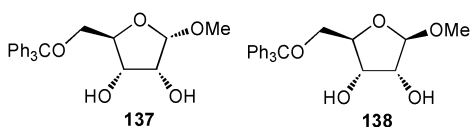
The coordination of sulfate by the triazolium based receptors **135** and **136** was investigated by Schubert and co-workers.⁹²

A different complex composition was obtained depending on the degree of methylation of the receptor. Proton NMR titration experiments in $\text{CD}_3\text{CN}/\text{CH}_3\text{OH}$ 4 : 1 show the formation of a 1 : 1 complex by **135** with a stability constant $\log K_a = 4.39$. On the other hand, the coordination of sulfate by the mono-methylated receptor **136** results in the formation of a 2 : 1 (L : A) complex. The stability constants in CD_3CN were determined to be $\log K_{11} = 3.73$ and $\log K_{21} = 3.1$.



Hydroxy and Lewis acid based receptors

The anion binding abilities of two D-ribose based epimers **137** and **138** in solution were reported by Kondo and co-workers.⁹³ Significant shifts of both OH-signals in proton NMR titration experiments in CDCl_3 and CD_3CN indicate the formation of O-H···anion hydrogen bonds. The calculated stability constants fitted to a 1 : 1 binding mode reveal a preferred anion binding by **138** over **137**, presumably due to the electrostatic and/or steric repulsion between the anomeric O atom in **137** and the anion. Both receptors show an enhanced binding of AcO^- over H_2PO_4^- , Cl^- and Br^- . A stronger affinity was observed in CD_3CN with respect to CDCl_3 for both receptors. A summary of the obtained stability constants is given in Table 12.

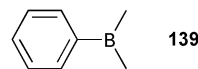


Competitive studies to investigate the F^-/CN^- selectivity of the simple Lewis acid dimethyl(phenyl)borane **139** were reported by Aldridge and co-workers.⁹⁴ The absorption change at 351 nm of **139** in UV-Vis titration experiments in CH_2Cl_2 were employed to calculate the stability constants $K_a [\text{M}^{-1}]$ of 1.9×10^5 for CN^- and 8.9×10^4 for F^- . Competitive studies in CD_2Cl_2 , monitored by multinuclear NMR experiments, reveal a replacement of F^- from $[\text{F} \subset \text{139}]^-$ by an excess of CN^- , whereas no spectral change was observed if $[\text{CN} \subset \text{139}]^-$ was treated with an excess of F^- . The crystal structures $[\text{F} \subset \text{139}](n\text{-Bu}_4\text{N})$ and $[\text{CN} \subset \text{139}]\cdot[\text{K}(18\text{-crown-6})]$ show the

Table 12 Stability constants $K_a [\text{M}^{-1}]$ of **137** and **138** in CDCl_3 and CD_3CN at 298 K. Anions added as their tetrabutylammonium salts

Anion	CDCl_3		CD_3CN	
	137	138	137	137
AcO^-	71.8 ± 13.1	2450 ± 40	149 ± 27	3380 ± 440
H_2PO_4^-	16.0 ± 0.6	2030 ± 320	39.4 ± 1.6	459 ± 109
Cl^-	6.7 ± 0.3	148 ± 21	33.2 ± 1.5	235 ± 3
Br^-	2.6 ± 0.1	36.8 ± 0.7	6.5 ± 0.3	30.9 ± 7.3

formation of covalent bonds between the borane receptor and the anion. The B-F distance is 1.482 Å, whereas CN^- is bound by the C atom with a B-C distance of 1.631 Å and a B-C-N angle of 173.4°.



The same group also reported the F^-/CN^- binding ability of 1,2-diborylferrrocene **140** and **141**.⁹⁵ UV-Vis titration experiments of **140** in THF give a stability constant of $3.7 \times 10^4 \text{ M}^{-1}$ for CN^- whereas the binding of F^- appears to be very slow. Competitive experiments, monitored by ^{11}B NMR show the quantitative formation of $[\text{CN} \subset \text{140}]^-$ upon the addition of **140** to a equimolar solution of F^- and CN^- . The crystal structures $[\text{F} \subset \text{141}]\cdot[\text{K}(18\text{-crown-6})]$ and $[\text{CN} \subset \text{141}]\cdot[\text{K}(18\text{-crown-6})]$ reveal different binding modes for the anions. The CN^- anion is C-bound with a B-C distance of 1.648 Å and coordinated in the *exo* position to one borane atom. Whereas F^- is bound by one borane centre with a B-F distance of 1.471 Å, but located in the *endo* position (Fig. 22).

The anion binding ability of the sulfonium fluorosilane Lewis acid receptor **142** was reported by Gabbai and co-workers.⁹⁶ The addition of tetrabutylammonium salts of Cl^- , Br^- or I^- to **142** in CDCl_3 results in the formation of neutral silane **143**, whereas the presence of $n\text{-Bu}_4\text{NF}$ gives the stable complex $[\text{F} \subset \text{142}]$. Changes in the absorption spectrum were employed to determine the stability constant K_a of $7 \times 10^6 \text{ M}^{-1}$ for the formed 1 : 1 complex in CHCl_3 . The crystal structure of $[\text{F} \subset \text{142}]$ reveals a trigonal-bipyramidal geometry of the Si atom (Fig. 23). The F-atoms occupy the axial positions with a F-Si-F angle of 177.3° and Si-F distances of 1.706 and 1.732 Å. The F atom with the longer Si-F bond is involved in interactions towards the S-atom with a S···F distance of 2.741 Å.

Armand and co-workers employed the simple boron esters **144–147** to form Lewis acid anion complexes from LiF and to dissolve the salts as an electrolyte in battery solvents such as ethylene carbonate/dichloromethane (EC/ CH_2Cl_2) or dimethyl-formamide (DMF).⁹⁷

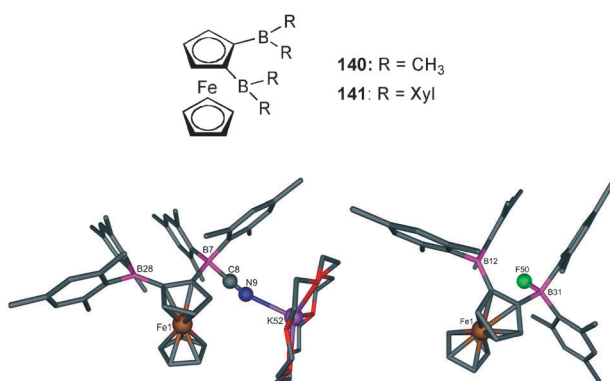


Fig. 22 Crystal structure of $[\text{CN} \subset \text{141}]\cdot[\text{K}(18\text{-crown-6})]$ (left) and $[[\text{F} \subset \text{141}]\cdot[\text{K}(18\text{-crown-6})]]$ (right) with selected atom labels, hydrogen atoms and $[\text{K}(18\text{-crown-6})]^+$ cation in $[[\text{F} \subset \text{141}]\cdot[\text{K}(18\text{-crown-6})]]$ omitted for clarity.

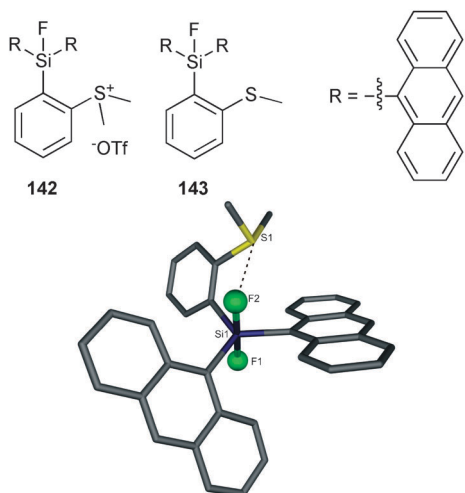
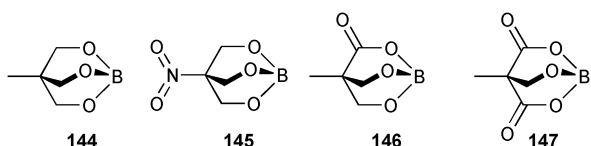


Fig. 23 Crystal structure of $[F \subset 142]$ with selected atom labels, $S \cdots F$ interaction represented as dotted line, hydrogen atoms omitted for clarity.

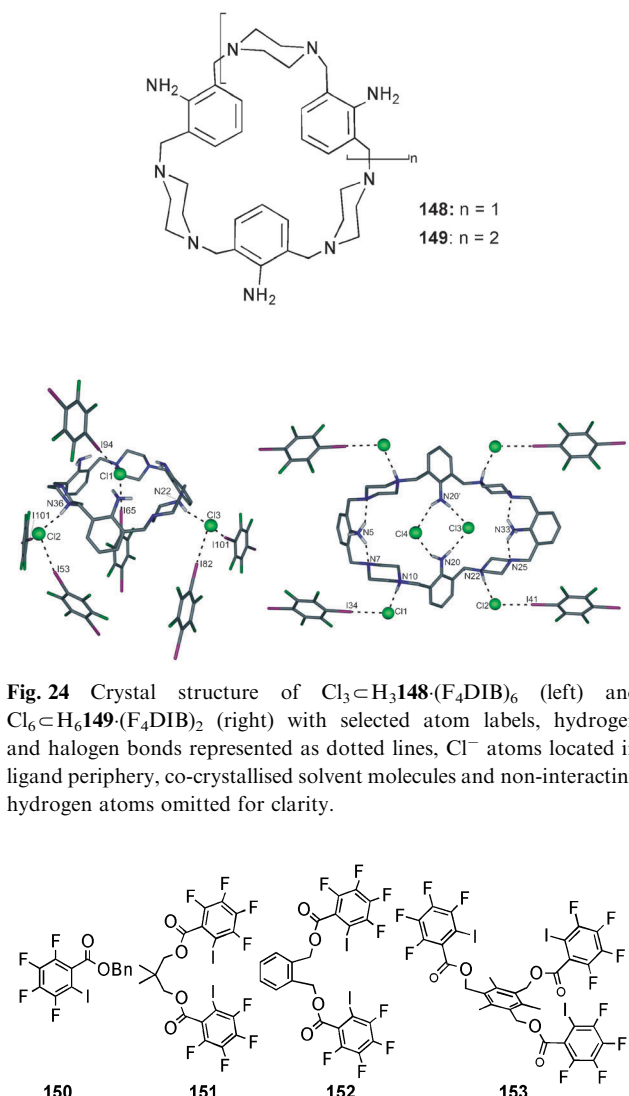


Anion recognition by halogen bonds

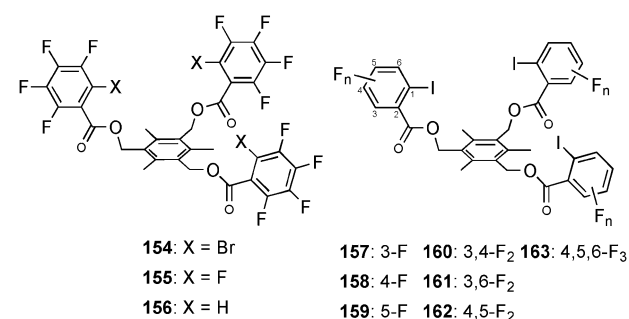
Halogen bonding is an emerging field in the recognition of anions. Crystallisation of the chloride complexes of triamino (**148**) and tetraamino (**149**) piperazine cyclophane in the presence of 1,4 diiodotetrafluorobenzene (F_4DIB) results in the formation of $C-I \cdots Cl$ halogen bonds in the solid state.⁹⁸ Each of the three chloride ions in $Cl_3 \subset H_3 148 \cdot (F_4DIB)_6$ is coordinated by two $C-I \cdots Cl$ halogen bonds with $I \cdots Cl$ distances ranging from 3.129 to 3.289 Å and $C-I \cdots Cl^-$ angles between 168.7 and 175.6°. Where in $Cl_6 \subset H_6 149 \cdot (F_4DIB)_2$ only four Cl^- ions are bound by one $C-I \cdots Cl$ interaction each with a $I \cdots Cl$ distance of 3.087 and 3.117 Å and a $C-I \cdots Cl^-$ angle of 179.8 and 178.2°, respectively (Fig. 24).

Taylor and co-workers investigated the possibility to coordinate a single anion by multiple halogen bonds in solution.⁹⁹ Fluorine NMR titrations were performed with the mono-, bi- and tridentate ligands **150–153** at 295 K in acetone- d_6 . The addition of tetrabutylammonium salts results in a downfield shift of the ^{19}F NMR signals and can be fitted to a 1:1 binding model. The calculated stability constant K_a [M^{-1}] for Cl^- increases considerably with the number of available iodine atoms in the receptor from 70 for **150**, 1.1×10^3 for **151**, 1.8×10^3 for **152** and 1.9×10^4 for **153** and demonstrate the chelating effect of the halogen bond. Additional ^{19}F NMR titrations with **153** reveal an anion binding selectivity in the order $Cl^- (1.9 \times 10^4 M^{-1}) > Br^- (3.8 \times 10^3 M^{-1}) > I^- (7.6 \times 10^2 M^{-1}) \gg TsO^- (10 M^{-1}) > HSO_4^- (< 10 M^{-1}) > NO_3^- (< 10 M^{-1})$.

The same group examined the influence of the type of donor atom and the number and position of adjacent electron withdrawing fluorine atoms on the strength of the halogen bonds.¹⁰⁰ The Cl^- stability constants were calculated employing a 1:1 binding mode from ^{19}F NMR titration experiments in acetone- d_6 of the tridentate ligands **153–163**. The obtained results of the

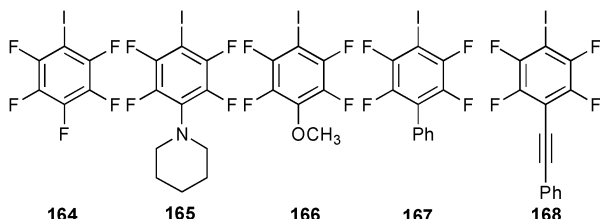


series of tetrafluoro-phenyl ligands **153–156** point at the presence of significant halogen bonding for the iodine-based receptor only. The stability constant K_a [M^{-1}] for **153** is 1.9×10^4 , where negligible values were obtained for the bromide-based receptor **154** (K_a [M^{-1}] = < 10), CH-anion hydrogen bond receptor **156** (K_a [M^{-1}] = < 5) and pentafluoro-phenyl receptor **155** (K_a [M^{-1}] = < 5). The investigation of ligands **157–163** demonstrates a striking correlation between the complex stability and the number and position of fluorine atoms present in the iodophenyl-moiety. A stability constant K_a [M^{-1}] of 18 was calculated for **157**, whereas K_a = 38 for **160**, K_a = 2.8×10^2 for **163** and

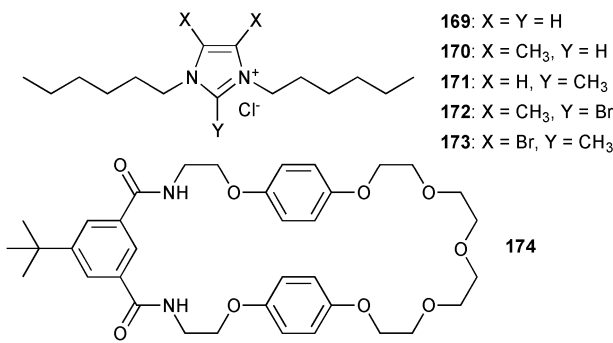


$K_a = 1.9 \times 10^4$ for **153**. Positional isomers **158** and **159** reveal stability constants of $K_a = 3 \text{ M}^{-1}$ and $K_a = 7 \text{ M}^{-1}$, respectively, and the bi-fluorinated **161** and **162** give values of $2.2 \times 10^2 \text{ M}^{-1}$ and 15 M^{-1} , respectively.

Significant smaller effects on the complex stability were observed for a series of *para*-substituted iodoperfluoroarenes **164–168**.¹⁰¹ Fluorine NMR titrations, fitted to a 1:1 binding mode in cyclohexane-*d*₁₂ at 298 K with tri-*n*-butylphosphine oxide, reveal stability constants $K_a [\text{M}^{-1}]$ of 12 for **164**, 5.6 for **165**, 3.9 for **166**, 3.3 for **167** and 1.3 for **168**.



Beer and co-workers reported the first example of an imidazolium-based pseudorotaxane that employs halogen bonds in order to assemble.¹⁰² The interpenetration of a series of bromo- and methyl-functionalized imidazolium derivatives **169–173** with known macrocycle **174** were studied by ¹H NMR spectroscopy in CDCl₃ at 293 K. The calculated stability constants from titration experiments reveal a pronounced association with the 2-bromo-imidazolium chloride thread **172** ($K_a [\text{M}^{-1}] = 254$) over the value obtained for the hydrogen bonded equivalent **170** ($K_a [\text{M}^{-1}] = 97$) and point at halogen bond mediated anion templated interpenetration. The almost identical behaviour of **169** ($K_a [\text{M}^{-1}] = 92$) and **170** is consistent with chloride ion hydrogen bonding in unsubstituted imidazolium systems occurring primarily through the acidic 2-position. The obtained stability constant with the 2-methyl-imidazolium thread **171** ($K_a [\text{M}^{-1}] = 245$) was explained by the authors with an altered coordination of the thread towards the anion template. Detailed analysis of the NMR spectra point at a chelating coordination of the chloride ion by hydrogen bonds originating from the 4- and 5-positions of the imidazolium subunit. In contradistinction the strongly linear nature of halogen bonds prevents a chelating effect with thread **173** and results in no noticeable interpenetration.



Anion recognition by anion-π interactions

A more recent objective in anion receptor chemistry is the use of anion-π interactions to bind anionic guests and is a topic of some controversy.¹⁰³ Frontera and co-workers synthesised the

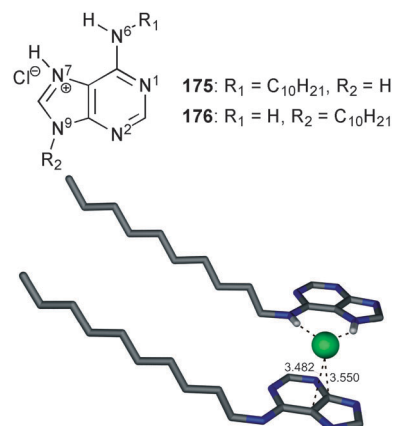


Fig. 25 Crystal structure of Cl-**176**, hydrogen and anion-π interactions represented as dotted line, non-interacting hydrogen atoms omitted for clarity.

hydrochloride salts of N⁹- and N⁶-decyladenine **175** and **176**, respectively, in order to investigate the influence of the substitution pattern on the formation of anion-π contacts.¹⁰⁴ The crystal structures of both salts reveal the presence of Cl⁻···π interactions with N⁶-decyladenine **176** only (Fig. 25). The shortest chloride-carbon distances are 3.482 and 3.550 Å. Further, the Cl⁻ ion is bound by two N-H···Cl⁻ hydrogen bonds of other ligand molecules with N···Cl⁻ distances of 2.892 and 2.784 Å.

Anion-π interactions of the pentafluorobenzyl-substituted ammonium salt **177** and the two pyridinium salts **178** and **179** were reported by Albrecht and co-workers.¹⁰⁵ All crystal structures of the Cl⁻, Br⁻, and I⁻ salts of **177** show the position of the anion on top of the π-system of the pentafluorophenyl ring (Fig. 26), while no anion-π attractions were observed in the PF₆⁻ salt of **177**. The observed C-anion distances are in the range of C···Cl = 3.757–3.951 Å (Cl-**177**), C···Br = 3.809–4.046 Å (Br-**177**) and C···I = 3.833–4.207 Å (I-**177**) and point at only a slight off-centre location of all three anions. On the other hand, the Br···π binding mode in the complexes of (Br-**178**) and (Br-**179**) depend on the substitution of the receptor. CH-anion hydrogen bonding in Br-**178** forces the

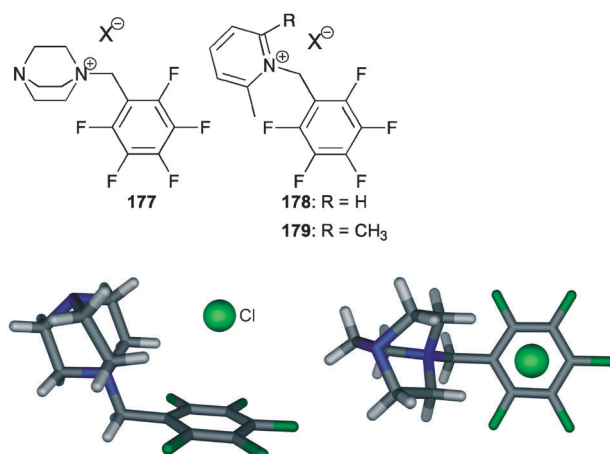


Fig. 26 Side (left) and top view (right) of the crystal structure of Cl-**177**, Br⁻ and I⁻ are very similar, structures not shown.

anion to a location towards the rim of the pentafluorophenyl group. This results in C···Br⁻ distances of 3.756 and 3.609 Å for the η^2 type interaction to the C₆F₅ unit. The additional methyl group in **179** and subsequent steric effects result in an orthogonal orientation of the pyridinium ring with respect to the C₆F₅ group. Thus the methyl substituent points over the centre of the aromatic ring and fixes the Br⁻ ion in a η^6 fashion with C···Br distances ranging from 3.492 to 3.976 Å.

The same group explored the formation of anion-π interactions between pentafluorophenyl substituted receptors **180** and **181** and polyhalide anions, such as Br₃⁻, I₃⁻ and I₄²⁻.¹⁰⁶ Crystal structure analysis reveals a η^3 and a slightly off-centre η^6 type interaction of the tribromide anion towards the C₆F₅ units of two quinoline receptors **180** (Fig. 27). The C···Br interactions in the η^3 interaction of Br1 range from 3.596 to 3.917 Å. Where C···Br3 distances are between 3.430 to 4.015 Å. The tribromide anion is unsymmetrical with a Br1–Br2 distance of 2.644 Å and a Br2–Br3 distance of 2.469 Å. The anion is bound to the protonated receptor by an N–H···Br hydrogen bond to Br1 with a N···Br distance of 3.624 Å. In contrast, the crystal structure of the bromide complex of **180** reveals a η^1 anion-π motive with a C···Br distance of 3.876 Å. The diffusion of HI into a solution of pentafluorobenzylidbenzylamine **181** in toluene and subsequent crystallisation results in the anion complex containing four protonated ligands, two triiodide ions and one tetraiodide dianion (Fig. 27). Both triiodide anions are linear with I–I bond lengths of 2.896 and 2.921 Å. The observed I–I distances of the symmetrical dianion I₄²⁻ are 2.762 Å (I–I_{internal}) and 3.363 Å (I–I_{terminal}). Anion-π interactions were observed for the triiodide anion, which is positioned in a side-on fashion to the C₆F₅ moiety of the receptor. The C···I distances to the central iodine atom I2 range from 3.804 to 4.082 Å. The tetraiodide dianion is involved in N–H···I hydrogen bonds (N···I distance 3.496 Å) and in anion-π interactions to two electron-poor phenyl rings with C···I distances of 3.661 and 4.068 Å.

Anion-π interactions of the extended π-electron deficient receptor **182** were investigated in the solid state and in solution

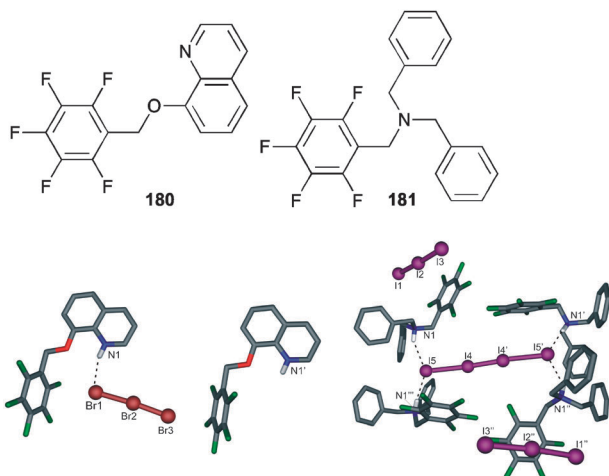


Fig. 27 Crystal structure of (Br₃)·H**180** (left) and (I₄)·(I₃)₂·(H**181**)₄ (right) with selected atom labels, hydrogen bonds represented as dotted lines, co-crystallised solvent molecules and non-interacting hydrogen atoms omitted for clarity.

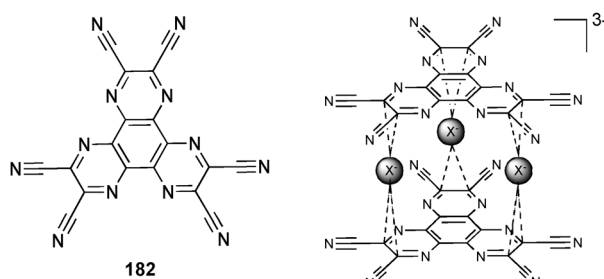
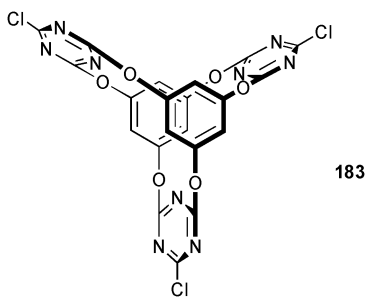


Fig. 28 Schematic draw of **182** (left) and diagram of the stacked [X₃·**182**]³⁻ adduct (right).

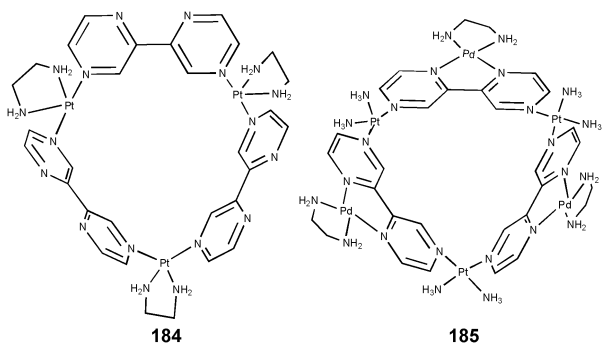
by Chifotides and co-workers.¹⁰⁷ The crystal structure of the Br⁻ complex reveals a stacked assembly of [Br₃·**182**]³⁻ units linked by one Br⁻ ion as observed previously for the iodide complex of **182** (Fig. 28).¹⁰⁸ In both structures the three equivalent halide ions are bound to the pyrazine external carbon atoms C_{ext} in a η^2 , η^2 fashion, with distances up to 0.35 Å shorter than the sum of the van der Waals radii. The observed C···Br distances range from 3.245 to 3.280 Å where C···I distances are between 3.337 and 3.419 Å. UV-Vis, ¹³C and halogen NMR studies are evidence for the formation of the similar [X₃·**182**]³⁻ assembly of the tetrabutylammonium salts of Cl⁻, Br⁻, I⁻ and **182** in CD₃NO₂ and THF-d₈ solution. Job plot experiments provide evidence for a 2:3 (or 1:1.5) (L:A) stoichiometry of the present complex. Downfield shifts of the single ¹³C_{ext} resonances by 1–3 ppm upon the addition of the halides point at comparable interactions between the anions and the receptor in solution as observed in the solid state. Additional ³⁵Cl, ⁸¹Br and ¹²⁷I NMR studies in CD₃NO₂ and THF-d₈ exhibit a single resonance with a considerable downfield shift with respect to the corresponding free halide ions and support the formation of similar [X₃·**182**]³⁻ assemblies in solution. Quantitative analyses in THF of the new absorption bands at 630, 419 and 408 nm for I⁻, Br⁻ and Cl⁻, respectively, as a function of the respective concentration of the anion were performed to determine the K_{CT} [M⁻¹] values of 3780 for Cl⁻, 2200 for Br⁻ and 940 for I⁻. Comparable experiments in CH₃NO₂ reveal K_{CT} [M⁻¹] values of 71 for Cl⁻, 48 for Br⁻ and 20 for I⁻ employing the absorption bands at 557, 406 and 390 nm, respectively. The observed order K_{CT,Cl} > K_{CT,Br} > K_{CT,I} in both solvents is in accordance with the order of Lewis basicity and thus the electron donating ability of the anion in the CT complex.

The anion-π interactions of the conformationally rigid triazine ring containing cage **183** were studied by Wang and co-workers in both solid state and solution.¹⁰⁹ Isothermal titration calorimetry in acetonitrile reveals the formation of 1:1 complexes with the tetrabutylammonium salts of F⁻, Cl⁻ and Br⁻. The calculated stability constants K_a [M⁻¹] are 361 for F⁻, 146 for Cl⁻ and 95 for Br⁻. Proton NMR studies of the complex formation give no evidence for the anion binding being originated by hydrogen bonding in solution. The C₃ symmetric crystal structure of chloride complex shows a 1:3 (host:guest) stoichiometry with one Cl⁻ ion located in each of the three ligand clefts. The anion forms η^1 interaction to a carbon atom of one triazine ring with a C···Cl distance of 3.342 Å and is further bound by a C–H···Cl (C···Cl distance

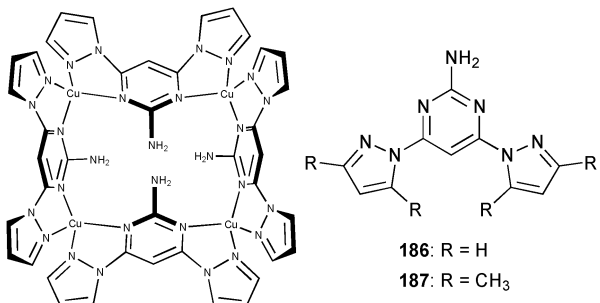
3.541 Å) and an O–H···Cl (O···Cl distance 3.541 Å) hydrogen bond to the ligand backbone and a co-crystallised water molecule.



Lippert and co-workers observed the presence of anion–π interactions towards the oxo-anions NO_3^- ¹¹⁰ and SO_4^{2-} ¹¹¹ encapsulated in the cationic triangular Pt_3 -tris(2,2'-bipyrazine) based metallo-macrocycles **184** and **185**, respectively. Two O atoms of a sandwiched NO_3^- anion in **184** form two O···π interaction with the pyrazine rings with O···π distances of 3.270 and 3.587 Å. Where one O atom of the positionally disordered SO_4^{2-} atom in **185** is involved in two anion–π interactions with O···π distances between 2.898 and 3.063 Å.



The anion–π interactions towards the anion encapsulated in the 2 × 2 grid like metallo-macrocycles formed by four Cu(I) centres linked by the four aminopyrimidine based ligands **186** and **187** were reported by Manzano and co-workers.¹¹² The crystal structures of the ClO_4^- complex of **186** and **187** as well as the BF_4^- and OTf^- (trifluoromethanesulfonate anion) complex of **187** reveal close contacts between the encapsulated anion and the centroid of the aminopyrimidine moiety of the ligand. The shortest O···centroid distance in the ClO_4^- complexes is 3.084 Å in **186** and 2.848 Å in **187**, respectively. The OTf^- O···centroid distance is 2.868 Å in **187**, where 2.848 Å is the shortest observed F···centroid distance in the BF_4^- complex of **187**.



Ion pair recognition

Ditopic receptors for ion pair recognition continue to be developed by a number of groups world-wide. Such systems provide a distinct binding site for cationic and anionic species and enable an enhanced binding due to electrostatic attraction. This was demonstrated by Sessler and co-workers in their continued work on calix[4]arene strapped calix[4]pyrroles such as **188**.¹¹³ Quantitative proton NMR studies in 10% $\text{CD}_3\text{OD}/\text{CDCl}_3$ show no significant proton shift when CsClO_4 or $n\text{-Bu}_4\text{NF}$ is added. However, when CsF or CsClO_4 and $n\text{-Bu}_4\text{NF}$ are added simultaneously a significant change in the proton signals of both the calix[4]arene and the calix[4]pyrrole moiety is observed. ITC experiments in the same solvent mixture reveal a stability constant of $K_a = 1.3 \times 10^4 \text{ M}^{-1}$ for a 1:1 binding mode of CsF and **188**. No indication of similar ion pair binding was observed in proton NMR studies with other metal ions, such as Li^+ , Na^+ , K^+ , Rb^+ or NH_4^+ . This suggests that anion binding by **188** occurs only in the presence of Cs^+ . Comparable experiments with CsClO_4 and tetrabutylammonium salts of Cl^- , Br^- and NO_3^- show ion pair binding for all studied anions, with CsF as the preferred ion pair. In the crystal structure, the CsF ion pair is solvent-bridged by a co-crystallised water molecule (Fig. 29). As expected, the F^- anion is bound by four NH···F bonds (N···F distance between 2.793 to 2.809 Å) in the calix[4]pyrrole moiety and the Cs^+ ion is bound by ion-dipole interactions with two oxygen atoms and by cation–π interactions involving the calix[4]arene moiety in the 1,3-alternate conformation.

In a similar fashion, Jabin and Menand¹¹⁴ employed the known tren-capped calix[6]arene **189**¹¹⁵ for the recognition of anions and contact ion pairs. Proton NMR experiments in CD_3CN of a 1:1 mixture of the host **189** and the tetrabutylammonium salts of Cl^- , Br^- , CN^- and AcO^- reveal a slow exchange at 243 K, which enables the calculation of the stability constants from the integration of the appropriate signals. Where the constants for N_3^- and NO_3^- were calculated from titration experiments performed at 298 K. A preferred binding of Cl^- ($K_a = 48\,300 \text{ M}^{-1}$) over Br^- ($K_a = 1930 \text{ M}^{-1}$), CN^- ($K_a = 640 \text{ M}^{-1}$), N_3^- ($K_a = 215 \text{ M}^{-1}$), AcO^- ($K_a = 160 \text{ M}^{-1}$) and NO_3^- ($K_a = 98 \text{ M}^{-1}$) was observed.

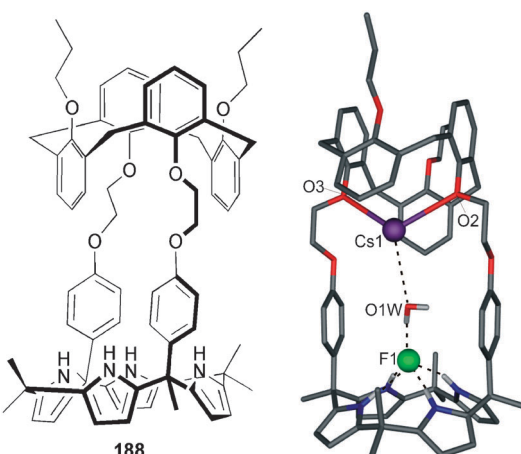
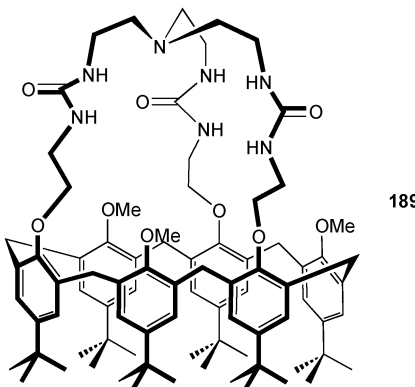
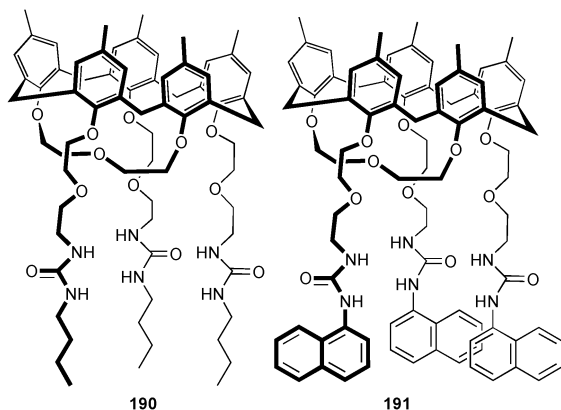


Fig. 29 Schematic drawing of **188** (left) and crystal structure of $(\text{Cs}-\text{H}_2\text{O}-\text{F}) \subset \text{188}$ (right) with selected atom labels, hydrogen bonds represented as dotted line, co-crystallised solvent molecules and non-interacting hydrogen atoms omitted for clarity.

Comparable experiments in the presence of PrNH_3Cl reveal a significant enhanced stability constant of $K_a > 1.6 \times 10^9 \text{ M}^{-2}$ ($K_a = [\text{PrNH}_3\text{Cl} \subset 189]/[189][\text{PrNH}_3^+][\text{Cl}^-]$) for the ion pair in CDCl_3 at 258 K.



Gattuson and co-workers employed the (1,3)-bridged calix[5]arene-crown-3 receptors **190** and **191** for the recognition of ion pairs.¹¹⁶ Proton NMR titration experiments were performed in CD_2Cl_2 with n-butylammonium ($n\text{-BuNH}_3^+$) hexafluorophosphate, tetrabutylammonium halides and n-butylammonium halides to assess stability constants of the $n\text{-BuNH}_3^+$ cation and the anions Cl^- , Br^- and I^- , both independent and as ion pair. The stability constants calculated using a 1:1 binding mode are summarised in Table 13 and show clearly an enhanced binding for the ion pair.



The recognition of amino acid ammonium salts (tetrabutyl- and tetramethylammonium) by heteroditopic chiral uranyl-salen receptor substituted with 1-oxypyrenyl groups (**192**) reported Tomaselli and co-workers.¹¹⁷ UV-Vis spectral studies

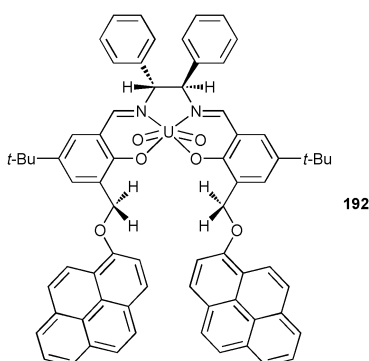


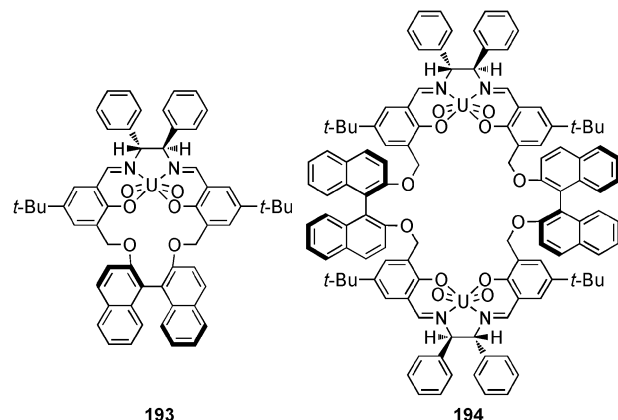
Table 13 Conditional stability constants of **190** and **191** in CD_2Cl_2 at 298 K

	190	191
$n\text{-Bu-NH}_3^+{}^a$	$(5.3 \pm 0.3) \times 10^3 \text{ M}^{-1}$	$(2.1 \pm 0.1) \times 10^4 \text{ M}^{-1}$
$\text{Cl}^-{}^b$	$39 \pm 14 \text{ M}^{-1}$	$577 \pm 66 \text{ M}^{-1}$
$\text{Br}^-{}^b$	$7 \pm 5 \text{ M}^{-1}$	$178 \pm 15 \text{ M}^{-1}$
$\text{I}^-{}^b$	$< 5 \text{ M}^{-1}$	$27 \pm 2 \text{ M}^{-1}$
$n\text{-Bu-NH}_3\text{Cl}$	$> 10^{10} \text{ M}^{-2}$	$> 10^{10} \text{ M}^{-2}$
$n\text{-Bu-NH}_3\text{Br}$	$> 10^{10} \text{ M}^{-2}$	$> 10^{10} \text{ M}^{-2}$
$n\text{-Bu-NH}_3\text{I}$	$> 10^{10} \text{ M}^{-2}$	$> 10^{10} \text{ M}^{-2}$

^a Added as PF_6^- salt. ^b Added as the $n\text{-Bu}_4\text{N}^+$ salt.

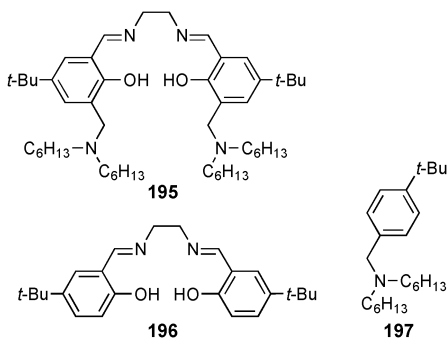
indicate a 1:1 binding stoichiometry in CHCl_3 solution. High binding affinities were noted along with good enantiomeric selectivity for L-Phe over D-Phe with binding constants of 2.50×10^6 and $7.36 \times 10^4 \text{ M}^{-1}$, respectively. T-ROESY NMR experiments show cation- π and CH- π interactions of the pyrene moieties and the ammonium cations and result in the formation of stable complexes with chiral carboxylate guests.

The same group also employed the chiral uranyl-salen macrocycles **193** and **194** for the recognition of chiral and achiral ammonium halide salts (tetramethylammonium, tetraethylammonium, tetrabutylammonium, acetylcholine, trimethyl-anilinium, benzyltrimethylammonium and (a-methylbenzyl)-trimethylammonium).¹¹⁸ Detailed T-ROESY NMR experiments show that the binding of the cation occurs by CH- π and π - π interactions of the binaphthyl, or the salicylaldehyde moiety, or the phenyl rings of the diimine bridge, where the halide ion is bound on the uranyl side.



Tasker and co-workers continued their work on the use of polytopic ligands for the extraction of metal salts. The authors show a significant enhanced metal-to-ligand loading and extraction ability ($\approx 250\%$ Zn to receptor) by the coordination of Zn^{2+} and anionic chlorozincate species, such as ZnCl_4^{2-} , $\text{Zn}_2\text{Cl}_6^{2-}$ or ZnCl_3^- , in the polytopic salen based ligand system **195**.¹¹⁹ Comparable dual host extraction experiments with 1:2 mixture of the simple salen ligand **196** and the tertiary amine **197** result in a reduced Zn extraction power (loading up to 150% Zn to receptor **196**). Proton NMR shifts of the azomethine and the 3-aminomethyl signals of **195** at ZnCl_2 loading $> 100\%$ indicate the coordination of Zn^{2+} in the salen moiety and the interaction of a chlorozincate species with the anion binding sides.

On the other hand, Plieger and co-workers used an *in situ* formed metallo-macrocycles based on the 2:2 coordination of



Cu(II) and the salicyl-aldimine ligand **198** for the binding of anions (Fig. 30).¹²⁰ Crystal structures of the ClO_4^- and NO_3^- complexes show the uptake and coordination of the anion by multiple NH and CH hydrogen bonds in the metallo-macrocycle. In addition, the ClO_4^- ion is coordinated by direct Cu–O– ClO_4^- interactions as previously observed for BF_4^- and SO_4^{2-} complexes.¹²¹ Changes in the UV-Vis absorption of the cationic Cu(II)-complex $[\text{Cu}(\text{b}198_2)]^{4+}$ upon the addition of acids in isopropanol were employed to calculate the stability constants. Job plot experiments show the formation of 1:1 complexes. The calculated stability constants show a preferred uptake of SO_4^{2-} ($\log K_a = 5.07$) over H_2PO_4^- ($\log K_a = 4.34$), ClO_4^- ($\log K_a = 3.38$), BF_4^- ($\log K_a = 3.03$) and NO_3^- ($\log K_a = 2.95$) and reflect the influence of the anion charge, size and ability to form coordinative bonds to the metal centres in the complex.

Huang and co-workers synthesised the unsymmetric diamide bis(*m*-phenylene)[32]crown-10 cryptands **199** and **200** and studied their ion pair binding of various dipyridinium dication salts **201**–**203**.¹²² Single crystal X-ray diffraction and proton NMR titrations in CD_3CN show the interaction of the amide groups and the CH_2 crown ether backbone with the Cl^- ions and dipyridinium cations. Job plot experiments based on UV-Vis absorption data in $\text{CHCl}_3/\text{CH}_3\text{OH}$ show a 1:1 stoichiometry. The highest stability constant for the binding of the 4,4'-bispyridinium chloride salt **201** was obtained for cryptand **200** ($K_a = 1.7 \times 10^4 \text{ M}^{-1}$ for **200** and $K_a = 4.8 \times 10^3 \text{ M}^{-1}$ for **199**), presumably due to the additional anion binding site supplied by the acidic phenyl hydrogen atom. The effect of the nature of the anion on the ion pair binding in **199** and **200** was investigated by comparing experiments with the Cl^- and PF_6^- salts of the bishexyl-dipyridinium dication salts

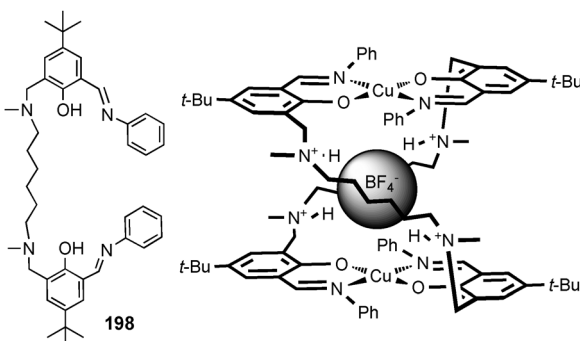
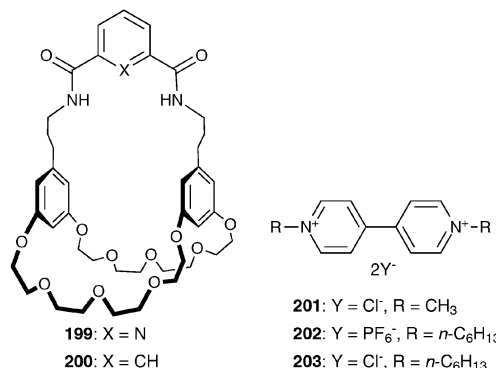
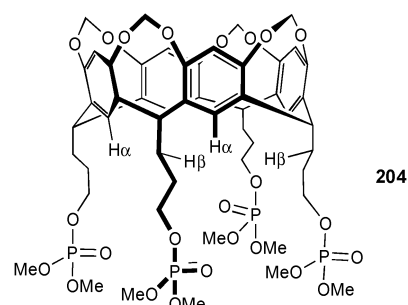


Fig. 30 Schematic draw of **198** (left) and diagram of the anion encapsulated 2:2 metallo-macrocycle formed by **198** and two Cu(II) metal centres (right).

202 and **203**. Stability constants of $7.8 \times 10^2 \text{ M}^{-1}$ with **199** and $6.3 \times 10^2 \text{ M}^{-1}$ with **200** for the PF_6^- salt **202** are significantly smaller than those obtained for the Cl^- salt **203** ($K_a = 2.4 \times 10^3 \text{ M}^{-1}$ for **199** and $K_a = 3.4 \times 10^3 \text{ M}^{-1}$ for **200**).

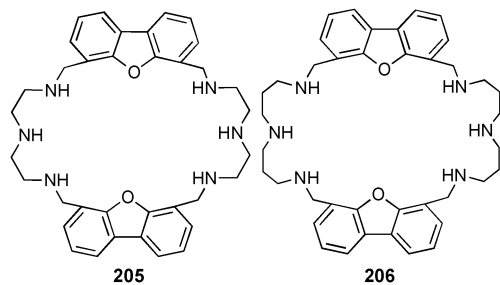


Another example of the recognition of ion pairs was reported by Dalcanale and co-workers.¹²³ Proton NMR titrations of the phosphate triester functionalized cavitand **204** in acetone- d_6 with the tetrabutylammonium salts of Cl^- , Br^- and I^- result in significant shifts of the aromatic CH ($\text{H}\alpha$) and the ArCH_2CH_2 protons ($\text{H}\beta$). The calculated stability constants $K_a [\text{M}^{-1}]$ are 150 for Cl^- , 140 for Br^- and 73 for I^- . Phosphorous NMR experiments show a negligible interaction towards the tetrabutylammonium cation ($\Delta\delta = -0.005 \text{ ppm}$). Comparable titration experiments with the n-octylammonium salts in CDCl_3 reveal stability constants of $1.5 \times 10^3 \text{ M}^{-1}$ for Cl^- and $2.1 \times 10^4 \text{ M}^{-1}$ for Br^- . Significant shifts of both the aromatic CH proton ($\text{H}\alpha$) in ^1H experiments and the phosphate triester signal in ^{31}P experiments are evidence that the ion pair is bound in the cavitand, resulting in higher stability constants for the binding of halide anions.

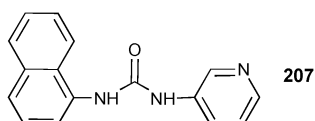


The recognition of carboxylate anions, such as oxalate (ox^{2-}), malonate (mal^{2-}), phthalate (ph^{2-}), isophthalate (iph^{2-}) and terephthalate (tpf^{2-}), in cascades formed between two Cu(II) centres in the hexaazamacrocycles **205** and **206** was reported by Delgado and co-workers.¹²⁴ The crystal structure reveals the cascade coordination of two phthalate anions by the two Cu(II) centres in the macrocycle **205**, where each metal centre is coordinated by three carboxylate oxygen atoms of the anions and three N-donor atoms of the ligand. The Cu–O bond distance of the single O-atom is 1.925 Å where the Cu–O distances of the two chelating carboxylate oxygen atoms are 2.387 and 2.866 Å. UV-Vis absorption titration experiments were utilized to obtain the stability constants of the 1:1 and 1:2 (host:guest) association of the dianions and the dicopper(II) complexes of **205** and **206**. In general, higher values were

observed for the larger macrocycle **206**, except for mal²⁻ where $\log K_{11} = 4.50$ and $\log K_{12} = 2.53$ for **205**, as opposed to $\log K_{11} = 4.06$ and $\log K_{12} = 2.96$ for **206**. The anions with a shorter distance between the two binding sites are preferred by both receptors, with stability constants for ox²⁻ of $\log K_{11} = 4.54$ and $\log K_{12} = 2.73$ for **205** and $\log K_{11} = 5.08$ and $\log K_{12} = 2.88$ for **206** and $\log K_a$ values for ph²⁻ of 4.01 and 2.75 for **205** and 4.08 and 3.13 for **206**. Consequently smaller values were obtained for iph²⁻ ($\log K_{11} = 3.43$ and $\log K_{12} = 1.82$ for **205** and $\log K_{11} = 3.78$ and $\log K_{12} = 2.81$ for **206**) and tph²⁻. For the latter only the formation of 1:1 complex was observed with $\log K_{11} = 3.07$ for **205** and $\log K_{11} = 3.61$ for **206**.

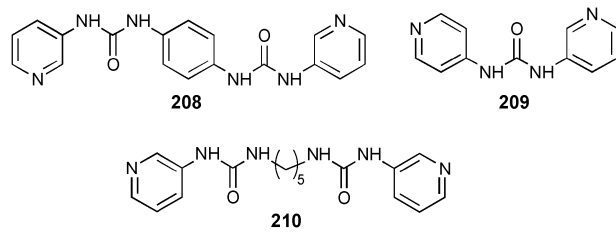


The simple monopyridylurea receptor **207** was employed by Wu and co-workers for the coordination of ZnSO₄.¹²⁵ Depending on the synthetic route two different complexes were isolated, both by slow evaporation of methanol. [Zn(SO₄)**207**₃]·CH₃OH was obtained when Zn(SO₄)·7H₂O dissolved in CH₃OH was added to a solution of **207** in CH₃OH, whereas {[Zn(μ_2 -SO₄)**207**₂]·0.5CH₃OH}_n was isolated when the ligand was added to the metal salt. The anion is coordinated by multiple N-H···O hydrogen bonds in both complexes (with N···O distances between 2.931 and 3.069 Å in [Zn(SO₄)**207**₃]·CH₃OH and between 2.775 and 3.017 Å in {[Zn(μ_2 -SO₄)**207**₂]·0.5CH₃OH}_n) and by direct metal anion interactions. The disordered tetrahedral coordination spheres of the metal centres are saturated by interactions to the N_{py} atom of the ligand.



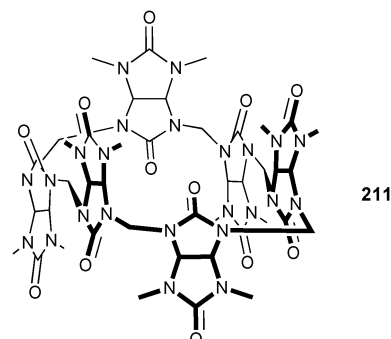
Similarly, Dastidar and co-workers^{126,127} employed a variety of bis-pyridylurea receptors for the separation of sulfate over other oxo-anions, such as nitrate and perchlorate by selective crystallisation in metal-organic frameworks. Upon the coordination of Zn(II) by **208** a 3-D framework is formed that coordinates a sulfate anion via six hydrogen bonds with three ligand molecules with N···O distances between 2.621 and 2.940 Å and a Zn(II)-O-SO₃ bond of 2.111 Å.¹²⁶ On the other hand, the treatment of **209** with CdSO₄ results in a framework where the sulfate anion is bound by four N-H···O hydrogen bonds with N···O distances between 2.835 and 3.200 Å originating from two ligands and a Cd(II)-O-SO₃ interaction of 2.339 Å.¹²⁷ Both crystallisations were repeated in the presence of mixtures of sulfate, perchlorate, nitrate and triflate as Zn(II) salts and a mixture of CdSO₄, Cd(NO₃)₂, Cd(ClO₄)₂, Cd(OAc)₂, CdCl₂ and CdBr₂, respectively. The isolated material shows comparable

FT-IR, XRPD and elemental analysis data to the results obtained for their sulfate salts, respectively and demonstrates the selective uptake of sulfate into the crystals. The same behaviour was observed by Wu and co-workers¹²⁸ for the pentyl linked bis-pyridylurea receptor **210**. Again, a selective uptake of sulfate was observed upon crystallisation of the Zn(II) linked framework.

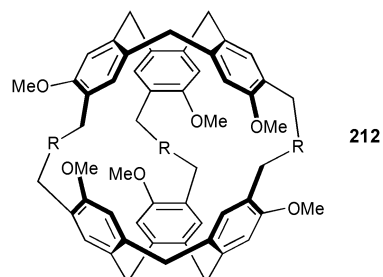


Others receptors

The novel halide selective macrocycle **211**, that was directly prepared by the condensation of 2,4-dimethylglycoluril with formaldehyde in the presence of HCl, was reported by Sindelar and co-workers.¹²⁹ Quantitative proton NMR studies in CD₃OD/CDCl₃ (2:1) show a preferred uptake of I⁻ over Br⁻, Cl⁻ and F⁻. The crystal structures of the Cl⁻ complex shows the uptake of the anion in the cavity and coordination by 12 weak C-H···anion bonds originating from the methine carbon atoms on the convex face of the glycoluril unit. The average C···anion distance in the Cl⁻ complex is 3.707 Å.



In contradistinction, Holman and co-workers encapsulated larger anions such as BF₄⁻ and PF₆⁻ in continued work on cryptophane cavitands of the general type **212**.¹³⁰



Commercially available amine terminated dendrimers (AT-PAMAM) have been employed by Anslyn and co-workers as anion receptors.¹³¹ UV-Vis studies employing anionic indicators such as fluorescein, pyrogallol red (PR) and pyrocatechol violet (PV) were performed in methanol/water (1:1 and 95:5 CH₃OH/H₂O for fluorescein, pH = 7 buffered with 25 mM HEPES) to monitor the level of anionic uptake by generation

3 to 7 AT-PAMAM. Bathochromic shifts observed upon the addition of the AT-PAMAM were found to be due to the deprotonation of the indicator as the interaction of the dendrimer lowers the pK_a of the indicator. The estimated stoichiometries were determined by extrapolating the binding isotherms saturation point. Stoichiometries by the generations 5, 6 and 7 of AT-PAMAM was found to be 3, 6 and 14 PV molecules respectively for each dendrimer while the PR uptake by generations 4, 5 and 6 was found to be significantly higher at 8, 16 and 32 molecules of PR per respective dendrimer. This showed the high level of anionic guests accommodated in the commercially available AT-PAMAM dendrimers.

Anion transport

Another application of anion receptor chemistry is the development of compounds that can bind and transport anions across lipid membranes, either as synthetic channels or as mobile carriers.⁴ J.T. Davis and co-workers facilitated sphingolipid C2-ceramide **213** as a mobile carrier for Cl^- and HCO_3^- transmembrane transport.¹³² Proton NMR studies show a significant shift of the NH and OH protons in water saturated CD_2Cl_2 upon addition of Cl^- or HCO_3^- anions and confirm that the ceramide head-group is a potent anion binder. Titration experiments reveal a stability constant $K_a [\text{M}^{-1}]$ of 1734 for $n\text{-Bu}_4\text{NCl}$ for a 1:1 binding mode. Transport ability was studied in egg-yolk phosphatidylcholine (EYPC) vesicles loaded with 100 mM NaCl and 2 mM lucigenin, a chloride-sensitive dye, and dispersed in a 100 mM solution of either NaNO_3 , NaHCO_3 or Na_2SO_4 . The addition of **213** (1 mol%) results in an increase in fluorescence and indicates the efflux of Cl^- when NO_3^- or HCO_3^- is present as external anion (Fig. 31). Comparable experiments with doubly charged SO_4^{2-} present as the

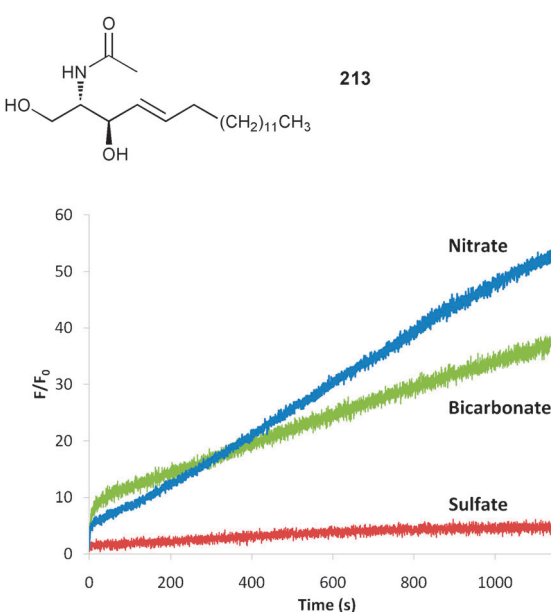


Fig. 31 Observed relative fluorescence in Cl^- transport assays promoted by **213** at 1 mol% receptor to EYPC liposomes (100 nm, 200 μM) with various external anions in 20 mM HEPES buffer ($\text{pH} = 7.4$). *Chem. Commun.* 2010, **46**, 3950–3952. Reproduced with permission of The Royal Society of Chemistry.

anion in the extravesicular solution show minimal Cl^- transport. This evidence suggests an anion-exchange mechanism and provides evidence against the formation of large pores by **213**, as observed in previous studies at high concentrations (> 10 mol%).¹³³

Judd and A. P. Davis continued their research on cyclosteroids such as **214** and **215**, containing a macrocyclic unit for anion recognition.¹³⁴ Transport studies were performed in 1-palmitoyl-2-oleoylphosphatidylcholine (POPC)/cholesterol (7:3 ratio) vesicles with pre-incorporated receptors in a 1:2500 ratio. The vesicles were loaded with 225 mM NaNO_3 and 1 mM lucigenin and dispersed in 225 mM NaNO_3 . The addition of NaCl (final concentration 25 mM) results in a Cl^- influx, indicated by quenched fluorescence (Fig. 32). Comparable experiments with the acyclic analogues **216** and **217** illustrate strikingly an enhanced $\text{Cl}^-/\text{NO}_3^-$ transport activity of the macrocyclic receptors **214** and **215**.

The trent based urea and thiourea receptors **218–221** were employed by Gale and co-workers for the transmembrane transport of Cl^- by either $\text{Cl}^-/\text{NO}_3^-$ or $\text{Cl}^-/\text{HCO}_3^-$ antiport mechanisms.¹³⁵ Therefore POPC vesicles loaded with 489 mM NaCl were dispersed in either NaNO_3 (489 mM) or Na_2SO_4 (167 mM) and upon the addition of the receptor the Cl^- efflux was monitored using a Cl^- selective electrode. For experiments investigating HCO_3^- transport, NaHCO_3 was added to the external Na_2SO_4 solution as a pulse after 120 s to give an overall HCO_3^- concentration of 40 mM. The observed Cl^-

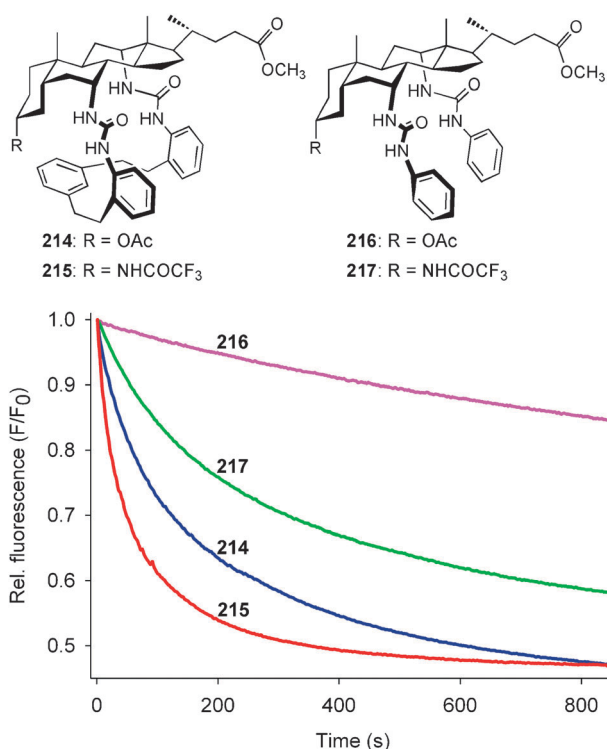
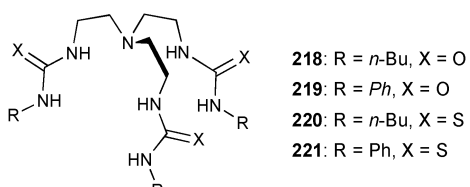
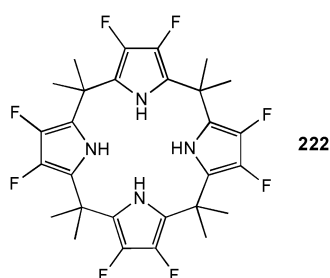


Fig. 32 Observed relative fluorescence promoted by **214–217** at 1:2500 receptor to lipid ratio in Cl^- transport assays into vesicles (7:3 POPC/cholesterol, 04 mM, 200 nm diameter). Vesicles loaded with 225 mM NaNO_3 and 1mM lucigenin, final external NaCl concentration 25 mM. *Chem. Commun.* 2010, **46**, 2227–2230. Reproduced with permission of The Royal Society of Chemistry.

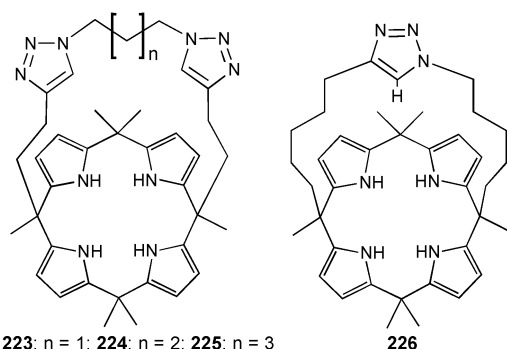
efflux reveals a significant activity of the thiourea receptors **220** and **221** (>90% for $\text{Cl}^-/\text{NO}_3^-$ and >75% for $\text{Cl}^-/\text{HCO}_3^-$ over the time of the experiment), whereas the urea analogues **218** and **219** are less active and point at a pronounced influence of the substituent (about 30% Cl^- efflux with phenyl substituted **218** and negligible transport for **219** with *n*-Bu moieties). Furthermore, the authors provide direct evidence of transmembrane transport of HCO_3^- by comparable ^{13}C NMR experiments. Distinct ^{13}C NMR signals for intravesicular ($\delta \approx 161$ ppm) and extravesicular $\text{H}^{13}\text{CO}_3^-$ ($\delta \approx 160$ ppm) are observed in the presence of **220** and **221** and the subsequent addition of Mn^{2+} results in a broadened signal of the extravesicular $\text{H}^{13}\text{CO}_3^-$ into the baseline, illustrating the transport of HCO_3^- by **220** and **221**.



Gale, Sessler and co-workers continued their work on *meso*-octamethylcalix[4]pyrroles as ion transporters through lipid bilayers.¹³⁶ An extended series of POPC vesicles studies reveal that the presence of electron-withdrawing fluorine substituents in **222** results in a change in the transport mechanism. Fluorinated **222** is capable of acting as a $\text{Cl}^-/\text{NO}_3^-$ and $\text{Cl}^-/\text{HCO}_3^-$ antiport agent, whereas the parent calix[4]pyrrole **88** functions as a membrane transporter for the cesium chloride ion pair only.

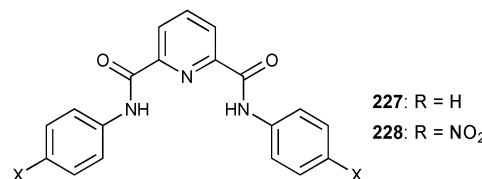


Gale and co-workers observed the same switch in transport mechanism for a series of strapped calix[4]pyrroles **223–225**.¹³⁷ The new receptors contain two triazole groups and show a decreasing dependence of the Cl^- transport activity on the type of group one metal counterion. This suggests that the predominant cesium chloride ion pair co-transport process for

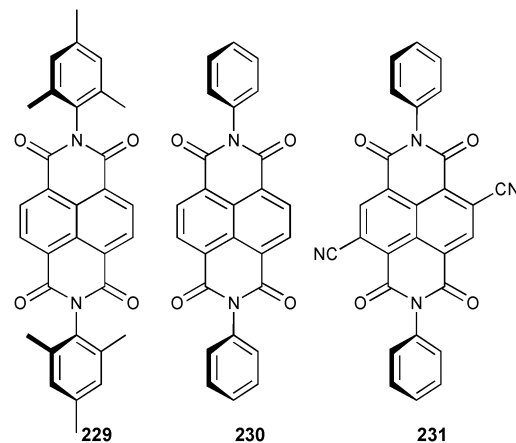


223, is replaced by a $\text{Cl}^-/\text{NO}_3^-$ antiport process with compound **225**. The transport efficiency of the previous generation compound **226**¹³⁸ lies between those of **224** and **225** for $\text{Cl}^-/\text{NO}_3^-$ antiport.

A switch between transmembrane anion transport mechanism from mobile carriers to synthetic channels was observed by Gokel and co-workers in their study of the dipicoline-amides **227** and **228**.¹³⁹ Fluorescence quenching in dioleoyl-phosphatidyl choline (DOPC) vesicles loaded with 225 mM NaNO_3 and 1 mM lucigenin shows an influx of Cl^- mediated by both receptors. Hill plot analysis of the transport mediated by **228** at various concentrations suggests that both mobile carrier and channel mechanisms may be present. Planar bilayer conductance technique¹⁴⁰ reveals the formation of channels for **228**, whereas no conductance behaviour was obtained for **227**.

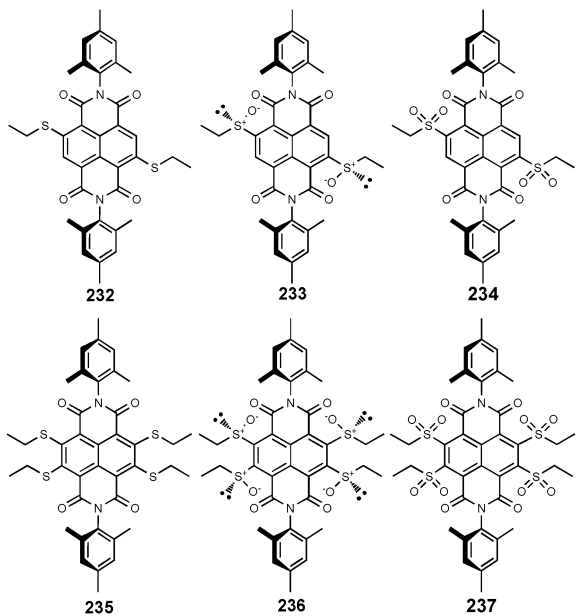


Matile and co-workers continued their work on synthetic channels formed by naphthalenediimides (NDI) derivatives to prove the functional relevance of anion–π interactions for the transmembrane transport of anions.¹⁴¹ Laser-induced ESI-MS and charge-transfer absorption spectra illustrate the formation of anion complexes of the simple NDI derivatives **229** and **230**, whereas transport studies using different fluorescent probes in EYPC vesicles prove anion transport facilitated by **231**. Therefore vesicles experiments were repeated with 8-hydroxy-1,3,6-pyrenetrisulfonate (HPTS), 5(6)-carboxyfluorescein (CF) and lucigenin (LG) encapsulated and the ‘effective’ monomer concentration needed to achieve 50% activity (EC_{50}) was determined for each experiment. The authors use a quantitative comparison of the obtained EC_{50} values for **231** for the transport of Cl^- (0.75 μM for LG, 0.33 μM for HPTS and >100 for CF) to conclude a pronounced anion over cation or dye transport due to the formed channels of the receptor. The authors explain their observations due to the presence of anion–π interactions.

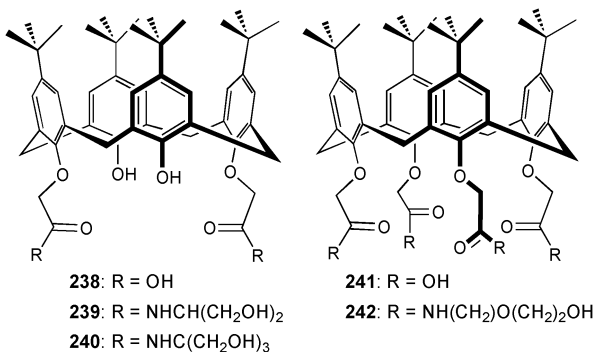


The same group also employed a series of sulfur substituted NDI derivatives for the transmembrane transport by channels employing anion–π interactions.¹⁴² The stepwise oxidation of

the sulfide donors in **232** or **235** to the sulfoxides **233** and **236** and the more powerful sulfones **234** and **237** results in an increase in the π - acidity of the NDI core and subsequently a higher anion transport activity was observed.

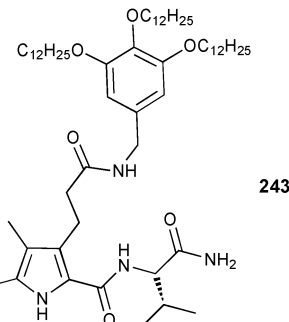


Bulk lipid membrane transport experiments were performed by Mutihac and co-workers to probe the acid and amido functionalized calix[4]arenes **238-242** as transporters for the amino acid esters L-tryptophane methylester (L-TrpOMe), L-phenylalanine methylester (L-PheOMe) and L-tyrosine methylester (L-TyrOMe).¹⁴³ A pH gradient was applied (source phase pH = 5.5, receiving phase pH = 1.5) across the CHCl₃ membrane and UV-Vis absorption spectroscopy was used to determine the amino acid concentration in the source phase and receiving phase after 24 h. The obtained transport yield shows a transport ability in the order L-TrpOMe > L-PheOMe ≫ L-TyrOMe for all receptors, with the acid **240** and the amido calix[4]arene **242** as the most efficient transporters.



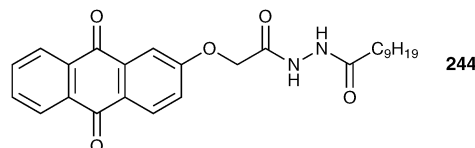
Another carrier for amino acids in bulk CHCl₃ lipid membranes was reported by Urban and Schmuck.¹⁴⁴ The low pK_a value of approximately 6–7 of the guanidinocarbonyl pyrrole group in **243** enables a pH dependent binding of amino acid under ambient conditions.¹⁴⁵ Thus, proton driven symport of the N-acetylated L-amino acid of alanine (Ala), valine (Val) tyrosine (Tyr), phenylalanine (Phe) and tryptophan (Trp) was observed in simple U-tube experiments from a source phase

(pH = 6) to the receiving phase with a pH of 8. The transport studies reveal a decreasing flux for Val over Phe, Ala, Trp and Tyr for single amino acid experiments, while competitive experiments show a reduced flux and an order of Trp > Phe > Val > Tyr > Ala. The authors explain this observation using the binding strength of **243** towards the amino acids. The lower stability constant for Val ($K_{\text{ass}} [\text{M}^{-1}] = 4.3 \times 10^3$) favours the release of the substrate into the receiving phase and result in the highest flux of Val ($1.1 \times 10^{-6} \text{ mol m}^{-2} \text{ s}^{-1}$) in the single amino acid experiments. In contradistinction, the stronger binding of Trp ($K_{\text{ass}} [\text{M}^{-1}] = 1.5 \times 10^4$) leads to preferred transport in the competitive setup (flux: $2.1 \times 10^{-7} \text{ mol m}^{-2} \text{ s}^{-1}$).

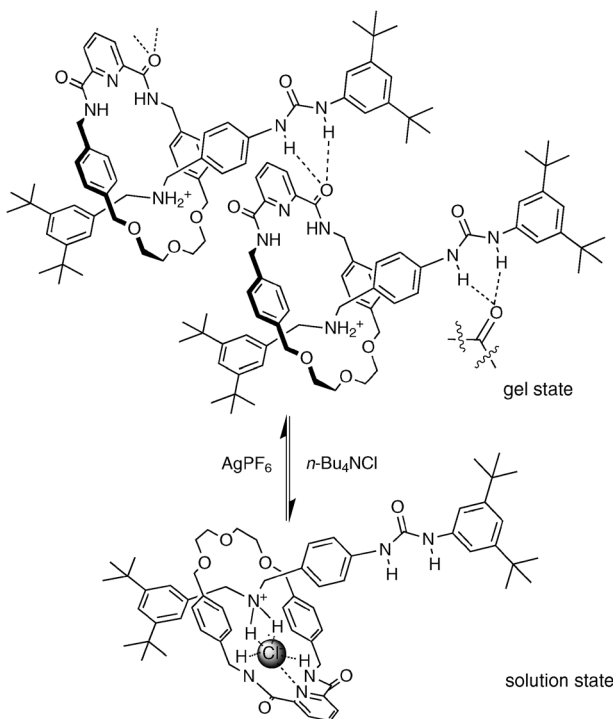


Anion-controlled gelation

Another interesting application of anions is in the field of organogels, in which they may be used to trigger gel–sol transitions. Chen and co-workers reported this process, along with a significant colour change, when H₂PO₄[−], AcO[−] and F[−] are added to the gel formed by **244** in CHCl₃, whereas Cl[−], Br[−] and I[−] do not cause a gel–sol transition.¹⁴⁶ Closer examination in UV-Vis and proton NMR experiments in DMSO-d₆ reveal a deprotonation of the hydrazine NH group in **244** upon the addition of H₂PO₄[−], AcO[−] and F[−].



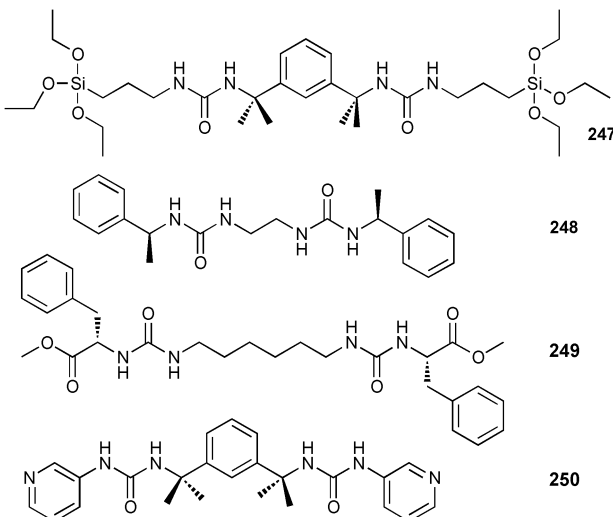
A novel anion induced sol–gel transition of an organogel based on the rotaxane formed from the macrocycle **245** and the thread **246** were investigated by Chiu and co-workers.¹⁴⁷ The addition of either AcO[−], Cl[−] or Br[−] as their tetrabutylammonium salts to the gel formed in 1-pentanol results in the gel becoming sol. Subsequent treatment with NaClO₄ or AgPF₆ restores the original gel after sonication. Comparable proton NMR studies in CD₃NO₂ show a switch of the interlocked macrocycle to the urea station upon the addition of n-Bu₄NaO, presumably due to stronger interaction of the AcO[−] ion with the ammonia group. Thus, the lack of the available urea group for intermolecular hydrogen bonding results in a gel–sol transition. The subsequent addition of NaClO₄ gives the original set of signals in the NMR spectra, presumably due to precipitation of NaOAc. When Cl[−] (or Br[−]) is added the change in the NMR spectra is less pronounced and the authors suspect a coordination of the anion by the amide groups of the macrocycle and the ammonia group of



Scheme 1 Proposed interactions in the gel and solution by **245** and **246**.

the thread (Scheme 1). Consequently the conformational change in the rotaxane results in the switch to the solution of the organogel.

Steed and co-workers utilized bis(urea) gelators **247–250** to aid the crystallisation of various organic compounds, including pharmaceuticals such as carbamazepine.¹⁴⁸ The inert gel matrix results in a slower crystallisation process and subsequently larger, more uniform crystals are formed. Furthermore, the gel inhibits the conversion of metastable polymorphs. After crystallisation the addition of AcO^- results in a gel–sol transition of the matrix and allows facile recovery of the formed crystals. The same group also reported metal-induced gel–sol transitions, where the metal ion competes with intramolecular urea-pyridine and urea-urea hydrogen bonds.¹⁴⁹

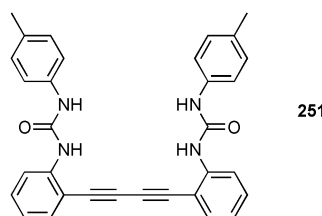


Anion sensing

Anion receptors can be combined with reporter groups to produce sensors that respond to the presence of anions *via* changes in their optical or electrochemical properties. Alternatively receptors may be used as part of a selective membrane in an electrode to produce device that responds selectively to analytes.

Fluorescent and luminescent sensors

In elegant work, Steed and co-workers have used the symmetric urea substituted ridged receptor **251** for sensing chloride.¹⁵⁰ The free receptor in $\text{CHCl}_3/\text{DMSO}$ solution (95/5) solution adopts a twisted conformation which upon binding to one equivalent of chloride, adopts a planar conformation. The formation of the planar complex switches-on fluorescence with an emission maximum at 395 nm ($\lambda_{\text{ex}} = 340$ nm). The most significant response was obtained with chloride over the other anions tested (Br^- , I^- , F^- , NO_3^- , AcO^- , H_2PO_4^- and HSO_4^-) due to the complementarity of chloride for the receptor site formed by the two urea groups in this receptor.



Severin and co-workers have developed a method for sensing of chloride anions in aqueous solution at $\text{pH} = 7.0$ (100 mM MOPS buffer) by fluorescence spectroscopy using turn-on chemosensing assemblies.¹⁵¹ Two closely related chloride sensors were synthesised by mixing the rhodium complexes **252** and **253** together and the fluorescent dyes **254** or **255** in buffered aqueous media. The authors proposed from extensive ESI-MS and proton NMR studies in $\text{H}_2\text{O}/\text{D}_2\text{O}$ 95/5 (v/v) an association of the fluorescent dye with the metal complexes *via* $\pi-\pi$ interactions between the Cp^* ligand and the aromatic ring system of the fluorophore producing an non-emissive ground state structure similar to that observed in the crystal structure (Fig. 33). Stability constants for a 2:1 receptor:fluorescent dye complex of **254** were calculated; $\log K_{11} = 3.53$ and $\log K_{21} = 2.86$ for receptor **252** and $\log K_{11} = 3.89$ and $\log K_{21} = 3.20$ for receptor **253**. The chloride recognition in the formed sensor is achieved by replacement of bound water molecule at the rhodium centre with stability constants $\log K_a = 2.82$ and 2.80 for free complexes **252** and **253**. Fluorescence studies of a solution of **252** (500 μM) and **254** (50 μM) results in a 325% enhancement of the emission intensity at 510 nm ($\lambda_{\text{ex}} = 480$ nm) upon the addition of NaCl (30 mM). In contrast, only minor spectral changes were observed upon the addition of NaF , NaNO_3 , Na_2SO_4 , NaH_2PO_4 , $\text{Na}_4\text{P}_2\text{O}_7$, NaHCO_3 and Na-salicylate , whereas NaAcO gives an I_F/I_0 value of 2. Interference problems were noted with the heavier halides Br^- and I^- as well as the pseudohalide CN^- . Comparable experiments with **253** and **254** show an enhanced sensitivity of an I_F/I_0 value of

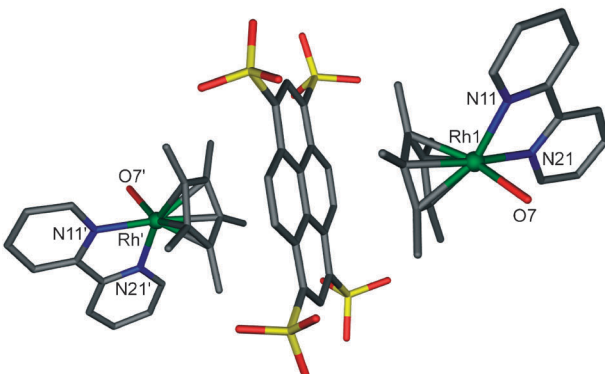
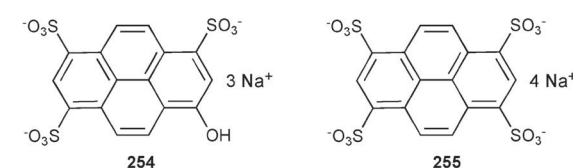
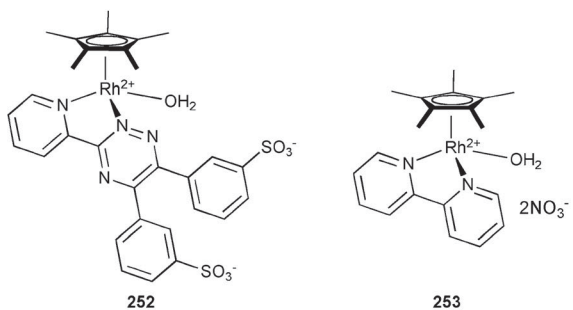
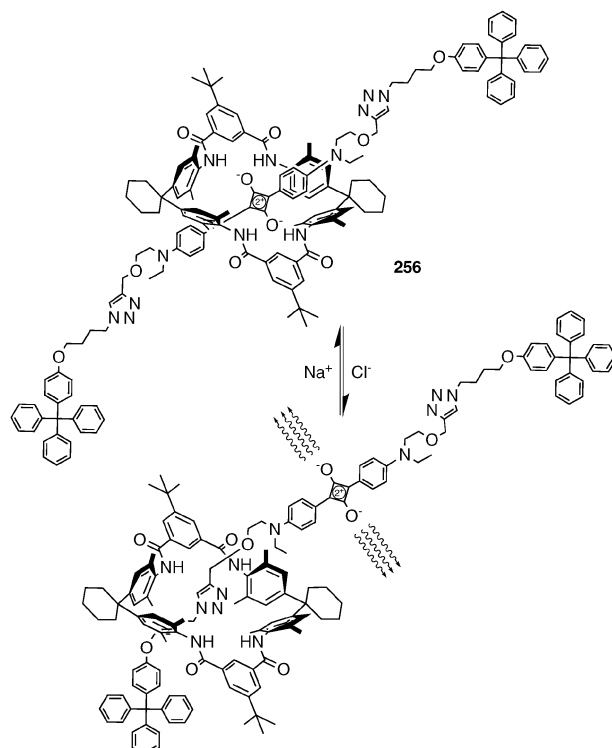


Fig. 33 Crystal structure of $\text{255}^-\text{253}_2$ with selected atom labels, hydrogen atoms and co-crystallised water omitted for clarity.

6.0 due to enhanced association of the dicationic rhodium complex **253** and the fluorescent dye.

The same group increased the sensitivity and selectivity for Cl^- of their sensor design by employing a micelle-base approach.¹⁵² The fluorophore **254** was encapsulated in micelles formed by cetyltrimethylammonium hydrogensulfate in aqueous solution at pH 7 containing **252**. The Cl^- binding of **252** reduces the net positive charge of the $\text{Cp}^*\text{Rh}(\text{III})$ fragment and the chloro-adduct may be considered as more amphiphilic. Subsequently the micelle/water partition constant K_p for Cl^- (**252**-H₂O) increases to 3700 compared to 7 for **252** allowing the complex to migrate into the micelle. Thus, quenching of **254** ($\lambda_{\text{ex}} = 360 \text{ nm}$, $\lambda_{\text{em}} = 528 \text{ nm}$) was obtained in the presence of Cl^- in a millimolar range, whereas no spectral change was observed upon the addition of AcO^- , H_2PO_4^- , $\text{HP}_2\text{O}_7^{3-}$, NO_3^- , SO_4^{2-} and HCO_3^- .

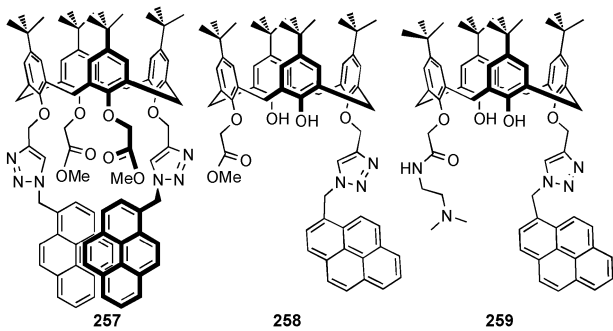
Reversible sensing of chloride has also been the focus of recent work by Smith and co-workers, through the synthesis of a squaraine based rotaxane **256**.¹⁵³ The interaction of the macrocycle with the squaraine dye in **256** results in a threefold decrease in fluorescence. Upon the addition of $n\text{-Bu}_4\text{NCl}$ to **256** in CHCl_3 the thread is displaced from its original position and the fluorescence returns at 655 nm ($\lambda_{\text{ex}} = 365 \text{ nm}$). Detailed ¹H NMR studies suggest a Cl^- triggered translocation of the macrocycle from the central squaraine portion of the thread to the triazole functionalities (Scheme 2). This is reversed when the chloride is precipitated out of solution with



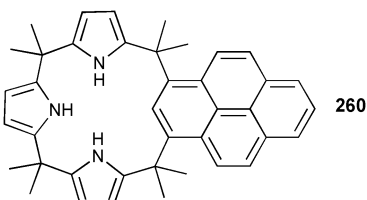
Scheme 2 Chloride triggered translocation in the rotaxane **256**.

a source of sodium ions. Fluorescence titration studies showed a stability constant of 340 M^{-1} for the 1:1 chloride rotaxane complex in CHCl_3 . This is considerably lower than that of the free macrocycle ($K_a > 10^5 \text{ M}^{-1}$ in CH_2Cl_2) and reflects the energy cost of translocation of the macrocycle away from the squaraine station in order to bind the anion. To investigate the practical potential of this system the rotaxane was immobilised on dipsticks that were shown to be able to reversibly detect chloride fluorometrically and colorimetrically in aqueous solution.

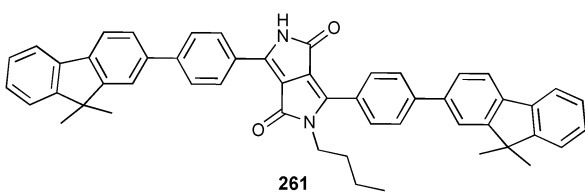
Matthews and co-workers have reported the synthesis of the new pyrenyl-appended triazole-based calix[4]arenes **257** and **259**¹⁵⁴ and compared them to the known fluorescent sensor **258**.¹⁵⁵ The fluorescent properties of these receptors were studied in CH_3CN with anions added as their tetrabutylammonium salts. The receptors were excited at 343 nm with receptor **257** displaying monomer and excimer bands at 395 and 475 nm respectively. However the fluorescence spectrum of receptors **258** and **259** showed the monomer band at 395 nm only, while **259** had the weakest emission due to photo-induced electron transfer (PET) caused by the addition of the pendant amide group. Compound **257** was found to exhibit fluorescent selectivity for iodide, with the monomer emission of the pyrene moiety increasing as the excimer emission decreases. This ratiometric change was due to the encapsulation of iodide in the receptors cavity, causing a conformational change resulting in the two pyrene subunits moving apart from one another. Upon addition of over 200 equivalents of iodide both signals from the monomer and excimer were quenched due to heavy atom effect imparted by I^- . A stability constant of 979 M^{-1} was determined for the 1:1 complex of receptor **257** with iodide.



Lee and co-workers have synthesised calix[1]pyreno-[3]pyrrole **260**, that uses fluoride induced conformational change to become a sensitive fluorescence sensor with a preferential affinity for C₇₀ in toluene/acetonitrile (5%) solution.¹⁵⁶ The [F-**260**] complex adopts a cone-like conformation that enable binding of electron deficient spherical guests. The binding affinity for fullerenes was found to increase with the addition of fluoride with the greatest affinity for C₆₀ and C₇₀ observed when three equivalents of fluoride were present. Minor fluorescence quenching was noted in the absence of fluoride.

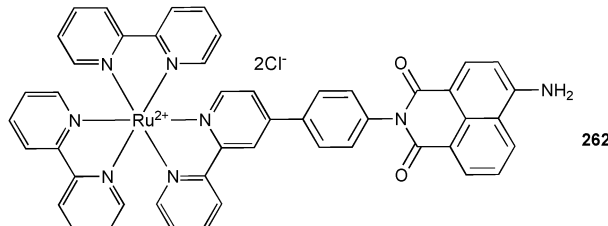


Deprotonation of the lactam group in the diketopyrrolo-pyrrole based receptor **261** was employed by Qu, Hua and Tian to produce a colorimetric and ratiometric red fluorescent sensor for fluoride.¹⁵⁷ Comparable UV-Vis absorption ($\lambda = 496$ and 594 nm) and fluorescent ($\lambda_{\text{ex}} = 435$ nm, $\lambda_{\text{em}} = 563$ nm) experiments in CH₂Cl₂ reveal a high fluoride selectivity over chloride, bromide and iodide as their tetrabutylammonium salts.

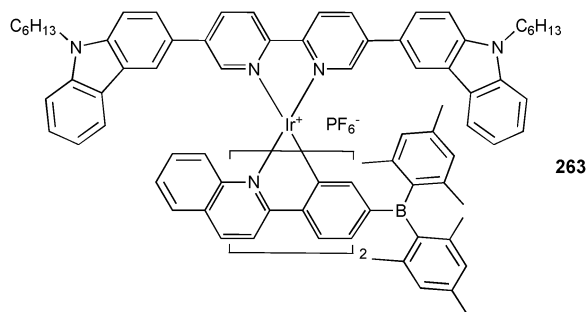


Gunnlaugsson and Elmes have synthesised a novel naphthalimide-ruthenium(II)-polypyridyl complex **262** for sensing fluoride via a change in luminescence caused by the modulation of the metal to ligand charge transfer (MLCT) emission.¹⁵⁸ The presence of tetrabutylammonium fluoride in CH₃CN could be detected by the naked eye as a colour change from yellow to red. Initial hydrogen bonding interactions of the anion with **262**, using the amine residue as the hydrogen bond donor, followed by deprotonation results in the observed spectral changes. Only minor changes were observed in the UV-Vis spectra in the presence of AcO⁻, Cl⁻ and HSO₄⁻. Fluorescence studies ($\lambda_{\text{ex}} = 435$ nm) in CH₃CN show a quenching of the emission at 615 nm upon the addition of F⁻ ($\log K_{11} = 4.20$, $\log K_{12} = 3.7$). Similar fluorescence quenching was observed with

AcO⁻ ($\log K_{11} = 4.25$, $\log K_{12} = 3.11$), Cl⁻ ($\log K_{11} = 2.90$) and H₂PO₄⁻ ($\log K_{11} = 4.52$), where the addition of tetrabutylammonium hydrogensulfate did not result in a significant spectral change. Competitive experiments show further quenching of the MLCT emission if F⁻ is added to a solution of **262** in the presence of an excess of H₂PO₄⁻, whereas the other studied anions do not result in any spectral changes.

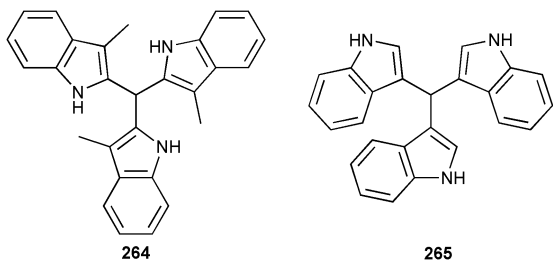


A carbazole and triarylboron containing iridium(III) complex **263** was synthesised by Huang and co-workers and has been shown to act as a ratiometric fluoride probe upon complex formation.¹⁵⁹ The addition of up to two equivalents of F⁻ to **263** in CH₃CN results in large change in the emission maxima from $\lambda_{\text{em}} = 584$ to $\lambda_{\text{em}} = 458$ nm if excited at $\lambda_{\text{ex}} = 379$ nm. The authors explained their observation with a triplet-singlet emission switch due to the coordination of the F⁻ by the boron centres. Subsequently the triplet emission of the metal centre is quenched and only singlet emission at $\lambda_{\text{em}} = 458$ nm of the carbazole moiety was detected. Selectivity studies with anions such as Cl⁻, Br⁻, I⁻, ClO₄⁻, NO₃⁻ present in 4 times excess gave no noticeable change in the emission intensity at 584 nm in CH₃CN, if **263** was excited at $\lambda_{\text{ex}} = 480$ nm. Minor quenching was observed in the presence of H₂PO₄⁻ and AcO⁻, whereas F⁻ results in significant quenching (I_1/I_0 of 0.1).

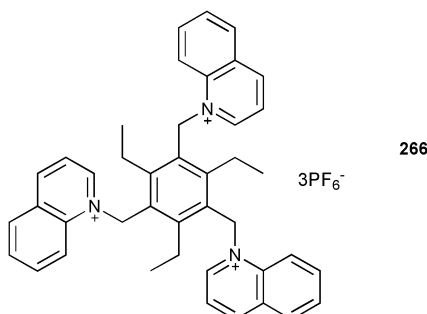


The spectroscopic response of tri(indolyl)methane receptors **264** and **265** upon addition of anions was investigated by Shoa and co-workers.¹⁶⁰ Fluorescence studies ($\lambda_{\text{ex}} = 283$ nm) in CH₃CN of **264** reveal no significant change in the emission intensity at 356 nm upon addition of Cl⁻, Br⁻, HSO₄⁻ and ClO₄⁻, added as their tetrabutylammonium salts, whereas the addition of tetrabutylammonium fluoride, acetate or dihydrogen phosphate, results in quenching of the fluorescence emission. The authors explain their observation as being due to the loss of planarity of the receptors upon complex formation with the latter anions. Titration experiments were employed to determine stability constants K_a of $3.39 \times 10^5 \text{ M}^{-1}$ for F⁻, $2.22 \times 10^5 \text{ M}^{-1}$ for AcO⁻ and $1.66 \times 10^5 \text{ M}^{-1}$ for H₂PO₄⁻ for a 1:1 binding mode. Comparable experiments with **265** reveal no significant interactions with any of the anions examined in this study. The authors suggest that in **265** the location of the link

in the 3-position may prevent the formation a convergent hydrogen bonding array.



Steed and co-workers have utilized the quinoline group in the tripodal receptor **266** for detection of anions. The strongest fluorescence quenching in CH_3CN at $\lambda_{\text{em}} = 408 \text{ nm}$ ($\lambda_{\text{ex}} = 317 \text{ nm}$) was observed for AcO^- over Br^- , Cl^- , I^- and NO_3^- , presence as their tetrabutylammonium salts. Extensive NMR studies in CD_3CN reveal the formation of 1 : 1 and 2 : 1 ($\text{L} : \text{A}$) as well as the presence of host dimer ($\log K = 1.57$) in solution. The obtained stability constants are summarised in Table 14.



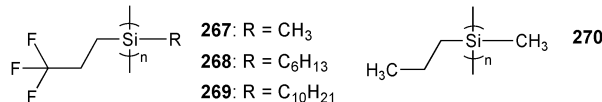
Naito and co-workers have employed a series of helical fluorinated poly(dialkylsilanes) (**267–269**) as fluorescent sensors for monovalent anions.¹⁶¹ The observed quenching of the emission maxima between 330 and 340 nm for **267–269** ($\lambda_{\text{ex}} = 300$ nm) in THF decreases from $\text{F}^- > \text{NO}_3^-$, $\text{Br}^- > \text{Cl}^- > \text{HSO}_4^- > \text{PF}_6^- > \text{I}_3^-$ and is in correlation to the surface charge density of these anions (surface charge density (mCm⁻³) F^- : -389, Cl^- : -254, Br^- : -227, NO_3^- : -207, HSO_4^- : -166, PF_6^- : -146 and I_3^- : -108). Furthermore, the sensitivity of these systems could be modified by changing the length of the alkyl chains. The authors explain their observations as being due to the stronger electrostatic interaction between compact anions, such as F^- with the positively charged Si polymer chain in the fluorinated helical poly(dialkylsilanes). Comparable experiments with the unfluorinated poly(dialkylsilane)

Table 14 Stability constants of **266** in CD₃CN.^a Anions added as their tetrabutylammonium salts

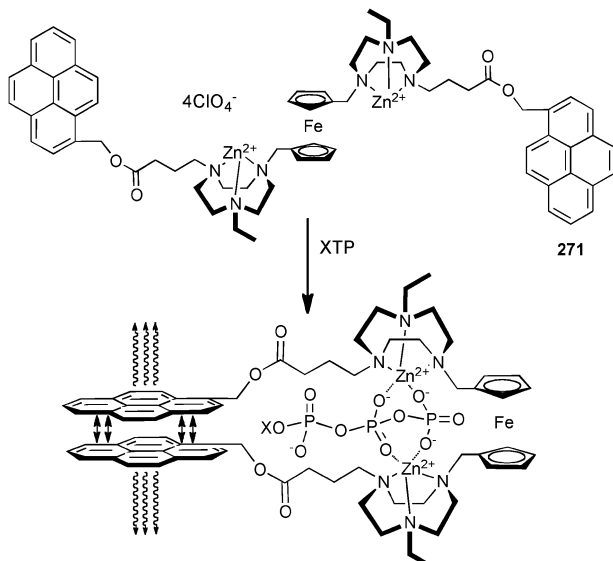
Anion	$\log \beta_{11}$	$\log \beta_{21}$
Cl^-	4.54(5)	8.01(8)
Br^-	4.75(5)	8.10(7)
I^-	3.391(1)	6.120(8)
NO_3^-	4.55(2)	8.18(3)
AcO^-	<i>b</i>	
H_2PO_4^-	<i>c</i>	
HSO_4^-	<i>c</i>	

^a Values in parentheses are standard deviation. ^b Stability constant to large to be determined by this method. ^c Precipitate.

270 show a minor quenching of the fluorescence in the presence of F^- only. Due to the non-ionic character of the Si main chain in the helix no electrostatic interactions are present between the polymer **270** and monovalent anions.



The sensing of phosphate nucleotides in the tweezer-like ferrocene linked pyrene functionalised Zn(II)-1,4,7-triazacyclononane (TACN) complexes **271** has been reported by Bond and co-workers.¹⁶² The binding of pyrophosphate, di- and triphosphate nucleotides between the two Zn(II) centres promotes a rearrangement of the pendant arms to a *cis*-orientation and results in an off-on fluorescence due to an enhanced excimer emission at 475 nm in 1:9 acetonitrile:tris/HCl buffer (pH 7.4, 10 mM) (Scheme 3). A summary of the obtained stability constants if given in Table 15. Phosphorous NMR studies in 1:9 CD₃CN:D₂O (tris/HCl buffer pD = 7.6, 10 mM, 293 K) with pyrophosphate (PPi) and adenosine



Scheme 3 Proposed mode of polyphosphate anion (XTP) binding by [271-4(Cl)₄O₄]⁻.

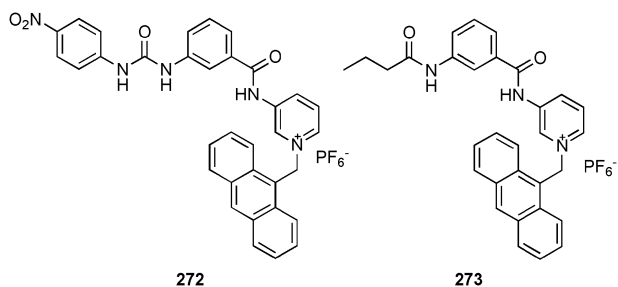
Table 15 Stability constants of polyphosphates by **271** in CH₃CN/H₂O (pH 7.4) at 293 K

Anion	$K_a [\text{M}^{-1}]$	Anion	$K_a [\text{M}^{-1}]$
PP _i ^a	$(4.45 \pm 0.41) \times 10^6$	TDP ^e	$(2.03 \pm 0.18) \times 10^4$
ATP ^b	$(9.31 \pm 0.84) \times 10^4$	AMP ^b	<u>f</u>
CTP ^c	$(2.32 \pm 0.19) \times 10^5$	CMP ^c	<u>f</u>
GTP ^d	$(2.13 \pm 0.29) \times 10^5$	GMP ^d	<u>f</u>
TPP ^e	$(5.05 \pm 0.46) \times 10^5$	TMP ^e	<u>f</u>
ADP ^b	$(9.63 \pm 0.93) \times 10^3$	H ₂ PO ₄ ⁻	<u>f</u>
CDP ^c	$(1.55 \pm 0.14) \times 10^4$	F ⁻	<u>f</u>
GDP ^d	$(1.41 \pm 0.12) \times 10^4$	AcO ⁻	<u>f</u>

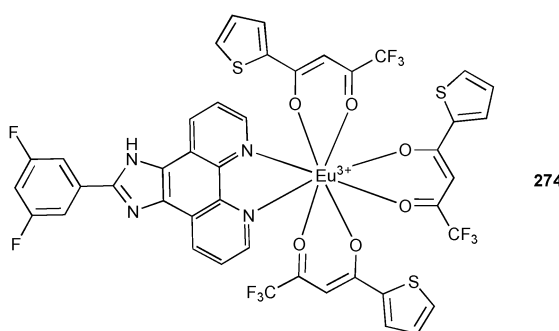
^a Pyrophosphate. ^b Adenosine tri-, di- and mono-phosphate (ATP, ADP and AMP). ^c Cytidine tri-, di- and mono-phosphate (CTP, CDP and CMP). ^d Guanosine tri-, di- and mono-phosphate (ATP, ADP and AMP). ^e Thymine tri-, di- and mono-phosphate (ATP, ADP and AMP). ^f Not determined due to small change in fluorescence emission.

tri-, di- and mono-phosphate (ATP, ADP and AMP) reveals the formation of 1:1 complexes for all anions in **271** and supports the formation of the proposed host–guest complex.

Ghosh and co-workers have used the pyridinium amide-urea conjugate anthracene appended receptor **272** to sense the presence of the L-N-acetylvaline and L-N-acetylalanine as their tetrabutylammonium salts.¹⁶³ Fluorescence studies of **272** in CH₃CN ($\lambda_{\text{ex}} = 370$ nm) reveal a moderate quenching of the emission at 415 nm upon the addition of L-N-acetylproline, (S)-mandelate, pyruvate and L-N-acetylphenylglycine, whereas L-N-acetylalanine and L-N-acetylvaline result in a broad emission observed at 492 nm of moderate intensity. Comparable experiments with amide-amide analogue **273** do not show the broad emission band at 492 nm highlighting the significance of the electron deficient urea motif in **272**. Titration experiments reveal selective binding of L-N-acetylvaline ($K_a = 1.87 \times 10^4$ M⁻¹) over L-N-acetylalanine ($K_a = 2.60 \times 10^3$ M⁻¹), acetate ($K_a = 2.20 \times 10^3$ M⁻¹), (S)-mandelate ($K_a = 1.60 \times 10^3$ M⁻¹), L-N-acetylproline ($K_a = 1.38 \times 10^3$ M⁻¹) and L-N-acetylphenylglycine ($K_a = 1.38 \times 10^3$ M⁻¹) in CH₃CN in a 1:1 binding mode.

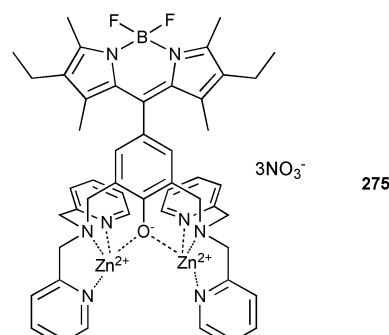


Wang and co-workers have employed the red luminescent Eu(III) complex **274** for the detection of F⁻ and AcO⁻ in DMSO solution.¹⁶⁴ Hydrogen bonding between the imidazole moiety and F⁻ (one equivalent, added as tetrabutylammonium salt) results in a change from red Eu(III) to a green emission ($\lambda_{\text{ex}} = 500$ nm), where the presence of tetrabutylammonium acetate gave rise to yellow-red to green emission change. Comparable experiments with HSO₄⁻ show minor spectral changes, whereas Cl⁻, Br⁻ and I⁻, added as their tetrabutylammonium salts, show no indication for hydrogen bonds towards **274**. Further the authors manufactured transparent poly-methyl methacrylate (PMMA) films containing 0.5 mg of **274** in 5 mg MMA. Recognition tests with F⁻ and AcO⁻ in DMSO reveal a slow response of the film upon presence of F⁻ only presumably due to the anion's higher basicity.

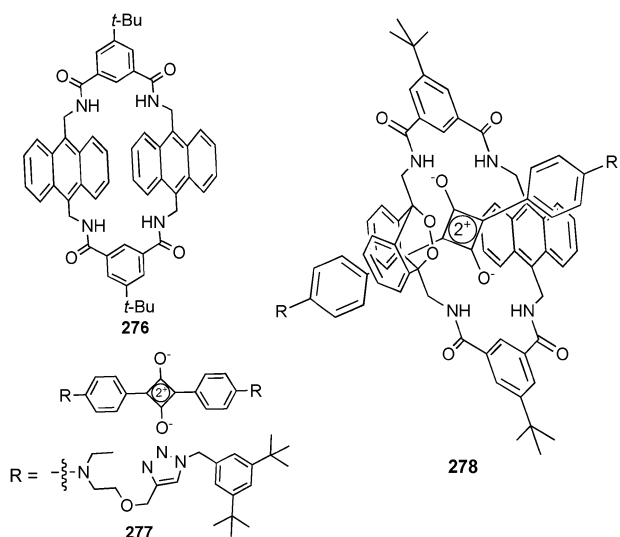


An electro-generated chemiluminescent (ECL) sensor based upon a BODIPY group in **275** that exhibits pyrophosphate

selectivity has been reported by Hong and co-workers.¹⁶⁵ The ECL emission maxima at 540 nm was quenched upon the coordination of the pyrophosphate by the dipicollylamine zinc(II) moiety in **275**. Competitive assays in CH₃CN (10 μM of **275**, 10 mM tri-n-propylamine, 0.1 M n-Bu₄NPF₆) with a 10-fold excess of I⁻, Cl⁻, F⁻, NO₃⁻, ClO₄⁻ and AcO⁻ show a slight change in the ECL intensity only, which significantly decreases if pyrophosphate (10 μM) was added to each solution. Comparable experiments show the same pronounced response for pyrophosphate in the presence of 10 μM of H₂PO₄⁻, ATP, ADP or AMP.

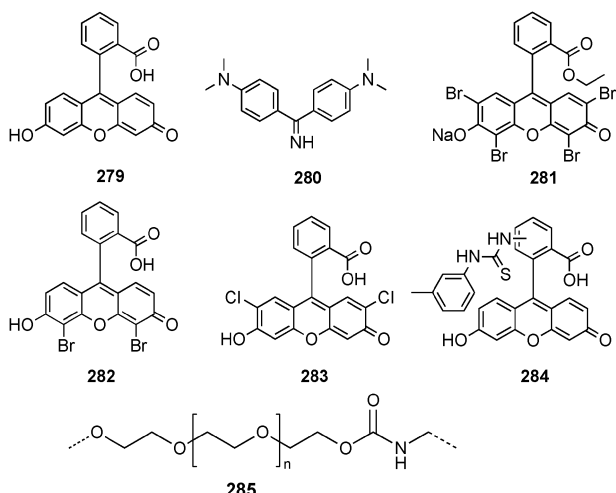


Smith and co-workers have employed the squaraine rotaxane **278** formed by the mono-oxidised macrocycle **276** and the squaraine thread **277** as chemiluminescent dye for effective imaging in tissue.¹⁶⁶ The temperature triggered reduction of the 9,10-anthracene endoperoxide moiety in **278** results in singlet oxygen release, which initiates a near infrared emission of the squaraine group at 733 nm. This light emission is used as an efficient *in vivo* imaging method in mice with a high target to background ratio at tissue depth of more than 2 cm. Radiation with red light in the presence of air regenerates the oxidised rotaxane **278**, which can be stored indefinitely at -20 °C.



Anzenbacher and co-workers have developed a simple sensor array capable of recognising ion pairs in water employing weak interactions of six pH indicators (**279**–**285**).¹⁶⁷ Only one of these indicators (**284**) has a hydrogen bonding thiourea group. The indicators were doped into a polyether-urethane matrix **285** which contained amide groups that interact with anions and an

oligo-ethylene glycol which interacts with the cations. Multiple studies were carried out with combinations of five different cations namely lithium, sodium, potassium, ammonium and tetrabutylammonium and seven different anions fluoride, chloride, iodide, bromide, acetate, nitrate and dihydrogen phosphate at five different pH levels (5, 6, 7, 8, and 9). The responses of the different pH indicator displacement events upon the addition of the different ion pairs were reported using a UV-excitation scanner with four different emission filters. These simple chemosensors were shown to be capable of sensing ion pairs over this wide pH range with a discrimination capacity and recognition efficiency of (6:35) and an accuracy of $\geq 93\%$, this is normally observed with very complex sensors.

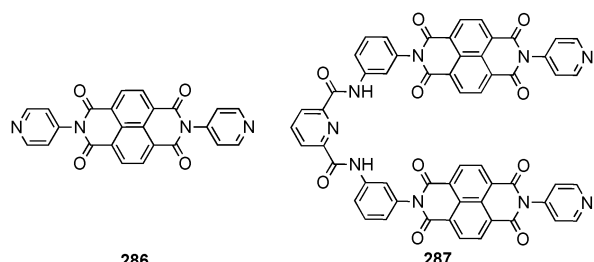


Colorimetric sensors

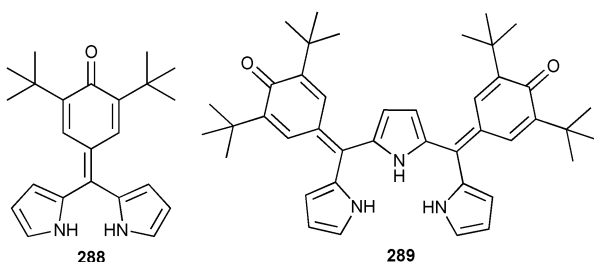
A dinuclear copper(II) bromide complex of **73** synthesised by Hossain and co-workers gives a selective response to iodide ($23\,900, 125\text{ M}^{-1}$) over fluoride ($2270, 20\text{ M}^{-1}$), chloride ($3200, 25\text{ M}^{-1}$) and bromide (no binding event observed) in 1:3 water:acetonitrile and water solutions buffered to pH 7.¹⁶⁸ The stability constants were calculated from UV-Vis titration experiments with the anions added as tetrabutylammonium salts (and bound in 1:1 stoichiometry). This macrocyclic receptor forms a bowl shape with metal cations at either end of the cavity separated by 7.101(4) Å in the solid state. The introduction of iodide anions to a solution of the receptor is thought to result in the replacement of groups previously linked to the copper(II) centres. This could be responsible for the colour change from blue to green and a unique λ_{\max} absorption value.

Saha and Guha have synthesised two receptors based on the π -electron deficient naphthalene diimide (NDI) group that interacts with the anion through anion- π interactions.¹⁶⁹ This results in charge/electron transfer events that trigger a two-step optical response towards fluoride with receptors **286** and **287**. The simple NDI receptor **286** was tested with a wide variety of anions added as their tetrabutylammonium salts in a variety of solutions (DMSO, DMF, DMAc, CH₃CN, (CH₃)₂CO and THF) containing up to 15% water. The first colour change exhibited was from colourless to orange which occurred when there were ≤ 5 equivalents of fluoride present. This colour change was triggered by the first electron transfer event between the

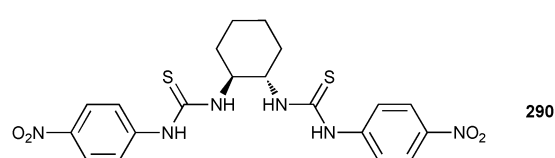
anion and NDI forming the NDI radical anion. When the quantity of fluoride was increased the solutions turned pink. This was due to the reduction of the NDI radical anion to NDI²⁻ by the fluoride anion. No other colour changes were noted with any other anion combinations even with up to 30 equivalents of the anions added. In order to test these compounds for any potential applications the more selective pincer scaffold of receptor **287** was exposed to anticavity toothpaste containing 0.24% w/v of NaF and fluoride free toothpaste in DMSO/water. A colour change was noted from colourless to a light orange with the former toothpaste but not with the fluoride free toothpaste.



Xie and co-workers have produced two pyrrole-hemiquinone based sensors for the fluoride anions through a colorimetric response *via* deprotonation of the receptor (an internal charge transfer process).¹⁷⁰ Upon the addition of forty equivalents of tetrabutylammonium fluoride to a DMSO solution of **288** a colour change was observed from dark orange (496 nm) to blue (568 nm); with **289** showing a colour change from wine red (459 and 571 nm) to grey (740 nm). With > 40 equivalents of anion a further colour change is noted to green (624 nm), this is due to a second deprotonation process. This doubly deprotonated species did not form upon addition of other basic anions such as cyanide, acetate and dihydrogen phosphate allowing differentiation between the anions. The double deprotonation is possible because of the increased acidity of the NH groups of **289** due to the additional hemiquinone electron withdrawing group.

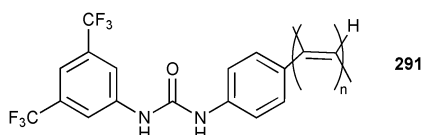


Lees and co-workers have reported a bis thiourea-based sensor **290** that gives a colorimetric response with cyanide.¹⁷¹ The red orange colour which is observed upon the addition of the cyanide to a DMSO solution of the receptor is due to the intramolecular charge transfer transition from the

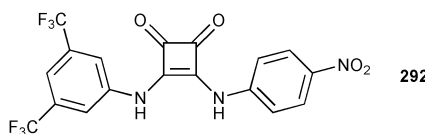


deprotonated thiourea nitrogen to the *para*-nitrophenyl substituent. UV-Vis and naked eye experiments with a variety of tetrabutylammonium salts showed a selective response to cyanide over other basic anions such as fluoride, acetate, and benzoate and dihydrogen phosphate although some colour changes were noted upon the addition of these anions.

Urea based polymers for anion sensing have been prepared by Kakuchi and co-workers.¹⁷² The affinity of polymer **291** for a variety of anions was tested in THF *via* UV-Vis spectroscopy, using the tetrabutylammonium salts of the anions studied. Selectivity was shown for acetate ($11\ 500\ M^{-1}$), benzoate ($11\ 700\ M^{-1}$), azide ($12\ 300\ M^{-1}$) and hydrogen sulfate ($11\ 500\ M^{-1}$) over nitrate ($4900\ M^{-1}$), chloride ($9100\ M^{-1}$), bromide ($5300\ M^{-1}$), and fluoride ($6500\ M^{-1}$), with stability constants calculated using the Hill equation. The addition of anions such as acetate, benzoate, fluoride, chloride triggered a colour change from yellow through orange to red was observed depending on the anion added. This colour change was found to be a direct result of complexation between the anion and receptor and was verified by ^1H NMR experiments.

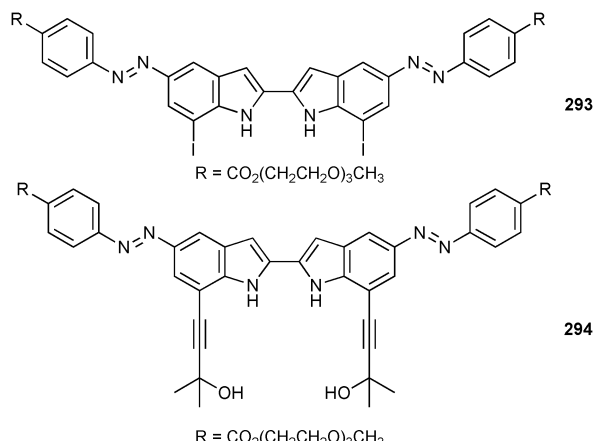


Taylor and co-workers have synthesised a variety of *N,N'*- diarylsquaramides and investigated the colorimetric response to anionic species of the *p*-nitrophenyl derivative **292**.¹⁷³ UV-Vis studies of the free receptor show a red shift in the absorption maxima by about 100 nm from approximately 380 nm (yellow) in CH_3CN to about 480 nm (red) in DMSO. The authors explain this observation with an ionization of free receptor and the formation of deprotonated species [**292-H**] $^-$ due to the different solvent polarity. Titration experiments with *n*-Bu₄NF in DMSO result in second deprotonation and subsequent colour change to blue, whereas no spectral change was observed upon the addition of AcO^- and H_2PO_4^- . Comparable experiments in CH_3CN show a similar colour change from yellow to red in the presence of AcO^- and H_2PO_4^- due to deprotonation of **292**. Surprisingly titrations with even weakly basic anions such as *p*-toluenesulfonate results in the same colour change in CH_3CN due to the high acidity of the NH groups in **292**. However, detailed UV-Vis and ^1H NMR investigations with *p*-toluenesulfonate (added as the tetrabutylammonium salt) in DMSO are evidence for a unique re-protonation process of the receptor in presence of an anion excess (10-30 equivalent). The observed UV-Vis absorption shifts back to yellow (395 nm) and points at presence of the free receptor **292**. Additional evidence for this re-protonation process are the appearance of sharp proton signals at about 10.6 ppm, which is very broad for free **292**.



Continuing their work on anion binding biindole scaffolds Jeong and co-workers have produced receptor **293** capable of

acting as a colorimetric anion sensor for the more basic anions such as acetate, dihydrogen phosphate, fluoride and cyanide.¹⁷⁴ Addition of these anions causes a colour change from yellow to orange/red due to complex formation or the deprotonation of the receptor in a 10% DMSO/ CH_3CN solution with anions added as the tetrabutylammonium salts. The addition of two further hydrogen bonding groups creates receptor **294** capable of binding anions strongly with a stability constant of $2 \times 10^5\ M^{-1}$ for fluoride binding in 1 : 1 stoichiometry determined *via* UV-Vis spectroscopy. Receptor **293** exhibits deprotonation under the same conditions.



Maeda and co-workers continued their work with dipyrrolyl-diketone boron based anion receptors **295–306** by tuning the electronic and optical properties with modifications of the substitution pattern on the pyrrole backbone.¹⁷⁵ Anion complexation was explored by ^1H NMR titration techniques in CD_2Cl_2 with the anions added as their tetrabutylammonium salts and confirmed a conformational change of the receptor to enable anion interactions through both pyrrole NH groups and the central CH hydrogen bond donor. The same binding pattern was observed in the solid phase (Fig. 34) with the pyrrole NH groups inverted compared to the free receptor. A combination of various observations showed that the substituents modulate the electronic, optical and fluorescent efficiencies as well as the solid state X-ray crystal structures. The UV-Vis titration data revealed that acetate is selectively bound over dihydrogen phosphate, chloride, bromide and hydrogen sulfate by all twelve receptors due to the higher basicity of this anion. Both the fluorescence and UV-Vis spectra of these receptors are perturbed upon the addition of anions. It was also shown that the singlet oxygen generation behaviour of these boron complexes was tuneable by anions. The combination of these properties is useful for both sensing anions and for agents to be used in photodynamic therapy.

Shores and co-workers utilised the anion triggered spin state switching of a series of heteroleptic iron(II) 2,2'-bi-1,4,5,6-tetrahydropyrimidine complexes such as **307** for the detection of Br^- .¹⁷⁶ Electronic absorption spectroscopy of **307** in CH_2Cl_2 with tetrabutylammonium bromide results in a distinct colour change from indigo to teal. Titration experiments give stability constants of $\log K_{11} = 6.2$ and $\log K_{12} = 5.6$, while quantitative experiments reveal an order of affinity of

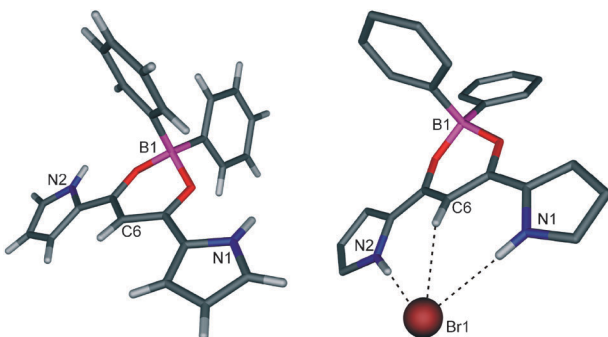
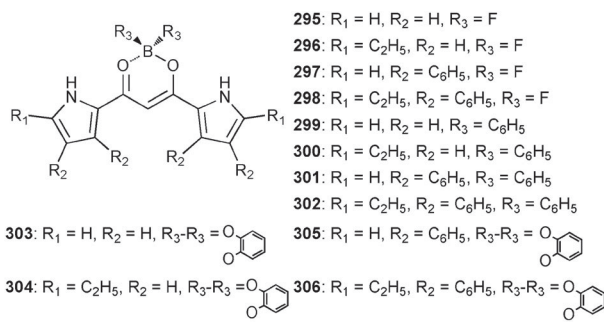
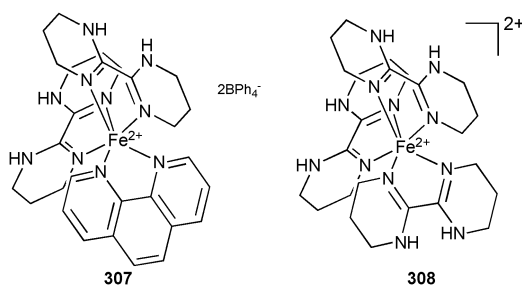


Fig. 34 Crystal structure of **299** (left) and $[\text{Br} \subset \text{299}]^+$ (right) with selected atom labels, hydrogen bonds represented as dotted lines, tetrabutylammonium cation and non-interacting hydrogen atoms in $[\text{Br} \subset \text{299}]^+$ omitted for clarity.

$\text{Br}^- > \text{Cl}^- > \text{I}^- > \text{NO}_3^- > \text{ClO}_4^-$ as observed for the previously reported for the symmetric homoleptic complex cation **308**.¹⁷⁷



Redox sensors

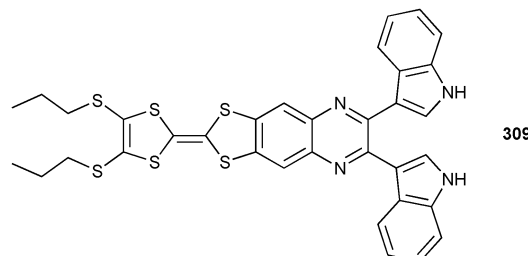
A number of new redox active sensors for anions have been reported in 2010. Sessler and co-workers employed this strikingly in the tetrathiafulvalene based receptor **309**, which also possesses an optical response due to the diindolylquinoxaline moiety.¹⁷⁸ Both, UV-Vis and cyclic voltammometric studies show selective detection of H_2PO_4^- . A summary of the obtained stability constants for a 1:1 binding mode in CH_2Cl_2 and ΔE of the first redox potential of the receptor are shown in Table 16. As expected results the addition of tetrabutylammonium dihydrogen phosphate in a cationic shift of 112 mV in the first oxidation wave ascribed to the tetrathiafulvalene unit. Comparable experiments with Cl^- , PhCOO^- and HSO_4^- produce only minor changes in $E_{1/2}^{1/1}$, while the addition of F^- caused a broadening and splitting in the cyclic voltammogram features.

Table 16 Stability constants for a 1:1 binding mode obtained by UV-Vis titrations and ΔE of the first redox potential of **309-X** ($X = \text{anion}$) in CH_2Cl_2 at 298 K

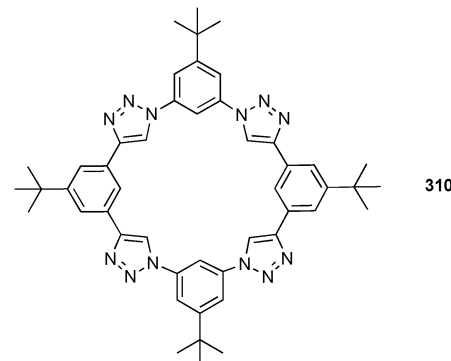
Anion	$K_a^a [\text{M}^{-1}]$	$\Delta E^{1b} [\text{mV}]$
F^-	3.6×10^3	-278 ^c
H_2PO_4^-	6.5×10^3	-112
PhCOO^-	9.5×10^2	-15
HSO_4^-	3.7×10^2	+19
Cl^-	1.1×10^3	0

^a Errors < ±10%. Anions used as their tetrabutylammonium salts. ^b ΔE^1 calculated again Ag/AgCl in the presence of 2 equivalent of anion and 0.3 M $n\text{-Bu}_4\text{NPF}_6$. ^c Value after suspected deprotonation.

Extensive NMR studies in CD_2Cl_2 and $\text{DMSO}-d_6$ are evidence for a deprotonation of **309** upon the addition of F^- .



Bachas and co-workers have employed the known triazolo-phane **310** for the selective potentiometric detection of halides in an ion-selective electrode.¹⁷⁹ Incorporation of **310** into a poly(vinyl chloride) based membrane (2% m/m of **310** in a membrane based on 60% m/m tridodecylmethylammonium chloride plasticised with 2-nitrophenyl octyl ether) afforded an electrode with a near-Nernstian response of -54.6 mV/decade with chloride detection limit of 5.6×10^{-6} M, whereas bromide is detected at a concentration of 8.5×10^{-6} M with a near-Nernstian response of -57.1 mV/decade.



Conclusions

In 2010 we have seen advances in a number of areas related to the supramolecular chemistry of anionic species. Research in the transmembrane transport of anionic species has demonstrated that very simple receptors can function as effective carriers. Halogen bonding is becoming increasingly important as a new non-covalent interaction with which to form complexes with halide anions and new systems containing triazole groups have extended this chemistry into new molecular

architectures including systems switchable by light. We can anticipate further exciting developments in the coming years.

Acknowledgements

PAG thanks the EPSRC/NSF and the EU for funding.

References

- 1 C. Caltagirone and P. A. Gale, *Chem. Soc. Rev.*, 2009, **38**, 520–563.
- 2 P. A. Gale, *Chem. Soc. Rev.*, 2010, **39**, 3746–3771.
- 3 P. A. Gale, *Chem. Commun.*, 2011, **47**, 82–86.
- 4 P. A. Gale, *Acc. Chem. Res.*, 2011, **44**, 216–226.
- 5 P. A. Gale, S. E. Garcia-Garrido and J. Garric, *Chem. Soc. Rev.*, 2008, **37**, 151–190.
- 6 P. A. Gale and R. Quesada, *Coord. Chem. Rev.*, 2006, **250**, 3219–3244.
- 7 A. J. Baer, B. D. Koivisto, A. P. Côté, N. J. Taylor, G. S. Hanan, H. Nierengarten and A. V. Dorsselaer, *Inorg. Chem.*, 2002, **41**, 4987–4989.
- 8 S. L. Jain, P. Bhattacharyya, H. L. Milton, A. M. Z. Slawin, J. A. Crayston and J. D. Woollins, *Dalton Trans.*, 2004, 862–871.
- 9 A. Dorazco-Gonzalez, H. Höpfl, F. Medrano and A. K. Yatsimirsky, *J. Org. Chem.*, 2010, **75**, 2259–2273.
- 10 Y. Xia, B. Wu, S. Li, Z. Yang, Y. Liu and X.-J. Yang, *Supramol. Chem.*, 2010, **22**, 318–324.
- 11 D. E. Gross, V. Mikkilineni, V. M. Lynch and J. L. Sessler, *Supramol. Chem.*, 2010, **22**, 135–141.
- 12 M. Arunachalam and P. Ghosh, *Org. Lett.*, 2010, **12**, 328–331.
- 13 M. Arunachalam and P. Ghosh, *Inorg. Chem.*, 2010, **49**, 943–951.
- 14 I. Ravikumar, P. S. Lakshminarayanan and P. Ghosh, *Inorg. Chim. Acta*, 2010, **363**, 2886–2895.
- 15 G. Ozturk, M. Colak and M. Togrul, *J. Inclusion Phenom. Macrocyclic Chem.*, 2010, **68**, 49–54.
- 16 M. Arunachalam and P. Ghosh, *Chem. Commun.*, 2009, 5389–5391.
- 17 P. S. Lakshminarayanan, E. Suresh and P. Ghosh, *Inorg. Chem.*, 2006, **45**, 4372–4380.
- 18 G. Ozturk, B. Gumgum, M. Kizil and S. Emen, *Synth. Commun.*, 2007, **37**, 3981–3988.
- 19 S. O. Kang, V. W. Day and K. Bowman-James, *J. Org. Chem.*, 2010, **75**, 277–283.
- 20 M. A. Hossain, S. O. Kang, J. M. Llinares, D. Powell and K. Bowman-James, *Inorg. Chem.*, 2003, **42**, 5043–5045.
- 21 S. O. Kang, V. W. Day and K. Bowman-James, *Inorg. Chem.*, 2010, **49**, 8629–8636.
- 22 J. Eckelmann, V. Saggiomo, F. D. Sonnichsen and U. Luning, *New J. Chem.*, 2010, **34**, 1247–1250.
- 23 S. Colombo, C. Coluccini, M. Caricato, C. Gargiulli, G. Gattuso and D. Pasini, *Tetrahedron*, 2010, **66**, 4206–4211.
- 24 L. Molina, E. Moreno-Clavijo, A. J. Moreno-Vargas, A. T. Carmona and I. Robina, *Eur. J. Org. Chem.*, 2010, 4049–4055.
- 25 T. Fiehn, R. Goddard, R. W. Seidel and S. Kubik, *Chem. Eur. J.*, 2010, **16**, 7241–7255.
- 26 A. J. McConnell, C. J. Serpell, A. L. Thompson, D. R. Allan and P. D. Beer, *Chem.–Eur. J.*, 2010, **16**, 1256–1264.
- 27 H.-B. Wang, J. A. Wisner and M. C. Jennings, *Beilstein J. Org. Chem.*, 2010, **6**, 50.
- 28 C. Jia, B. Wu, S. Li, Z. Yang, Q. Zhao, J. Liang, Q.-S. Li and X.-J. Yang, *Chem. Commun.*, 2010, **46**, 5376–5378.
- 29 P. S. Lakshminarayanan, I. Ravikumar, E. Suresh and P. Ghosh, *Chem. Commun.*, 2007, 5214–5216.
- 30 I. Ravikumar and P. Ghosh, *Chem. Commun.*, 2010, **46**, 1082–1084.
- 31 I. Ravikumar and P. Ghosh, *Chem. Commun.*, 2010, **46**, 6741–6743.
- 32 R. Custelcean, A. Bock and B. A. Moyer, *J. Am. Chem. Soc.*, 2010, **132**, 7177–7185.
- 33 R. Custelcean, P. Remy, P. V. Bonnesen, D.-e. Jiang and B. A. Moyer, *Angew. Chem., Int. Ed.*, 2008, **47**, 1866–1870.
- 34 C. Bazzicalupi, A. Bencini, A. Bianchi, A. Danesi, C. Giorgi and B. Valtancoli, *Inorg. Chem.*, 2009, **48**, 2391–2398.
- 35 C. Pérez-Casas, H. Höpfl and A. Yatsimirsky, *J. Inclusion Phenom. Macrocyclic Chem.*, 2010, **68**, 387–398–398.
- 36 K. Raatikainen, N. K. Beyeh and K. Rissanen, *Chem.–Eur. J.*, 2010, **16**, 14554–14564.
- 37 A. Sirikulkajorn, T. Tuntulani, V. Ruangpornvisuti, B. Tomapatanaget and A. P. Davis, *Tetrahedron*, 2010, **66**, 7423–7428.
- 38 E. M. Boyle, T. McCabe and T. Gunnlaugsson, *Supramol. Chem.*, 2010, **22**, 586–597.
- 39 C. M. G. dos Santos, T. McCabe, G. W. Watson, P. E. Kruger and T. Gunnlaugsson, *J. Org. Chem.*, 2008, **73**, 9235–9244.
- 40 A. Ghosh, D. Jose, A. Das and B. Ganguly, *J. Mol. Model.*, 2010, **16**, 1441–1448–1448.
- 41 V. Amendola, G. Bergamaschi, M. Boiocchi, L. Fabbrizzi and M. Milani, *Chem.–Eur. J.*, 2010, **16**, 4368–4380.
- 42 M. Boiocchi, L. Del Boca, D. Esteban-Gómez, L. Fabbrizzi, M. Licchelli and E. Monzani, *J. Am. Chem. Soc.*, 2004, **126**, 16507–16514.
- 43 D. Esteban-Gómez, L. Fabbrizzi, M. Licchelli and E. Monzani, *Org. Biomol. Chem.*, 2005, **3**, 1495–1500.
- 44 M. H. Al-Sayah and N. R. Branda, *Thermochim. Acta*, 2010, **503–504**, 28–32.
- 45 E. G. Klauber, C. K. De, T. K. Shah and D. Seidel, *J. Am. Chem. Soc.*, 2010, **132**, 13624–13626.
- 46 N. Takenaka, J. Chen, B. Captain, R. S. Sarangthem and A. Chandrasekhar, *J. Am. Chem. Soc.*, 2010, **132**, 4536–4537.
- 47 A.-S. Delépine, R. Tripier, M. Le Baccon and H. Handel, *Eur. J. Org. Chem.*, 2010, 5380–5390.
- 48 K. R. Dey, T. Horne, F. R. Fronczek and M. A. Hossain, *Inorg. Chem. Commun.*, 2010, **13**, 1515–1518.
- 49 J. S. Mendy, M. L. Pilate, T. Horne, V. W. Day and M. A. Hossain, *Chem. Commun.*, 2010, **46**, 6084–6086.
- 50 M. A. Saeed, D. R. Powell, F. R. Fronczek and M. A. Hossain, *Tetrahedron Lett.*, 2010, **51**, 4233–4236.
- 51 M. A. Hossain, M. A. Saeed, F. R. Fronczek, B. M. Wong, K. R. Dey, J. S. Mendy and D. Gibson, *Cryst. Growth Des.*, 2010, **10**, 1478–1481.
- 52 M. A. Saeed, J. J. Thompson, F. R. Fronczek and M. A. Hossain, *CrystEngComm*, 2010, **12**, 674–676.
- 53 M. A. Saeed, F. R. Fronczek, M.-J. Huang and M. A. Hossain, *Chem. Commun.*, 2010, **46**, 404–406.
- 54 H. Wu, M. A. Saeed, H.-M. Hwang, S. Zhao, Y.-M. Liu and M. A. Hossain, *J. Phys. Org. Chem.*, 2005, **24**, 1–5.
- 55 A. L. Cresswell, M. O. M. Piepenbrock and J. W. Steed, *Chem. Commun.*, 2010, **46**, 2787–2789.
- 56 H. B. Tanh Jeazet, K. Gloe, T. Doert, O. N. Kataeva, A. Jager, G. Geipel, G. Bernhard, B. Buchner and K. Gloe, *Chem. Commun.*, 2010, **46**, 2373–2375.
- 57 H. Maeda, *Top. Heterocycl. Chem.*, 2010, **24**, 103–144.
- 58 P. A. Gale and C.-H. Lee, *Top. Heterocycl. Chem.*, 2010, **24**, 39–73.
- 59 J. L. Sessler, S. Camiolo and P. A. Gale, *Coord. Chem. Rev.*, 2003, **240**, 17–55.
- 60 G. Mani, T. Guchhait, R. Kumar and S. Kumar, *Org. Lett.*, 2010, **12**, 3910–3913.
- 61 G. Mani, D. Jana, R. Kumar and D. Ghorai, *Org. Lett.*, 2010, **12**, 3212–3215.
- 62 G. Cafeo, H. M. Colquhoun, A. Cuzzola, M. Gattuso, F. H. Kohnke, L. Valenti and A. J. P. White, *J. Org. Chem.*, 2010, **75**, 6263–6266.
- 63 K. Hirose, *J. Inclusion Phenom. Macrocyclic Chem.*, 2001, **39**, 193–209.
- 64 C. Caltagirone, N. L. Bill, D. E. Gross, M. E. Light, J. L. Sessler and P. A. Gale, *Org. Biomol. Chem.*, 2010, **8**, 96–99.
- 65 D.-W. Yoon, D. E. Gross, V. M. Lynch, J. L. Sessler, B. P. Hay and C.-H. Lee, *Angew. Chem., Int. Ed.*, 2008, **47**, 5038–5042.
- 66 D. Gross, D.-W. Yoon, V. Lynch, C.-H. Lee and J. Sessler, *J. Inclusion Phenom. Macrocyclic Chem.*, 2010, **66**, 81–85.
- 67 M. Buda, A. Iordache, C. Bucher, J.-C. Moutet, G. Royal, E. Saint-Aman and J. L. Sessler, *Chem.–Eur. J.*, 2010, **16**, 6810–6819.
- 68 B. A. Moyer, F. V. Sloop, C. J. Fowler, T. J. Haverlock, H.-A. Kang, L. H. Delmau, D. M. Bau, M. A. Hossain, K. Bowman-James, J. A. Shriver, N. L. Bill, D. E. Gross, M. Marquez, V. M. Lynch and J. L. Sessler, *Supramol. Chem.*, 2010, **22**, 653–671.

- 69 P. A. Gale, *Chem. Commun.*, 2008, 4525–4540.
- 70 H. Juwarker, J.-m. Suk and K.-S. Jeong, *Top. Heterocycl. Chem.*, 2010, **24**, 177–204.
- 71 D. Makuc, M. Albrecht and J. Plavec, *Supramol. Chem.*, 2010, **22**, 603–611.
- 72 P. A. Gale, J. R. Hiscock, C. Z. Jie, M. B. Hursthouse and M. E. Light, *Chem. Sci.*, 2010, **1**, 215–220.
- 73 P. A. Gale, J. R. Hiscock, S. J. Moore, C. Caltagirone, M. B. Hursthouse and M. E. Light, *Chem.–Asian J.*, 2010, **5**, 555–561.
- 74 P. R. Edwards, J. R. Hiscock, P. A. Gale and M. E. Light, *Org. Biomol. Chem.*, 2010, **8**, 100–106.
- 75 P. Dydio, T. Zieliński and J. Jurczak, *Org. Lett.*, 2010, **12**, 1076–1078.
- 76 J.-i. Kim, H. Juwarker, X. Liu, M. S. Lah and K.-S. Jeong, *Chem. Commun.*, 2010, **46**, 764–766.
- 77 T. Wang, Y. Bai, L. Ma and X.-P. Yan, *Org. Biomol. Chem.*, 2008, **6**, 1751–1755.
- 78 T. Wang, H.-F. Wang and X.-P. Yan, *CrystEngComm*, 2010, **12**, 3177–3182.
- 79 T. Wang and X.-P. Yan, *Chem.–Eur. J.*, 2010, **16**, 4639–4649.
- 80 Y. Zhao, Y. Li, Y. Li, C. Huang, H. Liu, S.-W. Lai, C.-M. Che and D. Zhu, *Org. Biomol. Chem.*, 2010, **8**, 3923–3927.
- 81 K. N. Skala, K. G. Perkins, A. Ali, R. Kutlik, A. M. Summitt, S. Swamy-Mruthinti, F. A. Khan and M. Fujita, *Tetrahedron Lett.*, 2010, **51**, 6516–6520.
- 82 C. Rether, W. Sicking, R. Boese and C. Schmuck, *Beilstein J. Org. Chem.*, 2010, **6**, 3.
- 83 C. Schmuck, *Eur. J. Org. Chem.*, 1999, 2397–2403.
- 84 M. Arunachalam and P. Ghosh, *CrystEngComm*, 2010, **12**, 1621–1627.
- 85 M. Arunachalam and P. Ghosh, *Chem. Commun.*, 2009, 3184–3186.
- 86 Q.-S. Lu, J. Zhang, L. Jiang, J.-T. Hou and X.-Q. Yu, *Tetrahedron Lett.*, 2010, **51**, 4395–4399.
- 87 L. Yang, S. Qin, X. Su, F. Yang, J. You, C. Hu, R. Xie and J. Lan, *Org. Biomol. Chem.*, 2010, **8**, 339–348.
- 88 H.-Y. Gong, B. M. Rambo, E. Karnas, V. M. Lynch and J. L. Sessler, *Nat. Chem.*, 2010, **2**, 406–409.
- 89 S. Lee, Y. Hua, H. Park and A. H. Flood, *Org. Lett.*, 2010, **12**, 2100–2102.
- 90 Y. Hua and A. H. Flood, *J. Am. Chem. Soc.*, 2010, **132**, 12838–12840.
- 91 Y. Wang, F. Bie and H. Jiang, *Org. Lett.*, 2010, **12**, 3630–3633.
- 92 B. Schulze, C. Fribe, M. D. Hager, W. Gunther, U. Kohn, B. O. Jahn, H. Gorls and U. S. Schubert, *Org. Lett.*, 2010, **12**, 2710–2713.
- 93 S.-i. Kondo, Y. Kobayashi and M. Unno, *Tetrahedron Lett.*, 2010, **51**, 2512–2514.
- 94 C. Bresner, C. J. E. Haynes, D. A. Addy, A. E. J. Broomsgrove, P. Fitzpatrick, D. Vidovic, A. L. Thompson, I. A. Fallis and S. Aldridge, *New J. Chem.*, 2010, **34**, 1652–1659.
- 95 I. R. Morgan, A. E. J. Broomsgrove, P. Fitzpatrick, D. Vidovic, A. L. Thompson, I. A. Fallis and S. Aldridge, *Organometallics*, 2010, **29**, 4762–4765.
- 96 Y. Kim, M. Kim and F. P. Gabbai, *Org. Lett.*, 2010, **12**, 600–602.
- 97 D. Shanmukaraj, S. Grugeon, G. Gachot, S. Laruelle, D. Mathiron, J.-M. Tarascon and M. Armand, *J. Am. Chem. Soc.*, 2010, **132**, 3055–3062.
- 98 K. Raatikainen and K. Rissanen, *Cryst. Growth Des.*, 2010, **10**, 3638–3646.
- 99 M. G. Sarwar, B. Dragisic, S. Sagoo and M. S. Taylor, *Angew. Chem. Int. Ed.*, 2010, **49**, 1674–1677.
- 100 E. Dimitrijevic, O. Kvak and M. S. Taylor, *Chem. Commun.*, 2010, **46**, 9025–9027.
- 101 M. G. Sarwar, B. Dragisic, L. J. Salsberg, C. Gouliaras and M. S. Taylor, *J. Am. Chem. Soc.*, 2010, **132**, 1646–1653.
- 102 C. J. Serpell, N. L. Kilah, P. J. Costa, V. Félix and P. D. Beer, *Angew. Chem. Int. Ed.*, 2010, **49**, 5322–5326.
- 103 B. P. Hay and R. Custelcean, *Cryst. Growth Des.*, 2009, **9**, 2539–2545.
- 104 A. Garcia-Raso, F. M. Albertí, J. J. Fiol, Y. Lagos, M. Torres, E. Molins, I. Mata, C. Estarellas, A. Frontera, D. Quiñonero and P. M. Deyà, *Eur. J. Org. Chem.*, 2010, 5171–5180.
- 105 M. Albrecht, M. Müller, O. Mergel, K. Rissanen and A. Valkonen, *Chem.–Eur. J.*, 2010, **16**, 5062–5069.
- 106 M. Müller, M. Albrecht, V. Gossen, T. Peters, A. Hoffmann, G. Raabe, A. Valkonen and K. Rissanen, *Chem.–Eur. J.*, 2010, **16**, 12446–12453.
- 107 H. T. Chifotides, B. L. Schottel and K. R. Dunbar, *Angew. Chem., Int. Ed.*, 2010, **49**, 7202–7207.
- 108 P. S. Szalay, J. R. Galán-Mascarós, B. L. Schottel, J. Bacsa, L. M. Pérez, A. S. Ichimura, A. Chouai and K. R. Dunbar, *J. Cluster Sci.*, 2004, **15**, 503–530.
- 109 D.-X. Wang, Q.-Q. Wang, Y. Han, Y. Wang, Z.-T. Huang and M.-X. Wang, *Chem.–Eur. J.*, 2010, **16**, 13053–13057.
- 110 A. Galstyan, P. J. Sanz Miguel and B. Lippert, *Dalton Trans.*, 2010, **39**, 6386–6388.
- 111 A. Galstyan, P. J. Sanz Miguel and B. Lippert, *Chem. Eur. J.*, 2010, **16**, 5577–5580.
- 112 M. I. Ortiz, M. L. Soriano, M. P. Carranza, F. A. Jalon, J. W. Steed, K. Mereiter, A. M. Rodriguez, D. Quinonero, P. M. Deya and B. R. Manzano, *Inorg. Chem.*, 2010, **49**, 8828–8847.
- 113 S. K. Kim, J. L. Sessler, D. E. Gross, C.-H. Lee, J. S. Kim, V. M. Lynch, L. H. Delmau and B. P. Hay, *J. Am. Chem. Soc.*, 2010, **132**, 5827–5836.
- 114 M. Ménand and I. Jabin, *Chem.–Eur. J.*, 2010, **16**, 2159–2169.
- 115 M. Ménand and I. Jabin, *Org. Lett.*, 2009, **11**, 673–676.
- 116 C. Capici, R. De Zorzi, C. Gargiulli, G. Gattuso, S. Geremia, A. Notti, S. Pappalardo, M. F. Parisi and F. Puntiliero, *Tetrahedron*, 2010, **66**, 4987–4993.
- 117 F. P. Ballistreri, A. Pappalardo, G. A. Tomaselli, R. M. Toscano and G. T. Sfrazzetto, *Eur. J. Org. Chem.*, 2010, 3806–3810.
- 118 M. E. Amato, F. P. Ballistreri, S. Gentile, A. Pappalardo, G. A. Tomaselli and R. M. Toscano, *J. Org. Chem.*, 2010, **75**, 1437–1443.
- 119 T. Lin, V. Gasperov, K. J. Smith, C. C. Tong and P. A. Tasker, *Dalton Trans.*, 2010, **39**, 9760–9762.
- 120 M. Wenzel, S. R. Bruere, Q. W. Knapp, P. A. Tasker and P. G. Plieger, *Dalton Trans.*, 2010, **39**, 2936–2941.
- 121 P. G. Plieger, S. Parsons, A. Parkin and P. A. Tasker, *J. Chem. Soc., Dalton Trans.*, 2002, 3928–3930.
- 122 K. Zhu, L. Wu, X. Yan, B. Zheng, M. Zhang and F. Huang, *Chem. Eur. J.*, 2010, **16**, 6088–6098.
- 123 F. Tancini, T. Gottschalk, W. B. Schweizer, F. Diederich and E. Dalcanale, *Chem.–Eur. J.*, 2010, **16**, 7813–7819.
- 124 F. Li, S. Carvalho, R. Delgado, M. G. B. Drew and V. Felix, *Dalton Trans.*, 2010, **39**, 9579–9587.
- 125 X. Huang, Z. Yang, X.-J. Yang, Q. Zhao, Y. Xia and B. Wu, *Inorg. Chem. Commun.*, 2010, **13**, 1103–1107.
- 126 N. N. Adarsh and P. Dastidar, *Cryst. Growth Des.*, 2010, **10**, 483–487.
- 127 S. Banerjee, N. N. Adarsh and P. Dastidar, *Eur. J. Inorg. Chem.*, 2010, 3770–3779.
- 128 B. Wu, J. Liang, Y. Zhao, M. Li, S. Li, Y. Liu, Y. Zhang and X.-J. Yang, *CrystEngComm*, 2010, **12**, 2129–2134.
- 129 J. Svec, M. Necas and V. Sindelar, *Angew. Chem. Int. Ed.*, 2010, **49**, 2378–2381.
- 130 K. T. Holman, S. D. Drake, J. W. Steed, G. W. Orr and J. L. Atwood, *Supramol. Chem.*, 2010, **22**, 870–890.
- 131 J. C. Rainwater and E. V. Anslyn, *Chem. Commun.*, 2010, **46**, 2904–2906.
- 132 W. A. Harrell, M. L. Bergmeyer, P. Y. Zavalij and J. T. Davis, *Chem. Commun.*, 2010, **46**, 3950–3952.
- 133 L. J. Siskind and M. Colombini, *J. Biol. Chem.*, 2000, **275**, 38640–38644.
- 134 L. W. Judd and A. P. Davis, *Chem. Commun.*, 2010, **46**, 2227–2229.
- 135 N. Busschaert, P. A. Gale, C. J. E. Haynes, M. E. Light, S. J. Moore, C. C. Tong, J. T. Davis and J. W. A. Harrell, *Chem. Commun.*, 2010, **46**, 6252–6254.
- 136 P. A. Gale, C. C. Tong, C. J. E. Haynes, O. Adeosun, D. E. Gross, E. Karnas, E. M. Sedenberg, R. Quesada and J. L. Sessler, *J. Am. Chem. Soc.*, 2010, **132**, 3240–3241.
- 137 M. Yano, C. C. Tong, M. E. Light, F. P. Schmidtchen and P. A. Gale, *Org. Biomol. Chem.*, 2010, **8**, 4356–4363.
- 138 M. G. Fisher, P. A. Gale, J. R. Hiscock, M. B. Hursthouse, M. E. Light, F. P. Schmidtchen and C. C. Tong, *Chem. Commun.*, 2009, 3017–3019.
- 139 C. R. Yamnitz, S. Negin, I. A. Carasel, R. K. Winter and G. W. Gokel, *Chem. Commun.*, 2010, **46**, 2838–2840.

- Published on 14 November 2011. Downloaded on 20/01/2016 15:01:55.
-
- 140 B. Hill, *Ionic Pores of Excitable Membranes*, Mass: Sinauer Associates, Sunderland, 3 edn, 2001.
- 141 R. E. Dawson, A. Hennig, D. P. Weimann, D. Emery, V. Ravikumar, J. Montenegro, T. Takeuchi, S. Gabutti, M. Mayor, J. Mareda, C. A. Schalley and S. Matile, *Nat. Chem.*, 2010, **2**, 533–538.
- 142 J. Mišek, A. Vargas Jentzsch, S.-i. Sakurai, D. Emery, J. Mareda and S. Matile, *Angew. Chem., Int. Ed.*, 2010, **49**, 7680–7683.
- 143 L. Kim, A. Hamdi, A. Stancu, R. Souane, L. Mutihac and J. Vicens, *J. Inclusion Phenom. Macrocyclic Chem.*, 2010, **66**, 55–59.
- 144 C. Urban and C. Schmuck, *Chem.–Eur. J.*, 2010, **16**, 9502–9510.
- 145 S. Niebling, S. K. Srivastava, C. Herrmann, P. R. Wich, C. Schmuck and S. Schlucker, *Chem. Commun.*, 2010, **46**, 2133–2135.
- 146 J.-W. Liu, Y. Yang, C.-F. Chen and J.-T. Ma, *Langmuir*, 2010, **26**, 9040–9044.
- 147 S.-Y. Hsueh, C.-T. Kuo, T.-W. Lu, C.-C. Lai, Y.-H. Liu, H.-F. Hsu, S.-M. Peng, C.-h. Chen and S.-H. Chiu, *Angew. Chem., Int. Ed.*, 2010, **49**, 9170–9173.
- 148 J. A. Foster, M.-O. M. Piepenbrock, G. O. Lloyd, N. Clarke, J. A. K. Howard and J. W. Steed, *Nat. Chem.*, 2010, **2**, 1037–1043.
- 149 P. Byrne, G. O. Lloyd, L. Applegarth, K. M. Anderson, N. Clarke and J. W. Steed, *New J. Chem.*, 2010, **34**, 2261–2274.
- 150 A. N. Swinburne, M. J. Paterson, A. Beeby and J. W. Steed, *Chem.–Eur. J.*, 2010, **16**, 2714–2718.
- 151 T. Riis-Johannessen, K. Schenk and K. Severin, *Inorg. Chem.*, 2010, **49**, 9546–9553.
- 152 T. Riis-Johannessen and K. Severin, *Chem.–Eur. J.*, 2010, **16**, 8291–8295.
- 153 J. J. Gassensmith, S. Matthys, J. J. Lee, A. Wojcik, P. V. Kamat and B. D. Smith, *Chem.–Eur. J.*, 2010, **16**, 2916–2921.
- 154 J. S. Kim, S. Y. Park, S. H. Kim, P. Thuery, R. Souane, S. E. Matthews and J. Vicens, *Bull. Korean Chem. Soc.*, 2010, **31**, 624–629.
- 155 S. Y. Park, J. H. Yoon, C. S. Hong, R. Souane, J. S. Kim, S. E. Matthews and J. Vicens, *J. Org. Chem.*, 2008, **73**, 8212–8218.
- 156 J. Yoo, Y. Kim, S. J. Kim and C. H. Lee, *Chem. Commun.*, 2010, **46**, 5449–5451.
- 157 Y. Qu, J. L. Hue and H. Tian, *Org. Lett.*, 2010, **12**, 3320–3323.
- 158 R. B. P. Elmes and T. Gunnlaugsson, *Tetrahedron Lett.*, 2010, **51**, 4082–4087.
- 159 W. J. Xu, S. J. Liu, X. Y. Zhao, S. Sun, S. Cheng, T. C. Ma, H. B. Sun, Q. A. Zhao and W. Huang, *Chem. Eur. J.*, 2010, **16**, 7125–7133.
- 160 W. Wei, Y. Guo, J. A. Xu and S. J. Shao, *Spectrochim. Acta, Part A*, 2010, **77**, 620–624.
- 161 M. Naito, M. Nakamura, K. Terao, T. Kawabe and M. Fujiki, *Macromolecules*, 2010, **43**, 7919–7923.
- 162 Z. H. Zeng, A. A. J. Torriero, A. M. Bond and L. Spiccia, *Chem.–Eur. J.*, 2010, **16**, 9154–9163.
- 163 K. Ghosh, T. Sarkar and A. P. Chattopadhyay, *Beilstein J. Org. Chem.*, 2010, **6**, 1211–1218.
- 164 J. T. Lin, Q. M. Wang, C. L. Tan and H. Y. Chen, *Synth. Met.*, 2010, **160**, 1780–1786.
- 165 I. S. Shin, S. W. Bae, H. Kim and J. I. Hong, *Anal. Chem.*, 2010, **82**, 8259–8265.
- 166 J. M. Baumes, J. J. Gassensmith, J. Giblin, J. J. Lee, A. G. White, W. J. Culligan, W. M. Leevy, M. Kuno and B. D. Smith, *Nat. Chem.*, 2010, **2**, 1025–1030.
- 167 Y. L. Liu, M. A. Palacios and P. Anzenbacher, *Chem. Commun.*, 2010, **46**, 1860–1862.
- 168 J. S. Mendy, M. A. Saeed, F. R. Fronczek, D. R. Powell and M. A. Hossain, *Inorg. Chem.*, 2010, **49**, 7223–7225.
- 169 S. Guha and S. Saha, *J. Am. Chem. Soc.*, 2010, **132**, 17674–17677.
- 170 Q. G. Wang, Y. S. Xie, Y. B. Ding, X. Li and W. H. Zhu, *Chem. Commun.*, 2010, **46**, 3669–3671.
- 171 M. O. Odago, D. M. Colabello and A. J. Lees, *Tetrahedron*, 2010, **66**, 7465–7471.
- 172 R. Sakai, S. Okade, E. B. Barasa, R. Kakuchi, M. Ziabka, S. Umeda, K. Tsuda, T. Satoh and T. Kakuchi, *Macromolecules*, 2010, **43**, 7406–7411.
- 173 A. Rostami, A. Colin, X. Y. Li, M. G. Chudzinski, A. J. Lough and M. S. Taylor, *J. Org. Chem.*, 2010, **75**, 3983–3992.
- 174 G. W. Lee, N. K. Kim and K. S. Jeong, *Org. Lett.*, 2010, **12**, 2634–2637.
- 175 H. Maeda, M. Takayama, K. Kobayashi and H. Shinmori, *Org. Biomol. Chem.*, 2010, **8**, 4308–4315.
- 176 Z. P. Ni, A. M. McDaniel and M. P. Shores, *Chem. Sci.*, 2010, **1**, 615–621.
- 177 Z. Ni and M. P. Shores, *J. Am. Chem. Soc.*, 2009, **131**, 32–33.
- 178 C. Bejger, J. S. Park, E. S. Silver and J. L. Sessler, *Chem. Commun.*, 2010, **46**, 7745–7747.
- 179 E. M. Zahran, Y. R. Hua, Y. J. Li, A. H. Flood and L. G. Bachas, *Anal. Chem.*, 2010, **82**, 368–375.